

## Implementation of the Rigid Ring Tyre Model and Accompanying Soil Model in a Complete Vehicle Simulation Tool for Trucks

Master's thesis in Applied Mechanics

ALBIN BRANTIN  
OSCAR GRUNDÉN



MASTER'S THESIS IN APPLIED MECHANICS

Implementation of the Rigid Ring Tyre Model and Accompanying Soil Model  
in a Complete Vehicle Simulation Tool for Trucks

ALBIN BRANTIN  
OSCAR GRUNDÉN

Department of Applied Mechanics

Vehicle Dynamics

CHALMERS UNIVERSITY OF TECHNOLOGY

Göteborg, Sweden 2016

Implementation of the Rigid Ring Tyre Model and Accompanying Soil Model in a Complete Vehicle  
Simulation Tool for Trucks

ALBIN BRANTIN  
OSCAR GRUNDÉN

© ALBIN BRANTIN, OSCAR GRUNDÉN, 2016

Master's thesis 2016:58  
ISSN 1652-8557  
Department of Applied Mechanics  
Vehicle Dynamics  
Chalmers University of Technology  
SE-412 96 Göteborg  
Sweden  
Telephone: +46 (0)31-772 1000

Examiner: Bengt Jacobson  
Supervisors: Artem Kusachov, Fredrik Ijer

Cover:

A representation of the wheel plane and out of plane rigid ring model with soil model included.

Chalmers Reproservice  
Göteborg, Sweden 2016

Implementation of the Rigid Ring Tyre Model and Accompanying Soil Model in a Complete Vehicle Simulation Tool for Trucks

Master's thesis in Applied Mechanics

ALBIN BRANTIN

OSCAR GRUNDÉN

Department of Applied Mechanics

Vehicle Dynamics

Chalmers University of Technology

## ABSTRACT

Volvo got a library of Virtual Transport Models of their trucks (VTM). These models cannot simulate soft soil roads due to the currently implemented tyre model. A new tyre/soil model is being developed in conjunction with the University of Ontario Institute of Technology, which is to be implemented to work with the models in the VTM library.

The university model the tyre and soil using finite element method (FEM) and smoothed particle hydrodynamics (SPH), which is too computationally demanding to implement in VTM. The model that was to be implemented was instead a simplification comprising of springs, dampers and masses. The parameters of these elements are estimated from different FE-simulations done by the university. Once the tyre model is implemented it will be verified against the FE-model by comparing simulation results. In addition, the model will be compared to the currently implemented model to ensure an overall similarity between the models.

The overall results shows promise in the new tyre model. All of the single tyre simulations have given satisfactory results after some of the parameters were corrected. The soil model is however not able to completely capture the results of the FE-simulations but is considered acceptable. The full vehicle model has given good results even though the vertical soil model and the rolling resistance in the soil needs further investigation to capture an even more realistic dynamic response.

The rigid ring model on rigid ground is deemed to work properly and gives good results. The soil model has given acceptable results but it does not capture the full soil behaviour. Additionally the soil model has been non-physically altered to get good results. This warrants further studying of the model and its parameters in order to further refine the model. The rolling resistance in the soil also needs further investigation since the model is crude and uncertain. The implemented tyre model requires the same order of magnitude in simulation time as the original magic formula rigid ground model.

Keywords: Rigid Ring Tyre Model, Soft Soil Model, Tyre Modeling, Vehicle Dynamics



## PREFACE

This project acts as a continuation of an ongoing collaboration between Volvo Trucks, the University of Ontario Institute of Technology and the Pennsylvania State University. Volvo wants to implement a new tyre model into their full vehicle dynamic simulator, VTM. By adopting this tyre model into VTM the same tyre model will be used as in their FEM tool. In addition a soil model compatible with this model will be investigated and implemented.

## ACKNOWLEDGEMENTS

We want to give a huge thank you to our supervisor, at Volvo GTT, Fredrik Öijer who has helped us tremendously throughout the project. We would also like to thank Sachin Janardhanan and Inge Johansson and all the other people at the Chassis Strategy and Vehicle Analysis department at Volvo GTT who has been very helpful. Finally we would like to thank our examiner, Bengt Jacobson, and our supervisor, at Chalmers, Artem Kusachov, for their help in this project.



## NOMENCLATURE

SI-units and radians are used.

$C(v_x)$	slope compensation factor [ $\sim$ ]
$c_a$	first slope compensation constant [ $1/(m/s)^{c_b}$ ]
$c_b$	second slope compensation constant [ $\sim$ ]
$c_c$	third slope compensation constant [ $\sim$ ]
$c_l$	lateral tyre stiffness [ $N/rad$ ]
$c_{bx}$	longitudinal sidewall damping
$c_{by}$	lateral sidewall damping
$c_{bz}$	vertical sidewall damping
$c_{b\theta}$	wheel plane rotational damping of the sidewall
$c_{b\gamma}$	out of plane rotational damping of the sidewall
$c_{soil}$	vertical soil damping
$c'_{soil}$	equivalent vertical soil damping
$c'_{soil,app}$	approximate equivalent damping of the soil
$c_{tot}$	total vertical damping of the tyre
$c_{vr}$	vertical residual damping
$F_B$	bulldozing resistance force
$F_r$	rolling resistance force
$F_R$	rut rolling resistance force
$F_{sx}$	longitudinal slip force
$F_{sy}$	lateral slip force
$F_{wx}$	longitudinal force acting on tyre belt
$F_{wy}$	lateral force acting on tyre belt
$F_x$	longitudinal force acting on wheel rim
$F_{x,max}$	longitudinal slip force saturation for rigid ground
$F_{x,max,soil}$	longitudinal slip force saturation for soft soil ground
$F_y$	lateral force acting on wheel rim
$F_{y,max}$	lateral slip force saturation for rigid ground
$F_z$	vertical force acting on wheel rim
$F_{z0}$	static load
$I_{1y}$	wheel plane rotational inertia of wheel rim, with or without inertia of wheel axle
$I_{2x}$	out of plane rotational inertia of tyre belt
$I_{2y}$	wheel plane rotational inertia of tyre belt
$k_l$	lateral tyre tread stiffness
$k_{bx}$	longitudinal sidewall stiffness
$k_{by}$	lateral sidewall stiffness
$k_{bz}$	vertical sidewall stiffness
$k_{b\gamma}$	out of plane rotational stiffness of the sidewall
$k_{b\theta}$	wheel plane rotational stiffness of the sidewall
$k_{cx}$	longitudinal tyre tread stiffness
$k_f$	cornering stiffness
$k_k$	longitudinal tyre stiffness

$k_{\text{soil}}$	vertical soil stiffness
$k'_{\text{soil}}$	equivalent vertical component of soil stiffness
$k_{\text{soil},2}$	additional vertical soil stiffness
$k_{\text{tot}}$	total vertical stiffness of the tyre
$k_{vr}$	vertical residual stiffness
$M_{\text{in}}$	driving moment
$M_{y,r}$	reaction moment acting on wheel rim
$M_{y,b}$	reaction moment acting on tyre belt
$M_{y,\text{out}}$	moment used as output from the model
$m_1$	tyre rim mass, with or without wheel axle mass
$m_2$	tyre belt mass
$m_{\text{soil}}$	fictive mass of the soil
$m_{\text{tot,soil}}$	fictive mass of soil + mass of tyre
$R_0$	undeformed tyre radius
$R_e$	effective radius
$rrc$	rolling resistance coefficient [ $\sim$ ]
$r_a$	first rolling resistance constant [ $\sim$ ]
$r_b$	second rolling resistance constant [ $\sim$ ]
$r_c$	third rolling resistance constant [ $\sim$ ]
$u_x$	tyre tread deformation
$\dot{u}_x$	tyre tread deformation speed
$V_c$	velocity at the contact point
$v_x$	longitudinal velocity of wheel rim
$v_y$	lateral velocity of wheel rim
$v_z$	vertical velocity of wheel rim
$x_1$	longitudinal position of wheel rim
$x_2$	longitudinal position of where the sidewall meets the tyre tread
$y_1$	lateral position of wheel rim
$y_2$	lateral position of where the sidewall meets the tyre tread
$z_1$	vertical position of wheel rim
$z_2$	vertical position of where the sidewall meets the tyre tread
$z_3$	vertical position of tyre/soil interaction point
$z_r$	vertical position of the road
$\alpha_x$	longitudinal slip [ $\sim$ ]
$\alpha_y$	lateral slip [rad]
$\beta$	average local slope angle
$\beta'$	equivalent local slope angle
$\gamma_2$	out of plane angle of tyre belt
$\delta$	logarithmic decrement of oscillations [ $\sim$ ]
$\zeta$	dimensionless damping constant [ $\sim$ ]
$\theta_1$	wheel plane angle of wheel rim
$\theta_2$	wheel plane angle of tyre belt
$\sigma$	relaxation length of tyre
$\varphi_x$	lateral road slope
$\varphi_y$	longitudinal road slope
$\omega$	tyre frequency, soil frequency
$\omega_0$	nominal frequency

# CONTENTS

<b>Abstract</b>	<b>i</b>
<b>Preface</b>	<b>iii</b>
<b>Acknowledgements</b>	<b>iii</b>
<b>Nomenclature</b>	<b>v</b>
<b>Contents</b>	<b>vii</b>
<b>1 Introduction</b>	<b>1</b>
1.1 Background . . . . .	1
1.2 Project Motivation . . . . .	1
1.3 Envisioned Solution . . . . .	2
1.4 Objective . . . . .	2
1.5 Deliverables . . . . .	2
1.6 Limitations . . . . .	2
1.7 Method . . . . .	3
1.7.1 Single Tyre Simulations for Verification . . . . .	3
1.7.2 Complete Vehicle Simulations . . . . .	7
<b>2 Tyre Modelling</b>	<b>8</b>
2.1 VTM . . . . .	8
2.2 S-functions . . . . .	9
2.3 Present Tyre Model "PAC2002" . . . . .	9
2.4 Rigid Ring Tyre Model, Rigid Ground . . . . .	10
2.4.1 Vertical Reaction Force . . . . .	11
2.4.2 Longitudinal Reaction Force . . . . .	12
2.4.3 Wheel Plane Rotational Reaction Moment . . . . .	14
2.4.4 Lateral Reaction Force . . . . .	15
2.4.5 Out of Wheel Plane Rotational Reaction Moment . . . . .	17
2.5 Rigid Ring Tyre Model, Soft Soil Ground . . . . .	18
2.5.1 Vertical Reaction Force . . . . .	18
2.5.2 Longitudinal Reaction Force . . . . .	25
2.5.3 Lateral Reaction Force . . . . .	27
2.6 S-function Implementation . . . . .	27
2.6.1 Rigid Ground . . . . .	28
2.6.2 Soft Soil Ground . . . . .	28
2.6.3 Additional States for Single Tyre Model . . . . .	29
<b>3 Tyre Parameters</b>	<b>30</b>
3.1 Linearisation With Respect To Vertical Load . . . . .	30
3.2 Influence of Tyre Inflation Pressure . . . . .	30
3.3 Errors and Shortcomings in the Previous Work . . . . .	30
<b>4 Single Tyre Verification</b>	<b>32</b>
4.1 Vertical Stiffness, Rigid Ground . . . . .	32
4.2 Vertical Damping, Rigid Ground . . . . .	33

4.3	Soil Vertical Stiffness and Damping . . . . .	34
4.4	Wheel Plane Rotational Stiffness & Damping . . . . .	35
4.5	Longitudinal Tread & Tyre Stiffness, Rigid Ground . . . . .	35
4.6	Longitudinal Tread & Tyre Stiffness, Soft Soil Ground . . . . .	36
4.7	Out of Plane Sidewall Translational Stiffness & Damping . . . . .	37
4.8	Out of Plane Rotational Stiffness & Damping . . . . .	38
4.9	Cornering Stiffness, Rigid Ground . . . . .	38
4.10	Cornering Stiffness, Soft Soil Ground . . . . .	39
<b>5</b>	<b>Complete Vehicle Results</b>	<b>40</b>
5.1	Straight Line Acceleration Tests . . . . .	42
5.2	Step Steer Test . . . . .	46
5.3	Zigzag Steer Test . . . . .	49
5.4	Figure-8 test . . . . .	52
<b>6</b>	<b>Future Work</b>	<b>54</b>
6.1	More Detailed Rolling Resistance Modelling . . . . .	54
6.2	Different Vertical Soil Models . . . . .	55
6.2.1	Local slope . . . . .	55
6.3	Further Studying of Parameters . . . . .	55
6.3.1	Fictive Mass, Soil Damping and Removing Masses . . . . .	55
6.3.2	Vertical Residual Damping . . . . .	56
6.3.3	Longitudinal Tyre Stiffness for Soil . . . . .	56
6.4	Friction limit . . . . .	56
6.5	Optimising the S-function . . . . .	56
6.6	Real World Test Data . . . . .	56
<b>7</b>	<b>Conclusion</b>	<b>57</b>
	<b>References</b>	<b>58</b>
	<b>A Straight Line Acceleration Test</b>	<b>a</b>
	<b>B Step-Steer Test</b>	<b>c</b>
	<b>C Zigzag Test</b>	<b>e</b>
	<b>D Rigid Ring Tyre Model Parameter Values Used in This Project</b>	<b>g</b>

# 1 Introduction

One of the tools Volvo GTT uses to model the dynamic response of their trucks is VTM(Virtual Transport Models). One shortcoming with this tool is that it cannot take certain road conditions into account. Volvo GTT are, in collaboration with, the University of Ontario Institute of Technology, developing a tyre/ground model for soft soil road conditions but it is not implemented in VTM. The tyre model is based on FEM and Volvo requires a simplified model, called the rigid ring tyre model, to be implemented in VTM.

VTM uses rigid body dynamics in combination with spring, damper and mass elements. A VTM vehicle model takes steering wheel angle, driving torques and road topology as inputs and outputs full body dynamics of the vehicle.

## 1.1 Background

This project acts as a continuation and implementation of a collaboration with Volvo GTT and the University of Ontario Institute of Technology [1–9]. The project treats different tyre models, FEM-tyre and Rigid ring tyre model, in soft soil terrain. The soft soil has been simulated using both FEM(Finite Element Method) and SPH(Smoothed Particle Hydrodynamics) and compared with the studies of Wong [10]. The research collaboration has gone through different phases and what is of relevance starts in phase five. A small description of the relevant phases are given below:

- **Phase V:** Here the goal was to validate a newly developed FE soft soil model for two types of soils: a hard, dry soil and a sandy soil. The hard, dry soil was validated by comparing principle stresses, contours and sinkage to theoretical data, a good match was found. For sandy soil a rolling rigid wheel test was used and the shear and normal stresses were compared to experimental tests. Calibrating the soft sand was found to be difficult due to the low cohesion of the of the dry sand. A good approximation for sandy loam was however found.
- **Phase VI/VII:** In these phases the goal was to translate the FE soft soil model to a rigid ring tyre model and determine model parameters.
- **Phase VIII:** With the introduction of SPH-modelling soil parameters will now be estimated using a combination of results from SPH, FEA(Finite Element Analysis) and theoretical and experimental data. In the last part of this phase - five soils of interest are picked. One of which is the Clayey soil (Thailand), which will be used in this project. The FE- and SPH-model of this soil is compared with experimental data from Wong [10].
- **Phase XII:** In this phase parameters of the rigid ring tyre model for the five soils of interest are to be determined. They are found using the calibrated FE-models using the same procedure as in phase vi/vii.

## 1.2 Project Motivation

Volvo GTT cannot simulate soft soil ground conditions such as mud, clay and sand, in their Simulink based VTM-tool. A lot of their products typical use cases take place on non rigid ground, thus causing uncertainties in their dynamic behaviour. Volvo wants a more precise tyre model for the full vehicle model to capture the correct dynamic behaviour.

Soft soil can rather successfully be simulated using FEA with PAM-SHOCK solid elastic-plastic materials with element elimination as detailed in [5–7]. Simulations using SPH has also been conducted with successful results, these however, require considerably more computational power. To able to implement the soft soil tyre/ground model in VTM substantial simplifications are needed as both the other models are too computationally expensive. The simplified model is called the rigid ring tyre model and is a simple rigid ring using springs and dampers to control dynamic properties. This simplified model is not yet implemented in VTM and therefore the program can not take soft soil ground into account as of now.

### **1.3 Envisioned Solution**

Implement the rigid ring tyre model in combination with the soft soil model in VTM, as detailed in the progress reports [1–9]. The results from this implemented model will be studied to investigate possible improvements and modifications.

### **1.4 Objective**

A simplification of the FE tyre/soil model, called rigid ring model, with Clayey soil (Thailand) as soil shall be implemented in VTM and the results will be verified against the FE soil models and a VTM model using a rigid ground tyre model.

### **1.5 Deliverables**

To reach the objective of this project a list of deliverables was compiled.

1. Rigid ring tyre model for rigid ground implemented in VTM.
2. Rigid ring tyre model for rigid ground implementation verified.
3. Rigid ring tyre model for soft soil ground implemented in VTM.
4. Rigid ring tyre model for soft soil ground implementation verified.

### **1.6 Limitations**

The following limitations are set up to narrow the scope of the project:

1. No other model than the rigid ring tyre model will be investigated.
2. Only the soil investigated in progress report phase XII [8], Clayey Soil Thailand, is investigated in this project.
3. Ground memory, i.e. ground changes from tyre roll over, will be disregarded.
4. Only flat ground will be considered in the verifying simulations.
5. There are limiting amounts of real world test data to compare with and no physical tests to collect experimental data will be conducted.

6. No verification of the surrounding Simulink models will be conducted.
7. The velocity range of which the model must be working was set to 5-25 km/h as this is the typical range in which the vehicle operates on soft soil.
8. No combined slip model is targeted

## 1.7 Method

A literature study of the previous work has been carried out to get an overview of what has been done. The previous work consists of progress reports from previous projects [1–9]. The list of deliverables will be used as a check list to get an overview of the progress.

To implement the rigid ring tyre model for rigid and soft soil ground the VTM Simulink modules controlling ground/tyre characteristics will need to be modified.

The implementation of the rigid ring tyre model in VTM will be verified in two stages:

1. The rigid ring tyre model will be implemented without the soft soil additions. This model will be verified against the existing PAC2002 tyre model [11] by comparing the behaviour of the models. The implementation will be deemed verified when forces, slips and velocities show similar behaviour and magnitude. What lies within an acceptable fit will be discussed with the supervisor at Volvo. The model will also be verified by constructing similar simulations to those detailed in phase XII [8] using a single tyre model disconnected from the complete vehicle.
2. The soft soil implementation of the rigid ring model will be verified by constructing similar simulations to those detailed in the phase XII [8]. Here forces and displacements will be compared to FEA results. Additional simulations for verification will be provided from the University of Ontario Institute of Technology.

To verify complete vehicle dynamics for the different models a set of manoeuvres will be simulated with all models, rigid ring on rigid and soft soil ground and the currently implemented tyre model.

### 1.7.1 Single Tyre Simulations for Verification

To verify certain aspects of the tyre characteristics simulations taken from progress report phase XII [8] will be recreated in Simulink for an independent single tyre. In the previous work forces are applied as initial conditions and continued until the model reaches steady state, the forces are then suddenly released making the tyre oscillate. For the oscillations to match in Simulink stiffness, damping and mass need to be correct. In VTM it is easier to set the steady state position or angle as initial conditions instead and this is done for most cases. From the progress reports two standard vertical loads on the wheel centre has been used, 13.3 kN (3000 lbs) and 26.7 kN (6000 lbs). The 26.7 kN load is comparable to a small trucks load level while the 13.3 kN load is somewhat low for real world applications.

#### Rigid Ground

##### Vertical Stiffness

To verify the total vertical stiffness a static load is applied to the wheel rim of the tyre. By pressing the tyre into the rigid ground and measure the rim translation, the stiffness of the tyre can be verified.

The longitudinal and lateral part of the model is neglected in this simulation. A representation of the simulation can be seen in Figure 1.1.

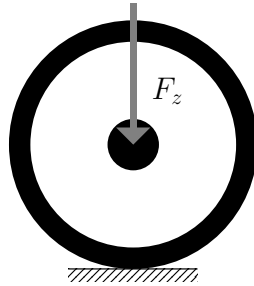


Figure 1.1: *Representation of the simulation for verifying the total vertical tyre stiffness.*

### Vertical Damping

The simulation to verify the vertical damping characteristics is a drop test simulation. The tyre is dropped from a height and the vertical displacement of the tyre is plotted over time. By measuring the decrease in oscillations the damping can be calculated. The longitudinal and lateral part of the model is neglected in this simulation. A representation of the simulation can be seen in Figure 1.2.

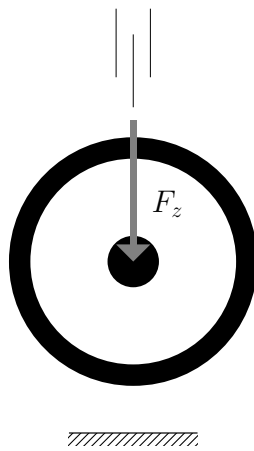


Figure 1.2: *Representation of the drop test simulation for verifying the total vertical tyre damping.*

### Wheel Plane Rotational Stiffness & Damping

To verify the wheel plane rotational components an initial condition of the tyre belt wheel plane angle, is set to non-zero while the rim of the tyre is fully constrained. When the simulation starts the tyre will start to oscillate because of the rotational stiffness and damping. The spring force is verified by comparing the force as it is fully wound up and the damping can be calculated by measuring the decrease in oscillations over time. A representation of the simulation can be seen in Figure 1.3.

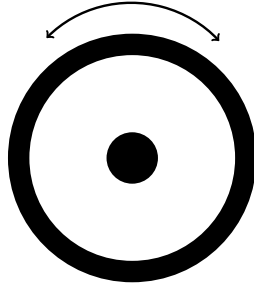


Figure 1.3: *Representation of the simulation for verifying the wheel plane rotational properties of the sidewall.*

### Longitudinal Tread & Tyre Stiffness

The longitudinal tread and tyre stiffness is verified by applying a driving torque on the wheel rim, which will accelerate the tyre. The wheel will develop slip since the rotational speed initially increases more than the longitudinal velocity. The driving torque is applied until 100% slip is reached and then terminated. By comparing the force generated in the slip model with the longitudinal slip, their relation can be found. A representation of the simulation can be seen in Figure 1.4.

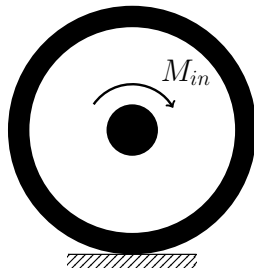


Figure 1.4: *Representation of the simulation for verifying tread and tyre stiffness in longitudinal direction.*

### Lateral Translational Stiffness & Damping

In this simulation the tyre rim is fully constrained. The initial condition on the lateral position of the tread is set to non-zero. By measuring the decrease in oscillations over time and compare with FE-model results these parameters can be verified. A representation of the simulation can be seen in Figure 1.5.

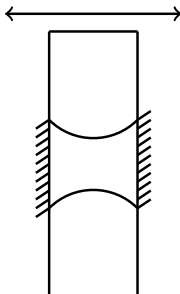


Figure 1.5: *Representation of the simulation for verifying the sidewall properties in lateral direction.*

### Out of Wheel Plane Rotational Stiffness & Damping

This simulation is carried out in the same way as for the wheel plane rotation, only now it is the out

of plane angle of the sidewall,  $\gamma_2$ , that has a non-zero initial condition. The out of plane angular oscillation is logged and the parameters can be verified.

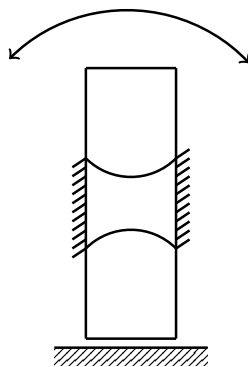


Figure 1.6: Representation of the simulation for verifying the out of wheel plane rotational properties of the sidewall.

### Cornering Stiffness

By setting a speed in a direction off from the longitudinal direction the cornering stiffness can be verified. By comparing the lateral force against the lateral slip the cornering stiffness can simply be found as the constant between them as it is modelled linearly.

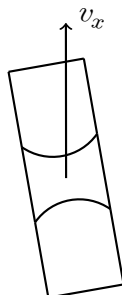


Figure 1.7: Representation of the simulation for verifying the cornering stiffness of the tyre.

### Soft Soil Ground

In the longitudinal and lateral direction the only difference between the rigid and soft soil ground implementation are the parameter values. Therefore no new tests for these are constructed.

In the vertical direction the model changes and a new test is needed. To check the soil parameters the vertical displacement of the tyre when driving at different longitudinal velocities with different loads is investigated.

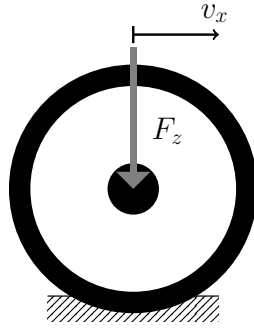


Figure 1.8: *Representation of the simulation for verifying various soil properties.*

## 1.7.2 Complete Vehicle Simulations

To verify the implementation of the tyre model in the complete vehicle, VTM simulations are needed to be constructed. Four simple manoeuvres were set up and simulated and the results from the currently implemented model and the rigid ring model, with and without soft soil, was compared.

### **Straight line acceleration test**

In the acceleration test a driving moment is applied and the vehicle starts to accelerate. By comparing the results the full vehicle longitudinal properties can be investigated.

### **Step-steer test**

To test the cornering behaviour of the models a step-steer test is constructed. By applying a steering angle and comparing the resulting forces the dynamic behaviour while turning can be investigated.

### **Zigzag test**

To further test the cornering behaviour of the models a more extreme turning test was introduced. By applying a step steer angle in one direction to be followed by a steering angle in the other direction the turning capabilities could be further tested beyond the previous step-steer test.

### **Figure-8 test**

The last test tries to incorporate all of the above aspects into one manoeuvre. While trying to maintain a constant speed the vehicle is driven in a figure-8. This will test both longitudinal and lateral properties in one test and not separate them as in the previous tests.

## 2 Tyre Modelling

The Simulink based tool VTM is assembled using several different modules. For this project the module of interest is the tyre module which contains the tyre and ground model. The currently implemented model is based on the magic tyre formula developed by Pacejka [11]. The new model that is to be implemented is called the rigid ring model. These both models will be implemented as S-functions(state space functions) in Simulink.

### 2.1 VTM

VTM uses rigid body dynamics in combination with spring, damper and mass elements. The program takes input such as steering angle, driving torque, and road topology. From this the full body dynamics of the vehicle is computed. VTM consists of different modules and a complete vehicle model consists of primarily six different modules; Cab, Chassis frame, load carrier, steered axles, non-steered axles and tyres. This project focuses on the tyre model which acts in the tyre module which therefore is the module that will be focused on. To be able to incorporate the tyre model efficiently without restructuring the entire program, the inputs and outputs of the tyre module will stay the same. The inputs to the tyre modules are:

- The wheel rim's three translational velocities
- The driving torque
- Road vertical position
- Road slopes, (pitch and roll)
- Scaling coefficients

The outputs consist of:

- Axle forces in all three directions
- Moment around the axle end around all three axis
- Wheel rotational speed
- Longitudinal and lateral slip
- The effective tyre radius

The scaling coefficients input will however not be needed in the new rigid ring tyre model. A representation of the tyre with all inputs and outputs can be seen in Figure 2.1, inputs are blue and outputs are red.

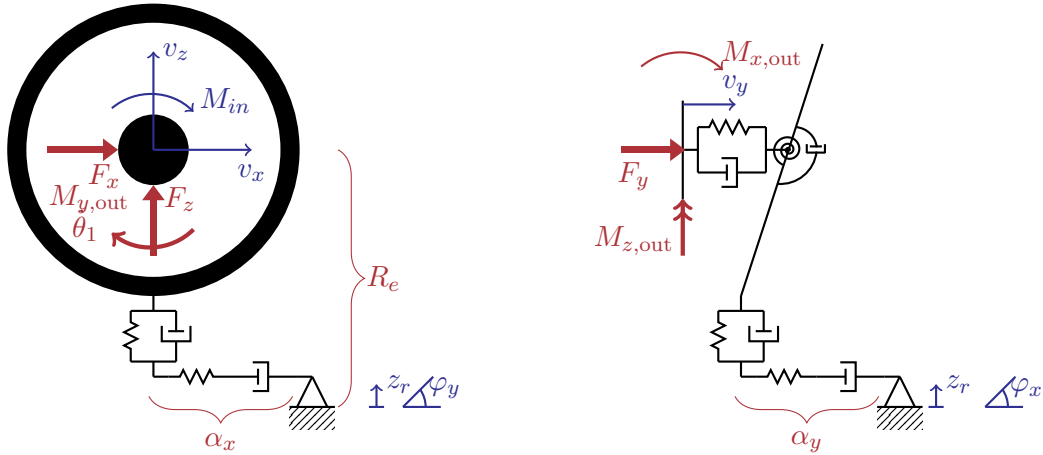


Figure 2.1: *Inputs and outputs of the rigid ring tyre model.*

## 2.2 S-functions

The tyre models are implemented as state space functions using Simulink's S-Function API. The general non-linear state space formulation can be seen below in equation 2.1.

$$\begin{aligned}\dot{\mathbf{x}}(t) &= \mathbf{f}(t, \mathbf{x}(t), \mathbf{u}(t)) \\ \mathbf{y}(t) &= \mathbf{h}(t, \mathbf{x}(t), \mathbf{u}(t))\end{aligned}\tag{2.1}$$

Where:  $\mathbf{x}$  represents the state vector  
 $\mathbf{y}$  represents the output vector  
 $\mathbf{u}$  represents the input vector  
 $\mathbf{f}$  represents the state equation  
 $\mathbf{h}$  represents the output equation

The first thing the S-function does is to read the input vector along with several constants. In the next step the output vector is calculated using the constants, states and input vector. In the first time step all states will be given an initial condition since the state vector derivative  $\dot{\mathbf{x}}(t)$  has not yet been defined. In the last step the state vector derivative is constructed which updates the states for the new time step.

S-functions in Simulink can be written in a number of programming languages and the S-function in this project will be written in C due to Volvo's preferences.

## 2.3 Present Tyre Model "PAC2002"

The currently implemented tyre model consists of the semi empirical model PAC2002 [11], which has only been developed to work for rigid ground. This model is developed by MSC Software and is based on Hans B. Pacejka's magic tyre formula which connects wheel slips to longitudinal and lateral forces. In this model the vertical force is modelled as a single spring and damper in parallel.

In the currently implemented model there is an error in the longitudinal slip which means that this property can not be compared between the models. Additionally the rolling resistance moment,

around the y-axis, and overturning moment, around the x-axis, are set to zero. In Figure 2.2 one can see a simple representation of the present tyre model.

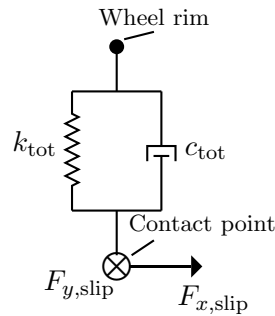


Figure 2.2: *Simple representation of the PAC2002-model*

## 2.4 Rigid Ring Tyre Model, Rigid Ground

The tyre model that is to be implemented in VTM is called the rigid ring tyre model. It consists of two rigid rings that are connected to each other via springs and dampers. The inner ring has the mass and inertia of the rim and inner part of the sidewall and the other ring has the mass and inertia of tyre belt and outer part of the sidewall. The springs and dampers between the two rings represent the elastic sidewall. The large deformation in the contact point will yield additional dynamics and a vertical residual spring and damper are added to the vertical model. This model uses the same inputs and outputs as the currently implemented model. However, whereas "PAC2002" is a semi empirical model the rigid ring tyre model is a completely physical model. An overview of the model can be seen in Figure 2.3.

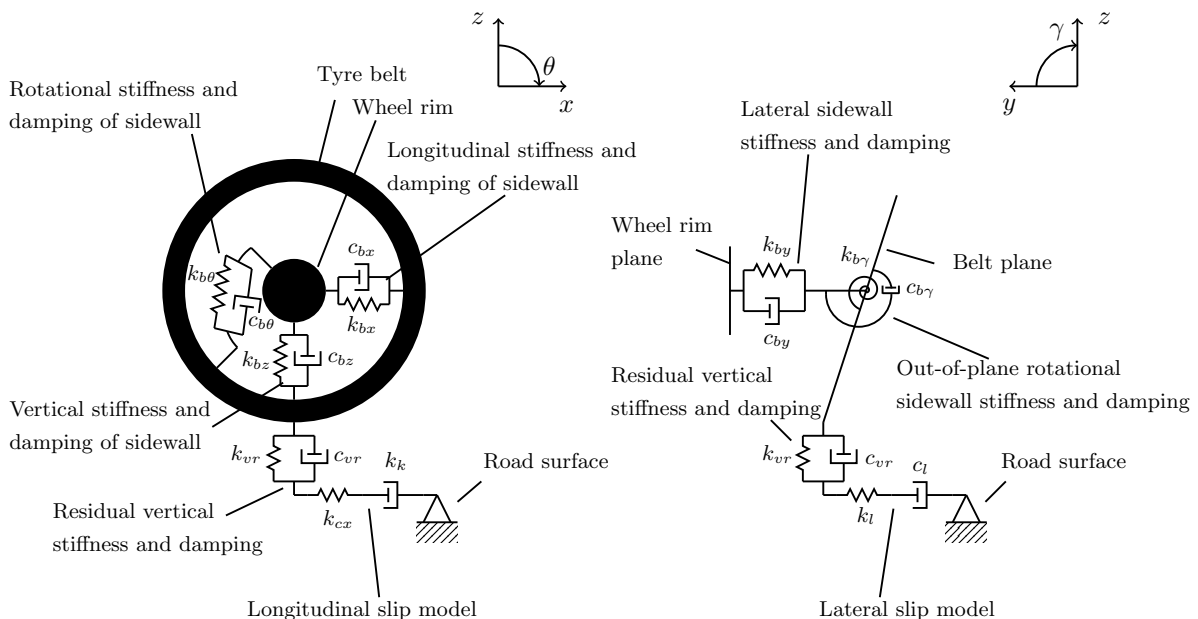


Figure 2.3: *Representation of the wheel plane (left) and out of plane (right) rigid ring model on rigid ground.*

### 2.4.1 Vertical Reaction Force

In the vertical direction there are two sets of a springs and dampers in parallel which are connected in series, see Figure 2.4.

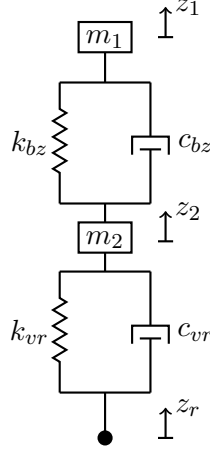


Figure 2.4: Representation of the vertical part of the rigid ring model on rigid ground. Here  $m_2$  and the separation of  $\bullet_{bz}$  and  $\bullet_{vr}$  parameters are new in the rigid ring model.

This yields the system of differential equations seen in equation 2.2.

$$\begin{bmatrix} 0 \\ 0 \\ 0 \end{bmatrix} = \begin{bmatrix} k_{bz} & -k_{bz} & 0 \\ -k_{bz} & k_{bz} + k_{vr} & -k_{vr} \\ 0 & -k_{vr} & k_{vr} \end{bmatrix} \begin{bmatrix} z_1 \\ z_2 \\ z_r \end{bmatrix} + \begin{bmatrix} c_{bz} & -c_{bz} & 0 \\ -c_{bz} & c_{bz} + c_{vr} & -c_{vr} \\ 0 & -c_{vr} & c_{vr} \end{bmatrix} \begin{bmatrix} \dot{z}_1 \\ \dot{z}_2 \\ \dot{z}_r \end{bmatrix} + \begin{bmatrix} m_1 & 0 & 0 \\ 0 & m_2 & 0 \\ 0 & 0 & 0 \end{bmatrix} \begin{bmatrix} \ddot{z}_1 \\ \ddot{z}_2 \\ \ddot{z}_r \end{bmatrix} \quad (2.2)$$

Where  $z_1$  is the position of the wheel rim,  $z_2$  is the position where the tyre tread begins and  $z_r$  is the position of the road.  $z_r$  and  $\dot{z}_r$  are known as the road is predefined and used as an input.  $z_1$  is considered known as  $\dot{z}_1$  is equal to  $v_z$  which is an input.  $m_1$  is the mass of the wheel rim and  $m_2$  is the mass of the tyre belt. For the complete vehicle model  $m_1$  is in addition to the mass of the rim also the mass of the wheel axle divided by the number of tyres on the axle, this is modelled outside the tyre model as well as the downwards force of the truck. The middle equation in 2.2 can be written as second order differential equation as seen in equation 2.3.

$$\underbrace{k_{vr}z_r + c_{vr}\dot{z}_r + k_{bz}z_1 + c_{bz}\dot{z}_1}_{A_z} = \underbrace{(k_{bz} + k_{vr})}_{B_z} z_2 + \underbrace{(c_{bz} + c_{vr})}_{C_z} \dot{z}_2 + m_2 \ddot{z}_2 \quad (2.3)$$

This equation can be rearranged to suit the general state space formulation and implemented in the S-Function by setting  $z_2$  and  $\dot{z}_2$  to states:

$$\ddot{z}_2 = \frac{A_z - B_z z_2 - C_z \dot{z}_2}{m_2} \quad (2.4)$$

From this  $\dot{z}_2$  and  $z_2$  can be found and inserting this in the first equation in 2.2 gives the vertical reaction force as in equation 2.5.

$$m_1 \ddot{z}_1 = F_z = k_{bz}(z_2 - z_1) + c_{bz}(\dot{z}_2 - \dot{z}_1) \quad (2.5)$$

## 2.4.2 Longitudinal Reaction Force

The longitudinal reaction force is calculated in two steps. The first step is to calculate the force generated by the longitudinal slip model, this force acts on the tyre sidewall. The second step is to calculate the force generated in the sidewall which acts on the rim. The force from the slip model,  $F_{sx}$ , is driven by the longitudinal slip,  $\alpha_x$ , and the tyre tread deformation,  $u_x$ , see Figure 2.5.

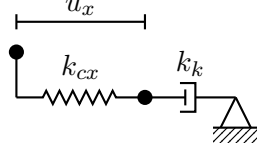


Figure 2.5: Representation of the longitudinal slip model belonging to the rigid ring model.

The longitudinal slip is defined as in equation 2.6.

$$\alpha_x = \frac{V_c}{v_x} \quad (2.6)$$

$$V_c = R_e \dot{\theta}_2 - v_x$$

where  $V_c$  is the velocity at the contact point,  $R_e = R_0 - (z_r - z_1)$  is the effective radius and  $R_0$  is the unloaded wheel radius.

The tyre tread deformation is the deformation of the spring denoted as  $k_{cx}$  and the slip acts on the damper denoted as  $k_k$ , see Figure 2.5. In steady state the force from the slip model can be defined in two ways:

$$F_{sx} = -k_k \alpha_x \quad (2.7)$$

$$F_{sx} = k_{cx} u_x \quad (2.8)$$

When steady state is not applicable the variation of  $u_x$  needs to be taken into account in the longitudinal slip changing equation 2.6 into:

$$\alpha_x = \frac{V_c + \dot{u}_x}{v_x} \quad (2.9)$$

By eliminating  $F_{sx}$  using equation 2.7 and 2.8 the following differential equation is obtained:

$$k_{cx} u_x = -k_k \cdot \frac{V_c + \dot{u}_x}{v_x} \quad (2.10)$$

Rearranging this equation suitable for state space implementation gives the following equation which can be implemented in the S-function, with  $u_x$  as a state:

$$\dot{u}_x = -v_x \frac{k_{cx}}{k_k} \cdot u_x - V_c \quad (2.11)$$

By inserting  $u_x$  into equation 2.8 the longitudinal force generated from the slip model can be found.

Since the slip force is modelled with a linear relation to the slip, the force needs to be saturated at a certain value. This value is chosen to better fit the non-linear nature of the slip/force relation. From FE-model simulation data these saturation values could be approximated for the two standard vertical loads 13.3 kN and 26.7 kN by calculating the mean force after the point where the tyre stiffness is no

longer considered linear. This happens around 15% slip for the lower load which resulted in a value of 9.6 kN and at 20% slip for the higher load which resulted in a value of 19.3 kN. See Figure 2.6 for the FEA simulation data and the approximated saturation value.

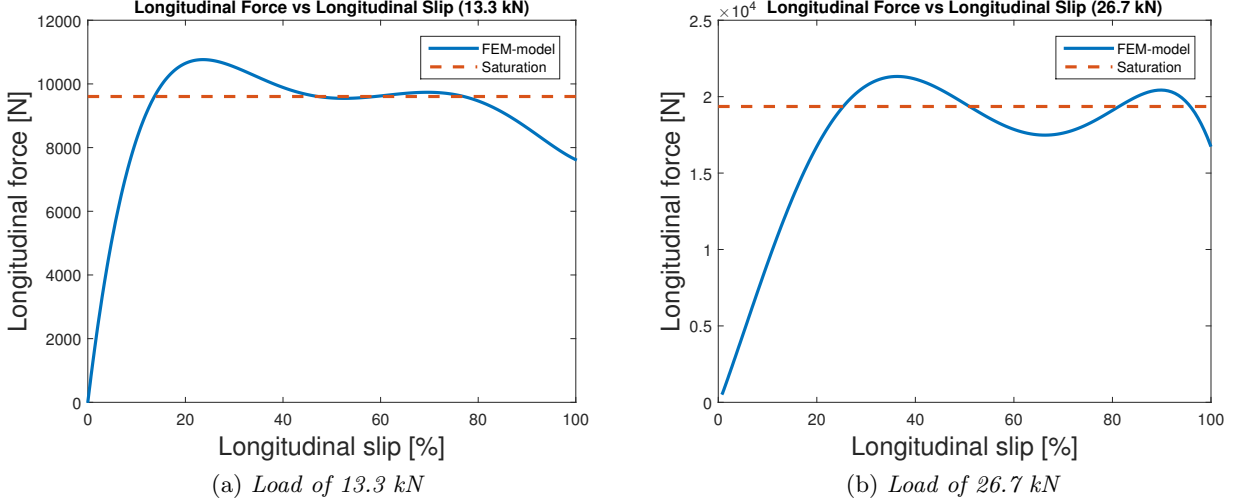


Figure 2.6: The longitudinal slip/force relation captured in the FEM-simulations of a transient acceleration test for two different loads, with saturation limits marked.

The force generated in the sidewall,  $F_{wx}$ , is driven by the velocity and displacement in the rim,  $x_1$ , and the tread,  $x_2$ , as well as the force from the slip model,  $F_{sx}$ , see Figure 2.7.

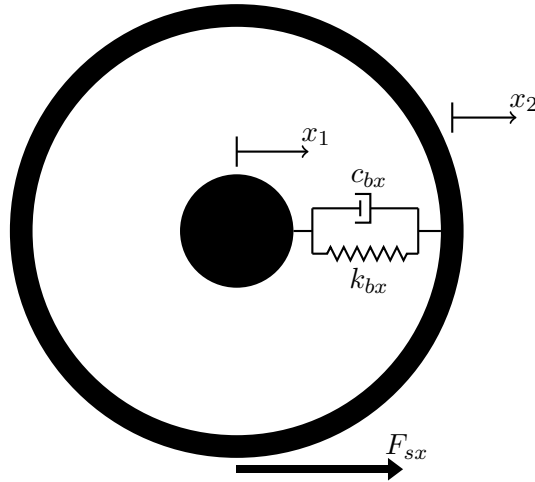


Figure 2.7: Representation of the two rigid rings in longitudinal direction.

From this the system of equations can be formulated as seen in equation 2.12.

$$\begin{bmatrix} 0 \\ F_{sx} \end{bmatrix} = \begin{bmatrix} k_{bx} & -k_{bx} \\ -k_{bx} & k_{bx} \end{bmatrix} \begin{bmatrix} x_1 \\ x_2 \end{bmatrix} + \begin{bmatrix} c_{bx} & -c_{bx} \\ -c_{bx} & c_{bx} \end{bmatrix} \begin{bmatrix} \dot{x}_1 \\ \dot{x}_2 \end{bmatrix} + \begin{bmatrix} m_1 & 0 \\ 0 & m_2 \end{bmatrix} \begin{bmatrix} \ddot{x}_1 \\ \ddot{x}_2 \end{bmatrix} \quad (2.12)$$

where  $m_1$  is the mass of the tyre rim and  $m_2$  is the mass of the tyre belt. For the complete vehicle model the mass of the wheel rim,  $m_1$ , will not be enough. In addition the axle mass divided by the number of tyres on the axle needs to be added, this is modelled outside of the tyre model.

The force acting on the rim,  $F_x$ , and the force acting on the tyre belt,  $F_{wx}$ , can be calculated as:

$$F_x = m_1 \ddot{x}_1 = k_{bx}(x_2 - x_1) + c_{bx}(\dot{x}_2 - \dot{x}_1) \quad (2.13)$$

$$F_{wx} = m_2 \ddot{x}_2 = F_{sx} - F_x \quad (2.14)$$

The velocity of the rim,  $\dot{x}_1$ , is the longitudinal velocity,  $v_x$ , which is one of the inputs, and the rims position,  $x_1$  is assigned as a state and updated with this velocity in each time step. The velocity of the tread is updated by calculating the acceleration of the tread, see equation 2.15, and the position is updated using the velocity. The tread position and velocity are therefore set as states.

$$\ddot{x}_2 = \frac{F_{wx}}{m_2} \quad (2.15)$$

### 2.4.3 Wheel Plane Rotational Reaction Moment

There are two wheel plane rotational degrees of freedom, see Figure 2.8. The rotation of the wheel rim,  $\theta_1$ , and the tyre belt,  $\theta_2$ . Between these a spring and damper works in parallel. In addition the longitudinal slip force,  $F_{sx}$ , acts on the bottom of the tyre belt, thus giving a rotational moment on the outer belt.

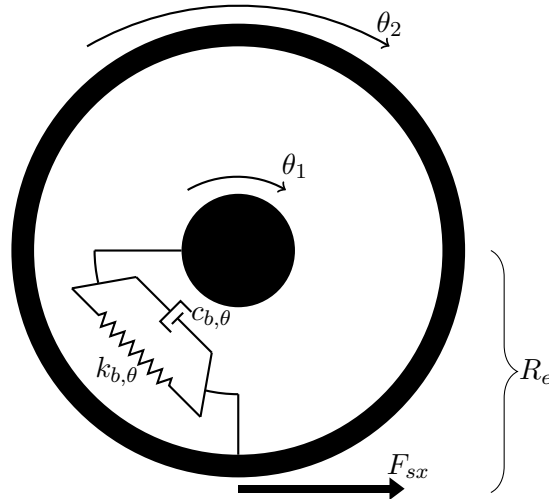


Figure 2.8: Representation of the rigid rings wheel plane rotational properties.

The equation system for the wheel plane rotation can be seen in equation 2.16.

$$\begin{bmatrix} M_{in} \\ -F_{sx} \cdot R_e \end{bmatrix} = \begin{bmatrix} k_{b\theta} & -k_{b\theta} \\ -k_{b\theta} & k_{b\theta} \end{bmatrix} \begin{bmatrix} \theta_1 \\ \theta_2 \end{bmatrix} + \begin{bmatrix} c_{b\theta} & -c_{b\theta} \\ -c_{b\theta} & c_{b\theta} \end{bmatrix} \begin{bmatrix} \dot{\theta}_1 \\ \dot{\theta}_2 \end{bmatrix} + \begin{bmatrix} I_{1y} & 0 \\ 0 & I_{2y} \end{bmatrix} \begin{bmatrix} \ddot{\theta}_1 \\ \ddot{\theta}_2 \end{bmatrix} \quad (2.16)$$

Where  $M_{in}$  is the driving torque,  $I_{1y}$  is the wheel plane moment of inertia of the rim and  $I_{2y}$  is the wheel plane moment of inertia of the belt. In the complete vehicle model the inertia from the wheel axle, divided by the number of tyres on the axle, needs to be included in  $I_{1y}$  as well.

From the system of equations the moments acting on the rim,  $M_{y,r}$ , and the tyre tread,  $M_{y,b}$ , can be found as:

$$I_{1y} \ddot{\theta}_1 = k_{b\theta}(\theta_2 - \theta_1) + c_{b\theta}(\dot{\theta}_2 - \dot{\theta}_1) + M_{in} = M_{y,r} \quad (2.17)$$

$$I_{2y} \ddot{\theta}_2 = k_{b\theta}(\theta_1 - \theta_2) + c_{b\theta}(\dot{\theta}_1 - \dot{\theta}_2) - F_{sx} \cdot R_e = M_{y,b} \quad (2.18)$$

The angle is updated with the angular velocity in each time step and the angular velocity is updated with the angular acceleration which can be seen in Equation 2.19 and 2.20. Therefore the two angles and the angular velocities are set as states.

$$\ddot{\theta}_1 = \frac{M_{y,r}}{I_{1y}} \quad (2.19)$$

$$\ddot{\theta}_2 = \frac{M_{y,b}}{I_{2y}} \quad (2.20)$$

#### 2.4.4 Lateral Reaction Force

The force generated in the lateral direction is divided into two parts as well. The force generated in slip model,  $F_{sy}$ , is calculated directly from the lateral slip angle,  $\alpha_y$ , by multiplying with the cornering stiffness,  $k_f$ .

$$F_{sy} = k_f \alpha_y \quad (2.21)$$

In steady state the slip angle is defined as  $\alpha_y = \frac{V_y}{V_x}$ , when steady state is not applicable the relaxation length of the tyre,  $\sigma$ , needs to be taken into consideration. This has been calculated from the spring and damper in the lateral slip model in previous work [8]. Using the relaxation length the following differential equation can be formulated:

$$\alpha_y + \frac{\sigma}{v_x} \dot{\alpha}_y = -\frac{v_y}{v_x} \quad (2.22)$$

By rearranging the equation suitable for state space implementation the lateral slip update can be implemented in the S-function. The rearranged equation can be seen below with  $\alpha_y$  as a state:

$$\dot{\alpha}_y = -\frac{v_x}{\sigma} \cdot \alpha_y - \frac{v_y}{\sigma} \quad (2.23)$$

Again the slip force is saturated in the same way as for the longitudinal direction since the non-linear force slip relation is modelled as bilinear, see Figure 2.9. For 13.3 kN vertical load the mean value was taken from the forces corresponding to a slip angle over  $4^\circ$  resulting in a saturation value of 8.5 kN. For 26.7 kN vertical load the slip angle limit was chosen to  $5^\circ$  and the saturation value resulted in 17 kN.

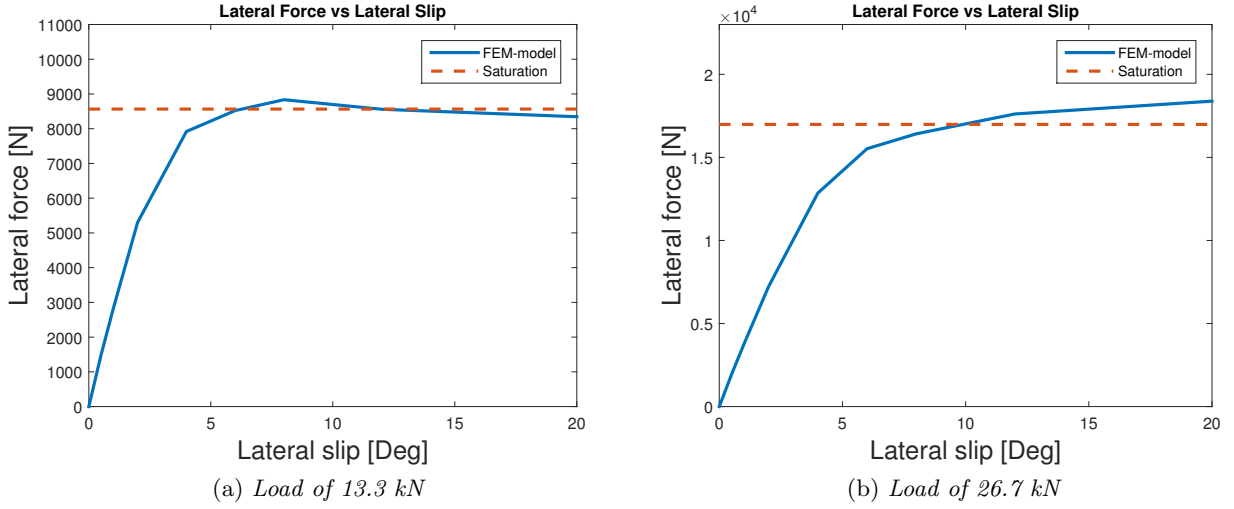


Figure 2.9: The lateral slip/force relation captured in the FEM-simulations for two different loads, with saturation limits marked.

The force generated in the tyre belt in the lateral direction is calculated in the same fashion as in the longitudinal direction, as is the update of the the states.

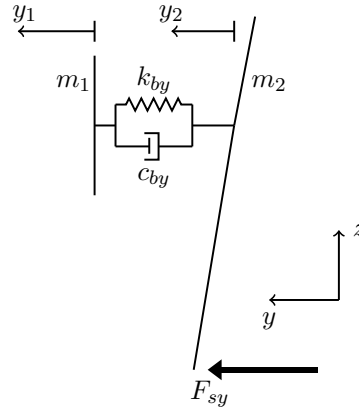


Figure 2.10: Representation of the two rigid rings in lateral direction.

The resulting system of equations can be seen in equation 2.24.

$$\begin{bmatrix} 0 \\ F_{sy} \end{bmatrix} = \begin{bmatrix} k_{by} & -k_{by} \\ -k_{by} & k_{by} \end{bmatrix} \begin{bmatrix} y_1 \\ y_2 \end{bmatrix} + \begin{bmatrix} c_{by} & -c_{by} \\ -c_{by} & c_{by} \end{bmatrix} \begin{bmatrix} \dot{y}_1 \\ \dot{y}_2 \end{bmatrix} + \begin{bmatrix} m_1 & 0 \\ 0 & m_2 \end{bmatrix} \begin{bmatrix} \ddot{y}_1 \\ \ddot{y}_2 \end{bmatrix} \quad (2.24)$$

Again, for the complete vehicle model the mass,  $m_1$ , is modelled outside the tyre model.

From this the force acting on the rim,  $F_y$ , and on the sidewall,  $F_{wy}$ , can be calculated as:

$$F_y = m_1 \ddot{y}_1 = k_{by}(y_2 - y_1) + c_{by}(\dot{y}_2 - \dot{y}_1) \quad (2.25)$$

$$F_{wy} = m_2 \ddot{y}_2 = F_{sy} - F_y \quad (2.26)$$

As for the longitudinal direction the tyre tread acceleration in lateral direction needs to be calculated

to update the states  $y_2$  and  $\dot{y}_2$  of the wheel:

$$\ddot{y}_2 = \frac{F_{wy}}{m_2} \quad (2.27)$$

### 2.4.5 Out of Wheel Plane Rotational Reaction Moment

The out of plane rotational reaction moment works the same as for wheel plane with a parallel spring and damper. As the wheel rim does not rotate out of plane the only angle is the belt angle,  $\gamma_2$ , and angular velocity,  $\dot{\gamma}_2$ .

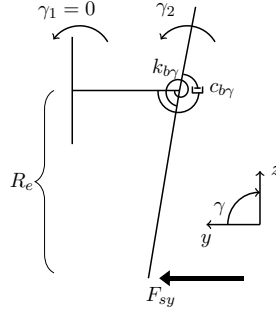


Figure 2.11: Representation of the rigid rings out of wheel plane rotational properties.

The moment equilibrium equation can be expressed as:

$$-F_{sy}R_e = k_{b\gamma}\gamma_2 + c_{b\gamma}\dot{\gamma}_2 + I_{2x}\ddot{\gamma}_2 \quad (2.28)$$

where the angle,  $\gamma_2$ , is updated with the angular velocity,  $\dot{\gamma}_2$ , which in turn is updated with the angular acceleration,  $\ddot{\gamma}_2$ , and can be obtained from moment equilibrium along with the moment acting on the wheel rim, as in equation 2.28. Here the angle and the angular velocity are assigned as states.

$$I_{2x}\ddot{\gamma}_2 = -F_{sy} \cdot R_e - k_{b\gamma}\gamma_2 - c_{b\gamma}\dot{\gamma}_2 = M_x \quad (2.29)$$

$$\ddot{\gamma}_2 = \frac{M_x}{I_{2x}} \quad (2.30)$$

Here  $I_{2x}$  is the out of wheel plane moment of inertia of the belt.

## 2.5 Rigid Ring Tyre Model, Soft Soil Ground

To take soft ground into consideration the model needs to be expanded. The ground and the tyre interacts at the contact point and this is where the model needs to be expanded. An illustration of the soft soil model can be seen in Figure 2.12. In addition to the rigid ground model a new set of spring and damper in parallel is added. The damper in the new block is connected to an additional spring in series.

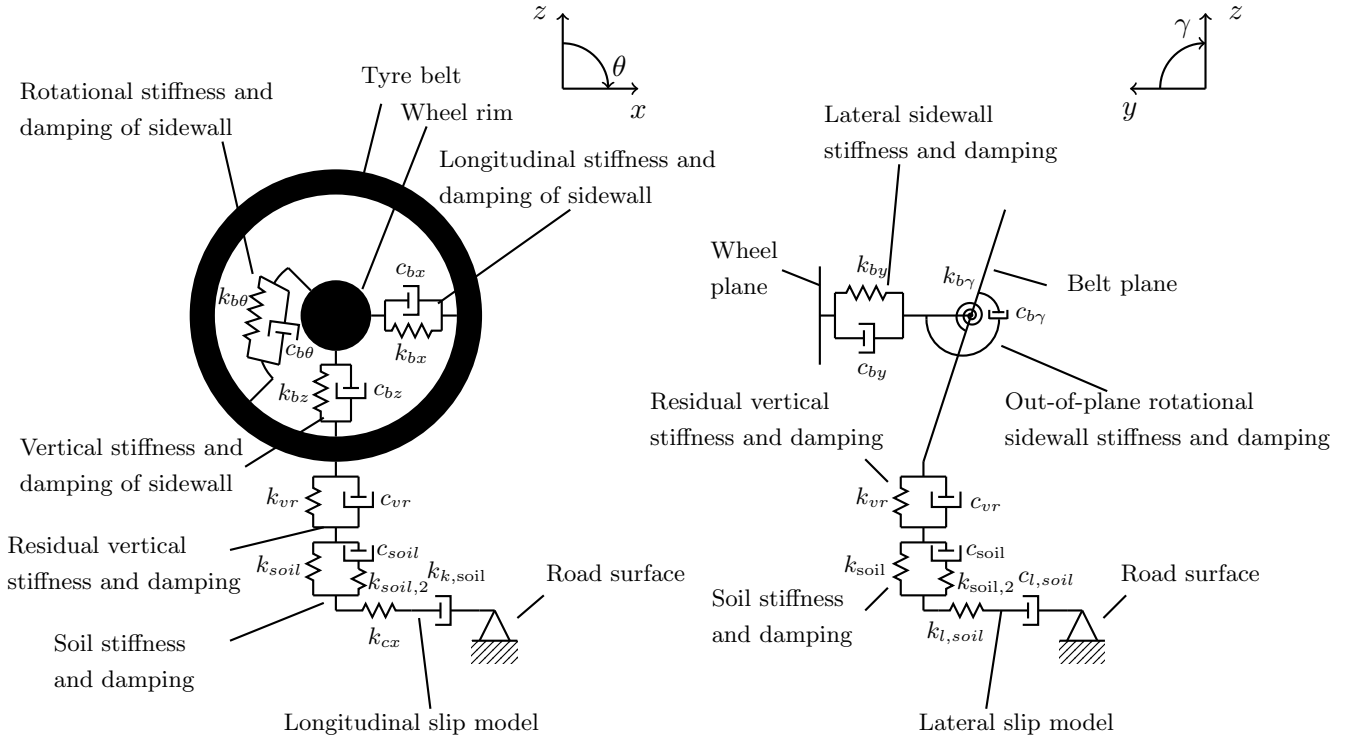


Figure 2.12: Representation of the the wheel plane (left) and out of plane (right) rigid ring model on soft soil ground.

### 2.5.1 Vertical Reaction Force

In the vertical direction the soil is modelled by expanding the rigid ground model. Initially the model only contained an extra spring,  $k_{soil}$ , as seen to the left in Figure 2.13. It was quickly found that this model was too crude. The soil needed a damping component,  $c_{soil}$ , as well as fictive mass,  $m_{soil}$ , to give the soil deformation an appropriate inertia [12]. Later on it was found that the damping was dependent on the longitudinal velocity. For different longitudinal velocities the oscillation of the sinkage,  $\omega(v_x)$ , was different. The damping could therefore be managed by changing the damper to a spring and damper in series instead [10] which then gives a damping dependent on the longitudinal velocity which is needed. The expanded model can be seen to the right in Figure 2.13.

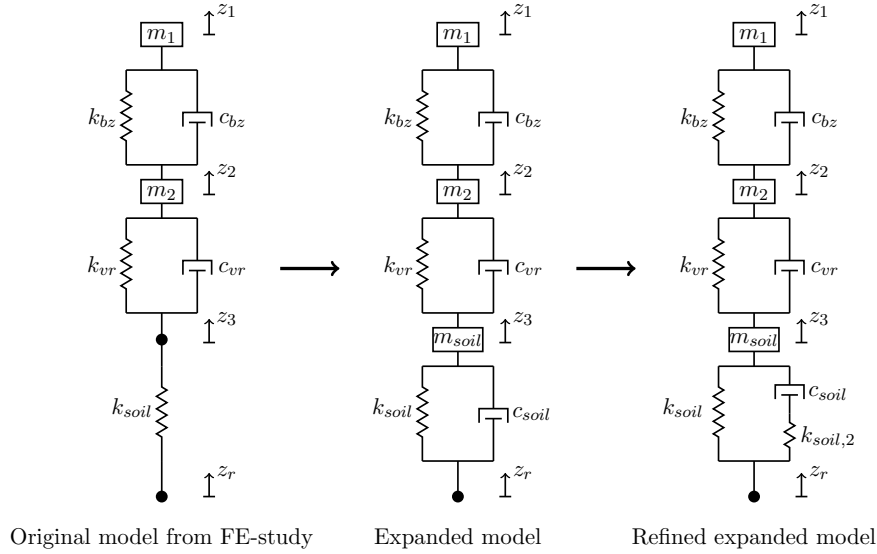


Figure 2.13: Representation of three investigated soil models implemented into the rigid ring model.

In previous work the parameters  $m_{soil}$ ,  $c_{soil}$  and  $k_{soil,2}$  has not been considered. The first step in calculating these are to find the frequency and damping. From the FEM results it was found that the frequency was linearly dependent on the velocity in longitudinal direction, see Figure 2.14. It can also be seen that the frequency changes throughout the oscillations but it is the oscillations with big amplitude that are of interest and the frequency of these are therefore used.

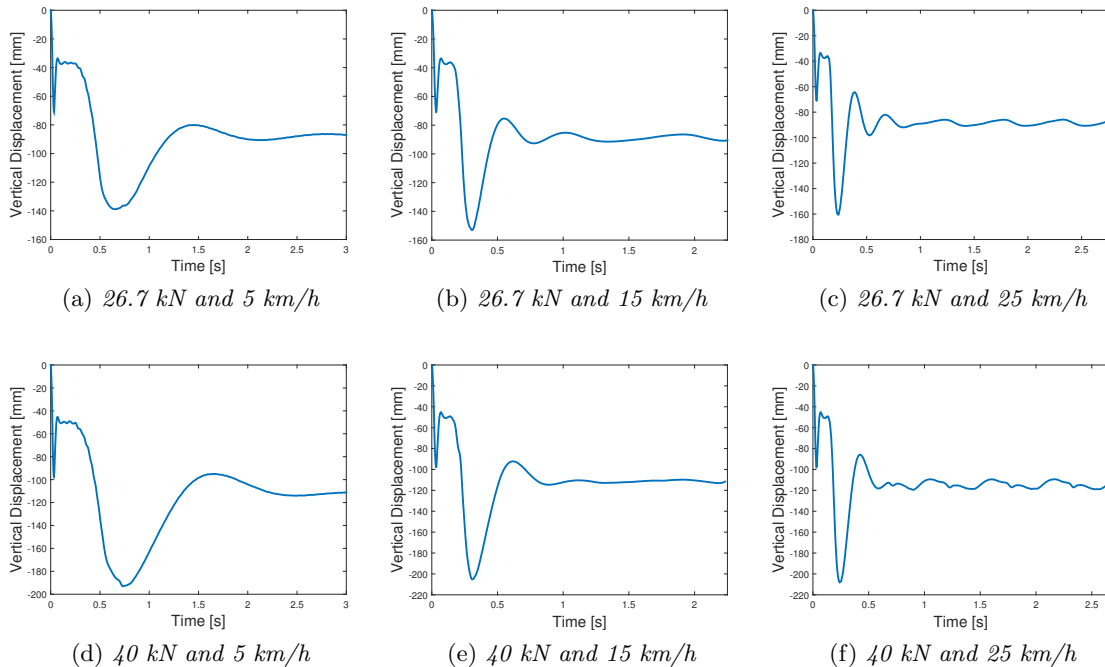


Figure 2.14: Vertical displacement of the wheel centre when driving into soil at different vertical loads and speeds simulated using FEM.

The frequency of the tyre sinkage oscillation were linearly dependent on the velocity making the

frequency easily calculated for all velocities within this velocity range, see below:

$$\omega(v_x) = \frac{d\omega}{dv_x} \cdot v_x + \omega_0 \quad (2.31)$$

where  $\frac{d\omega}{dv_x}$  and  $\omega_0$  were found using Matlab's curve fitting tool for the two different vertical loads. In Figure 2.15 a representation of equation 2.31 can be seen, plotted with the known frequencies from the FEM-model versus longitudinal velocity.

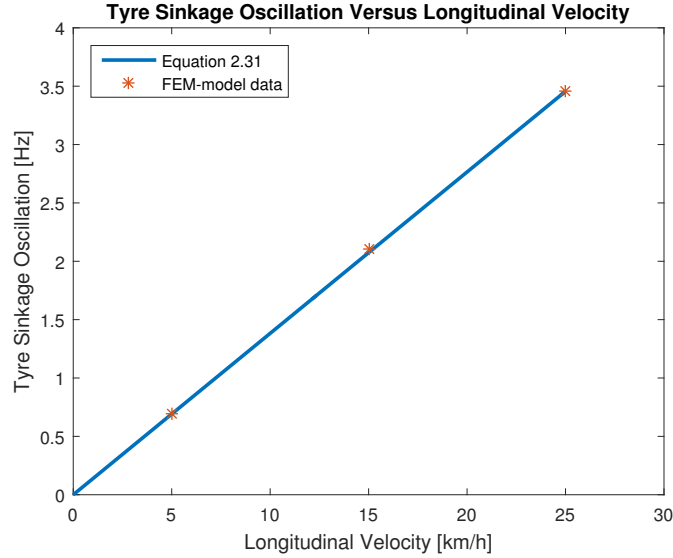


Figure 2.15: Frequency plotted against the longitudinal velocity including results from FEM-model and the corresponding values of  $\frac{d\omega}{dv_x}$  and  $\omega_0$  in equation 2.31 for a vertical load of 26.7 kN.

From this the damper can be seen as frequency dependent instead of velocity dependent. This can be modelled as a spring and damper in series, see Figure 2.16.

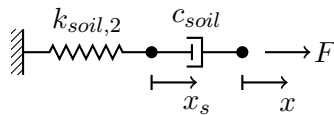


Figure 2.16: Representation of the spring and damper in series in the soil model.

This component will contribute with an equivalent stiffness,  $k'_{soil}$ , and damping,  $c'_{soil}$ . These can be expressed in terms of the stiffness,  $k_{soil,2}$ , the damping,  $c_{soil}$  and the frequency  $\omega$ . The derivation can be seen below:

$$\begin{aligned} F &= k_{soil,2} \cdot x_s \\ F &= c_{soil}(\dot{x} - \dot{x}_s) \\ F &= c_{soil} \left( \dot{x} - \frac{1}{k_{soil,2}} \dot{F} \right) \\ F &= F e^{i\omega t} \\ x &= x e^{i\omega t} \end{aligned}$$

$$\begin{aligned}
&\Rightarrow F = c_{soil} \left( i\omega x - \frac{1}{k_{soil,2}} i\omega F \right) \\
&F \left( 1 + i\omega \frac{c_{soil}}{k_{soil,2}} \right) = i\omega \cdot c_{soil} x \\
\frac{F}{x} &= \frac{i\omega \cdot c_{soil}}{1 + i\omega \frac{c_{soil}}{k_{soil,2}}} = \left\{ \frac{1}{\frac{1}{i\omega \cdot c_{soil}} + \frac{1}{k_{soil,2}}} = \frac{1}{\frac{1}{k_{soil,2}} - \frac{i}{\omega \cdot c_{soil}}} \right\} = \frac{\frac{1}{k_{soil,2}} + \frac{i}{\omega \cdot c_{soil}}}{\frac{1}{k_{soil,2}^2} + \frac{1}{(\omega \cdot c_{soil})^2}} \\
\Rightarrow k'_{soil}(\omega) &= \text{re} \left( \frac{F}{x} \right) = \frac{\frac{1}{k_{soil,2}}}{\frac{1}{k_{soil,2}^2} + \frac{1}{(\omega \cdot c_{soil})^2}} = \frac{k_{soil,2}}{1 + \left( \frac{k_{soil,2}}{\omega \cdot c_{soil}} \right)^2} \\
c'_{soil}(\omega) &= \text{im} \left( \frac{F}{x} \right) = \frac{\frac{1}{\omega^2 c_{soil}}}{\frac{1}{k_{soil,2}^2} + \frac{1}{(\omega \cdot c_{soil})^2}} = \frac{c_{soil}}{1 + \left( \frac{\omega \cdot c_{soil}}{k_{soil,2}} \right)^2}
\end{aligned} \tag{2.32}$$

To incorporate this soil behaviour the model needs to be further reworked. In Figure 2.17 a representation of the reworked soil model can be seen.

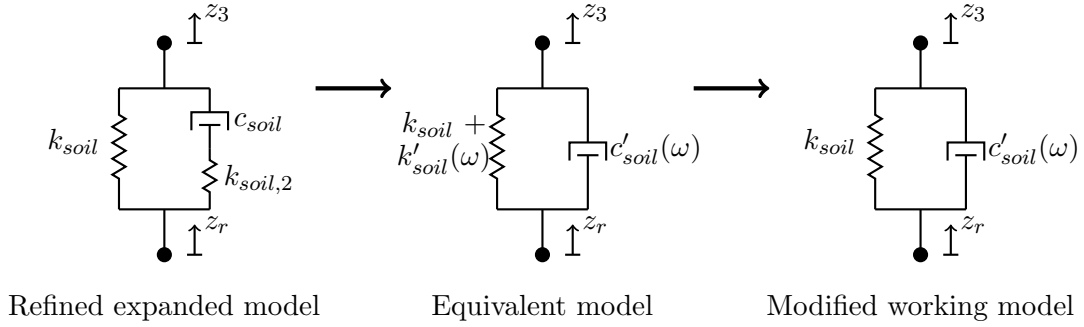


Figure 2.17: Representation of the evolution of the refined expanded soil model.

This model proved to be problematic since the equivalent stiffness,  $k'_{soil}$ , that arises from the damper and spring in series, was too high. In addition, the total vertical stiffness of the soil should not change, which it does with this model. However, the equivalent damping,  $c'_{soil}$ , gave successful results and the modified model was used. While not being completely physical it was implemented due to its relatively good way of mimicking the FEA soil characteristics.

With the tyre sinkage frequency calculated from equation 2.31, the fictive mass,  $m_{soil}$ , can be calculated by assuming that the tyre is completely rigid and fixed to the ground making the oscillation only being active in the soil. The original soil stiffness,  $k_{soil}$ , is then used to calculate the total mass oscillating. By removing the tyre mass the fictive mass of the soil can be found, see below.

$$m_{tot} = \frac{k_{soil}}{\omega^2} \tag{2.33}$$

$$m_{soil} = m_{tot} - m_{tyre} \tag{2.34}$$

An approximation of the equivalent damping,  $c'_{soil}$ , can then be calculated in the same way as in previous work [8], where the logarithmic decrement,  $\delta$ , and the dimensionless damping ratio,  $\zeta$ , are

calculated as:

$$\delta = \ln \left( \frac{p_1}{p_2} \right) \quad (2.35)$$

$$\zeta = \frac{\delta}{\sqrt{4\pi + \delta^2}} \quad (2.36)$$

Where  $p_1$  and  $p_2$  are extreme values in the oscillations in Figure 2.14. As the oscillations are nonlinear for the FE-model and the larger oscillations are of interest, the second oscillation was picked as this showed most promising result. To get the correct logarithmic decrement the steady state point was needed. This was calculated by taking the mean value of all the points after first oscillation. The first oscillation was neglected due to the non-linearity. The extreme values can then be calculated as below:

$$p_i = z(t_i) - z_m \quad (2.37)$$

Where  $z(t_i)$  is the vertical displacement at the extreme point and  $z_m$  is the mean (steady state) value.

The approximation can be calculated as:

$$c'_{soil} = 2\zeta \sqrt{m_{tot}k_{soil}} \quad (2.38)$$

It was found that for the case with a vertical load of 40 kN the damping of the soil is very non-linear. When driving in 5 km/h and 15 km/h the second oscillation can hardly be seen, see Figure 2.14d and 2.14e and when driving in 25 km/h the oscillations also becomes very irregular, see Figure 2.14f. For these cases the first two valley values were used instead of the peak values.

With these approximated values the model's system of equations can be formulated as seen in equation 2.39.

$$\begin{bmatrix} 0 \\ 0 \\ 0 \\ 0 \end{bmatrix} = \begin{bmatrix} k_{bz} & -k_{bz} & 0 & 0 \\ -k_{bz} & k_{bz} + k_{vr} & -k_{vr} & 0 \\ 0 & -k_{vr} & k_{vr} + k_{soil} & -k_{soil} \\ 0 & 0 & -k_{soil} & k_{soil} \end{bmatrix} \begin{bmatrix} z_1 \\ z_2 \\ z_3 \\ z_r \end{bmatrix} + \quad (2.39)$$

$$\begin{bmatrix} c_{bz} & -c_{bz} & 0 & 0 \\ -c_{bz} & c_{bz} + c_{vr} & -c_{vr} & 0 \\ 0 & -c_{vr} & c_{vr} + c'_{soil} & -c'_{soil} \\ 0 & 0 & -c'_{soil} & c'_{soil} \end{bmatrix} \begin{bmatrix} \dot{z}_1 \\ \dot{z}_2 \\ \dot{z}_3 \\ \dot{z}_r \end{bmatrix} + \begin{bmatrix} m_1 & 0 & 0 & 0 \\ 0 & m_2 & 0 & 0 \\ 0 & 0 & m_{soil} & 0 \\ 0 & 0 & 0 & 0 \end{bmatrix} \begin{bmatrix} \ddot{z}_1 \\ \ddot{z}_2 \\ \ddot{z}_3 \\ \ddot{z}_r \end{bmatrix}$$

From equation 2.39 the two middle equations can be rewritten as in equation 2.40 and 2.41. By defining  $\ddot{z}_2$  and  $\ddot{z}_3$  the states can be found consequently.

$$\ddot{z}_2 = \frac{k_{bz}(z_1 - z_2) + k_{vr}(z_3 - z_2) + c_{bz}(\dot{z}_1 - \dot{z}_2) + c_{vr}(\dot{z}_3 - \dot{z}_2)}{m_2} \quad (2.40)$$

$$\ddot{z}_3 = \frac{k_{vr}(z_2 - z_3) + k_{soil}(z_r - z_3) + c_{vr}(\dot{z}_2 - \dot{z}_3) + c'_{soil}(\dot{z}_r - \dot{z}_3)}{m_{soil}} \quad (2.41)$$

Here  $\dot{z}_1 = v_z$  and the states are:  $z_1, z_2, \dot{z}_2, z_3$  and  $\dot{z}_3$ .

Finally the force can be calculated by rearranging the first equation in equation 2.39 ending up in the equation below.

$$m_1 \ddot{z}_1 = Fz = k_{bz}(z_2 - z_1) + c_{bz}(\dot{z}_2 - \dot{z}_1) \quad (2.42)$$

## Soil Deformation

The model captured the large oscillations of the soil relatively well but underlying oscillations from the tyre itself were still present in the rigid ring model while being almost completely cancelled out in the FE-results. By increasing the vertical residual damping,  $c_{vr}$ , a better fit could be found. This was considered as a working solution as the damping in the contact point between the tyre and the soil should increase compared to the rigid ground. No exact value for this has been investigated but a correct behaviour was achieved when the residual damping,  $c_{vr}$ , was increased. The result from this change can be seen in Figure 2.19.

Another factor that needs to be taken into consideration is that when the tyre will sink down into the soil a local slope will arise. The angle of this slope can be approximated to the mean angle between the deepest point and the road plane, see Figure 2.18.

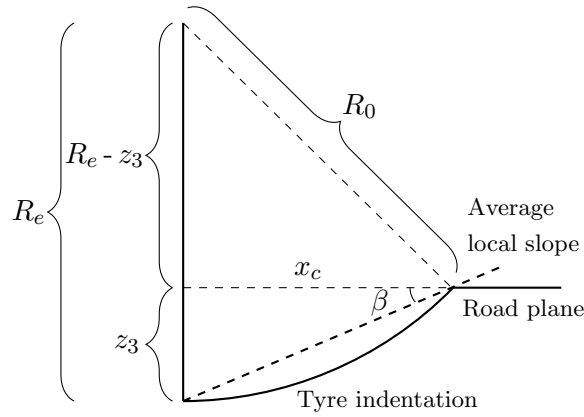


Figure 2.18: *Illustration of the local slope phenomenon.*

This angle can be calculated in the following way:

$$\beta = \tan^{-1} \left( \frac{z_3}{x_c} \right) \quad (2.43)$$

where  $x_c$  is:

$$x_c = \sqrt{R_0^2 - (R_e - z_3)^2} \quad (2.44)$$

When the tyre is moving in longitudinal direction the tyre will climb this slope and this change of  $z_3$  and  $\dot{z}_3$  needs to be taken into account.

$$\Delta x = v_x \Delta t \quad (2.45)$$

$$\Delta z_3 = \Delta x \tan(\beta) \quad (2.46)$$

$$\Delta \dot{z}_3 = v_x \tan(\beta) \quad (2.47)$$

The actual  $z_3$  and  $\dot{z}_3$  will then be calculated as:

$$z_3 = z_3 + \Delta z_3 \quad (2.48)$$

$$\dot{z}_3 = \dot{z}_3 + \Delta \dot{z}_3 \quad (2.49)$$

The simulation results in Figure 2.14 confirms the presence of an effect similar to the local slope climbing. To fit the results in Figure 2.14 the results needed to be shifted upwards which could not

be achieved by altering the soil parameters and maintain the static soil stiffness. It was found that the climb varied with the longitudinal velocity and a local slope coefficient,  $C(v_x)$ , was introduced. The equivalent local slope can be expressed as:

$$\beta' = C(v_x) \cdot \tan^{-1} \left( \frac{z_3}{x_c} \right) \quad (2.50)$$

The resulting oscillations of this model is compared with the FEA results in Figure 2.14 and the local slope coefficient,  $C(v_x)$ , is manually tuned to get a good fit with the FE-model. From equation 2.32 the model parameters,  $c_{soil}$  and  $k_{soil,2}$  can be obtained. With these two known the equivalent damping,  $c'_{soil}$ , can be calculated for all frequencies. These parameters can be verified for the velocity 25 km/h by comparing with the FEA simulation data to ensure that the parameters are correct within the range of 5-25 km/h.

With the values of  $C(v_x)$  found for the different simulations in Figure 2.14 Matlab's curve fitting tool was used to create a function that made  $C(v_x)$  valid for different velocities. A function that gave a sufficient result was on the form that can be seen below:

$$C(v_x) = c_a \cdot v_x^{c_b} + c_c \quad (2.51)$$

The constants,  $c_a$ ,  $c_b$  and  $c_c$ , are calculated for both 26.7 kN and 40 kN and then linearised to accommodate all loads.

Figure 2.19 shows results from the different stages of the implementation. The influence of how the parameters of the vertical damping and slope compensation could from this be verified and tuned in to match the FEM-model. Figure 2.19a shows the model with only  $c'_{soil}$  and  $m_{soil}$  implemented. One can see that the major oscillations are correct but there are small oscillations coming from the tyre itself. In Figure 2.19b the residual damping,  $c_{vr}$ , is increased and the small oscillations quickly disappears. Figure 2.19c shows the final result when the slope compensation,  $C(v_x)$ , is implemented to match the FEM-model.

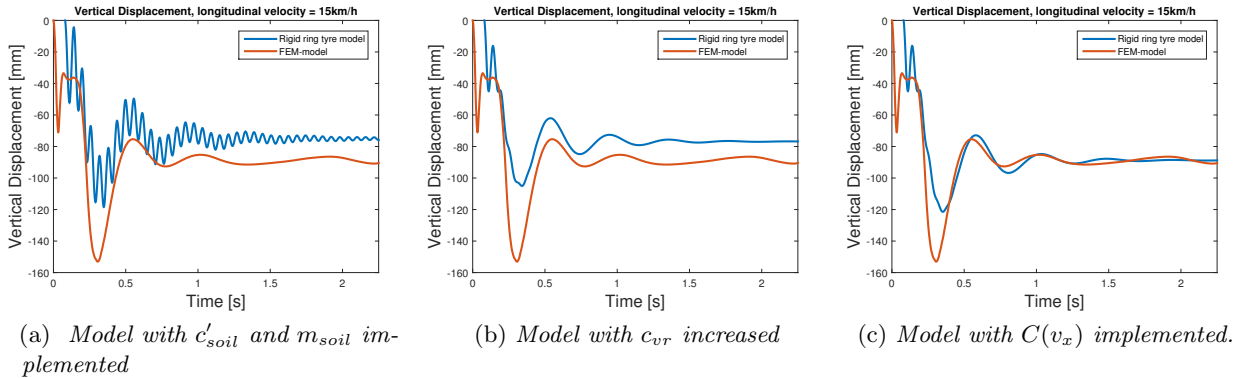


Figure 2.19: Results from the different stages of the implementation of the soil models vertical damping.

For 40 kN the equivalent damping constant  $c'_{soil}$  needed to be manually tuned in for 5 km/h as it was found that the approximated value of this was too high. In Figure 2.20 the difference between the approximated damping and the tuned one is shown.

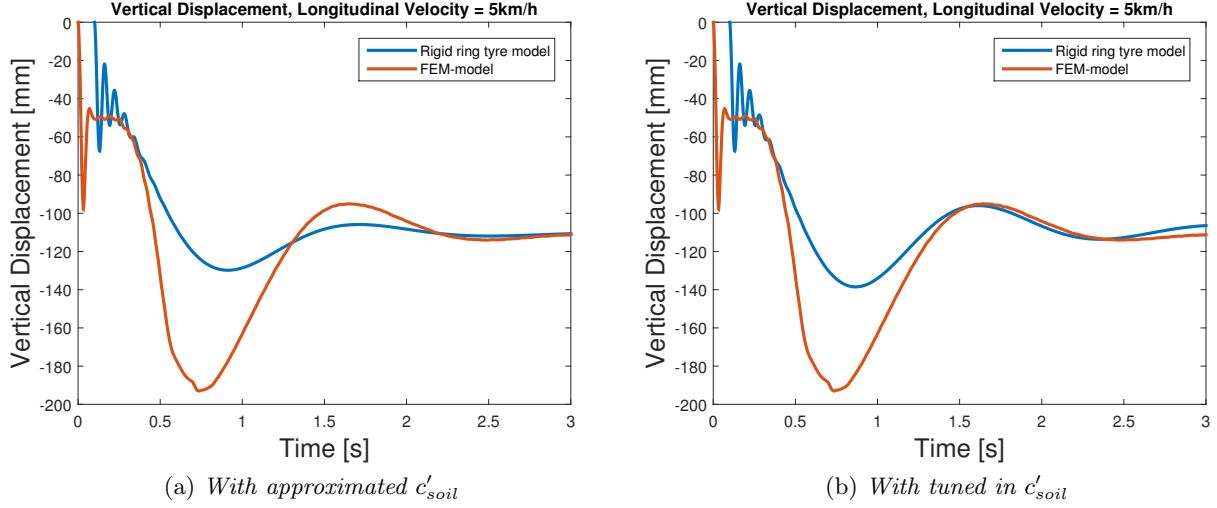


Figure 2.20: Result from simulation with approximated and tuned in equivalent damping constant  $c'_{soil}$ .

### 2.5.2 Longitudinal Reaction Force

There are only small changes in the longitudinal force model compared to the rigid ground. The equation for the effective rolling radius changes to:

$$R_e = R_0 - (z_3 - z_1) \quad (2.52)$$

For soft soil ground resistance forces such as rut deformation and the bulldozing effect, see chapter 6, needs to be taken into account. However the longitudinal slip constants,  $k_{k,soil}$  and  $k_{cx}$ , have already taken these effects into account since they are simply calculated from the resulting force in the tyre compared to the slip. This means that the only change in equation 2.7 - 2.11 are the values of the slip parameters and a new saturation value must be calculated from the FEM simulation data. For soft soil it was harder to define a range in which the saturation value should be calculated from. This curve is a second order polynomial fit calculated from a non-linear slip/force curve. The range was here instead defined by including all values above the value for 100% slip. In difference to rigid ground the tyre pressure had more influence on the maximum force therefore the saturation value was calculated for all tyre pressures. This resulted in the values shown in table 2.1. In Figure 2.21 the FE-model simulation data can be seen along with the saturation value for 85 PSI.

Table 2.1: Saturation value of longitudinal force for different vertical loads and tyre pressures

Vertical Load	55 PSI	85 PSI	110 PSI	UNIT
13.3	7.0	6.7	6.4	[kN]
26.7	13.3	12.9	12.2	[kN]

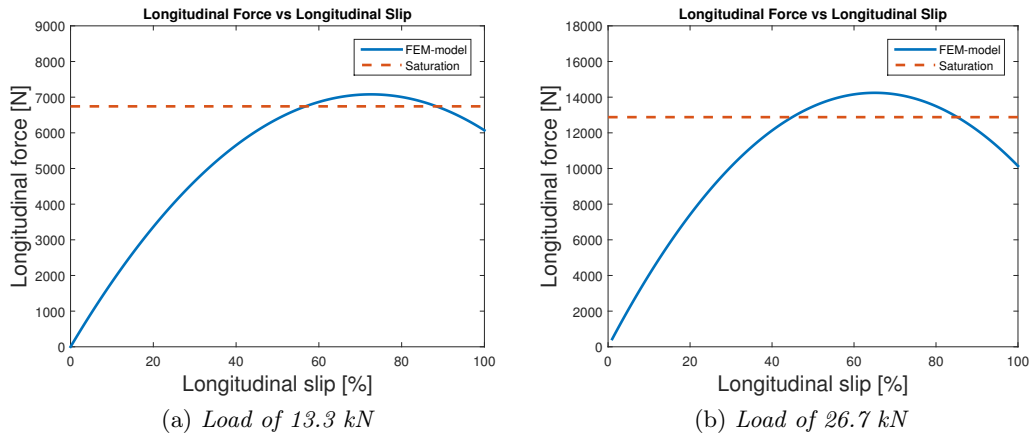


Figure 2.21: The slip/force relation, in the the wheel local longitudinal direction, captured in the FEM-simulations for two different loads, with saturation limits marked.

This model, in which the resistance forces are included in the tyre stiffness, proved too crude and gave non-satisfying results. During the simulations of the complete vehicle it was found that the soil model was not behaving as expected. The resulting velocities from a step-steer simulation, can be seen in Figure 2.22. This shows that the soil model has the highest velocity in both longitudinal and lateral direction. This seems reasonable for the lateral direction since the truck should skid somewhat more than the other models. However, the longitudinal velocity should be considerably lower than the other models. This behaviour likely originates from the fact that the resistance forces are not modelled externally. Since there is no applied torque during this simulation no considerable slip will build up and there will be no difference in the longitudinal direction between the models. However, since the rigid ground models have higher lateral slip stiffness they will have a greater force decelerating the vehicle than the soil model. This model is behaving more like ice than soil and the conclusion was drawn that the resistance forces needed to be modelled externally, i.e. not by lowering the tyre stiffness.

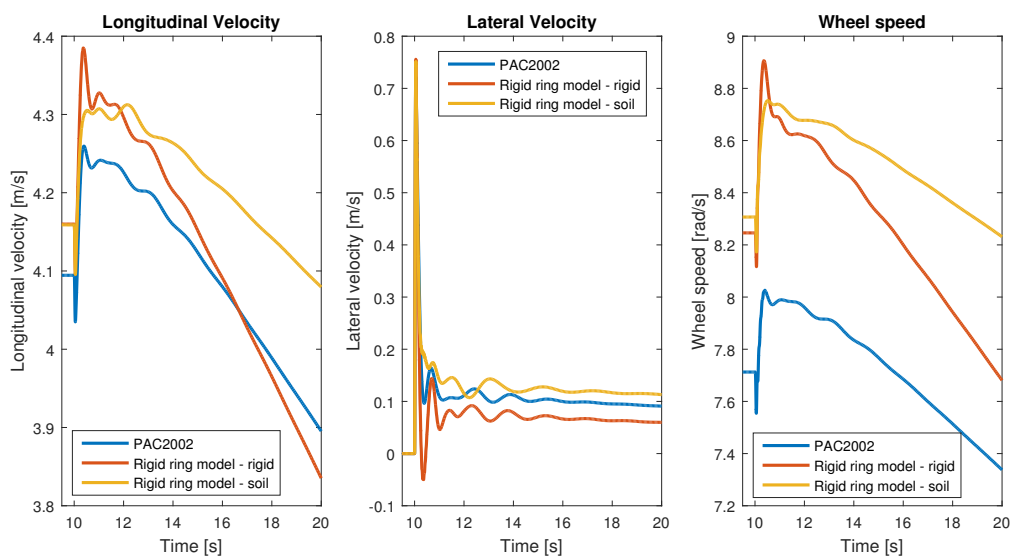


Figure 2.22: Velocities during the step steer simulation for all models with soil model without resistance force modelled externally.

Instead the same tyre stiffness will be used as for rigid ground (further research will be needed) and an external resistance force will be applied instead. The resistance force for clayey soil (thailand) has been investigated in a previous report [7]. The resistance coefficient has been investigated using both FEM and SPH but the SPH model is described as behaving more physical. The SPH value will therefore be used for the resistance. Three different loads were used and Matlab's curve fitting tool was used from these to be able to create a function to approximate the rolling resistance coefficient,  $rrc$ , for other loads than the ones used in the simulations. In Figure 2.23 the three points from the SPH results are shown along with the approximated function created in Matlab.

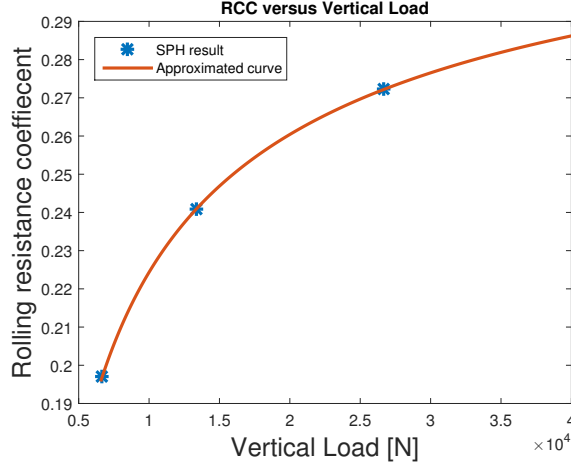


Figure 2.23: *Rolling resistance coefficient versus vertical load from SPH result and approximated function.*

The function that seemed appropriate was a power function as the increment of the rolling resistance coefficient decreases with the vertical load:

$$rrc = r_a \cdot F_z^{r_b} + r_c \quad (2.53)$$

where  $r_a, r_b$  and  $r_c$  are constants calculated with the curve fitting tool. This is what will be used until further testing and investigation has been performed. The saturation limit for the soft soil will however be kept and the rolling resistance force,  $F_r$ , is calculated as:

$$F_r = rrc \cdot F_z \quad (2.54)$$

### 2.5.3 Lateral Reaction Force

In the lateral direction equation 2.21 - 2.27 are still used but the cornering stiffness,  $k_f$ , and the relaxation length,  $\sigma$ , will change to the constants for soft soil ground. No saturation limit is needed as this does not have a maximum and varies linearly for soil, likely due to some resistance force from the soil.

## 2.6 S-function Implementation

In general three different tire models are implemented:

1. Variations of a single tire model disconnected from the complete vehicle.
2. Rigid ground model compatible with complete vehicle.
3. Soft soil ground model compatible with complete vehicle.

The first model will be used to verify all aspects of the tyre to the work documented in the previous progress report [8]. The second model will be used to compare and verify the rigid ground tire model to the currently implemented PAC2002 model. The third model is the final product of this project, it is the rigid ring model with soft soil ground implemented.

### 2.6.1 Rigid Ground

To construct the state space function for the rigid ground the following states are defined:

- Displacement of the wheel centre:  $x_1, y_1$  and  $z_1$
- Displacement of the tyre tread:  $x_2, y_2$  and  $z_2$
- Velocity of the tyre tread:  $\dot{x}_2, \dot{y}_2$  and  $\dot{z}_2$
- Tread deformation:  $u_x$
- Wheel plane angle of the wheel rim:  $\theta_1$
- Wheel plane angular velocity of the wheel rim:  $\dot{\theta}_1$
- Wheel plane angle of the tyre belt:  $\theta_2$
- Wheel plane angular velocity of the belt tread:  $\dot{\theta}_2$
- Out of plane angle of the tyre belt:  $\gamma_2$
- Out of plane angular velocity of the tyre belt:  $\dot{\gamma}_2$

The displacement of the wheel centre,  $x_1, y_1$  and  $z_1$ , is updated using the input velocities. The displacement of the tyre tread,  $x_2, y_2$  and  $z_2$ , is updated using their velocities,  $\dot{x}_2, \dot{y}_2$  and  $\dot{z}_2$ , which in turn are updated by their acceleration calculated from the equilibrium equations 2.4, 2.15 and 2.27. The tread deformation,  $u_x$ , is updated using its derivative in equation 2.11. The wheel plane rotational properties,  $\theta_1, \dot{\theta}_1, \theta_2$  and  $\dot{\theta}_2$  are updated from the equilibrium equations 2.19 and 2.20. The out of plane wheel belt angle,  $\gamma_2$ , and rotational speed,  $\dot{\gamma}_2$ , is updated using the equilibrium equation 2.30.

### 2.6.2 Soft Soil Ground

For the soft soil ground implementation two additional states are needed, the tyre sinkage into the soil,  $z_3$  and the sinkage velocity,  $\dot{z}_3$ .

- Tyre sinkage:  $z_3$
- Tyre sinkage velocity:  $\dot{z}_3$

$\ddot{z}_3$  can be found in the equilibrium equation 2.41 which is used to update  $\dot{z}_3$  which in turn is used to update  $z_3$ .

### 2.6.3 Additional States for Single Tyre Model

When constructing the independent single tyre model the velocities  $v_x$ ,  $v_y$  and  $v_z$  need to be updated internally within the tyre module. This requires that the wheel rim velocities are set up as states,  $\dot{x}_1$ ,  $\dot{y}_1$  and  $\dot{z}_1$ .

- Velocity of the wheel centre:  $\dot{x}_1$ ,  $\dot{y}_1$  and  $\dot{z}_1$

To update the velocities the wheel rim accelerations are needed and can be calculated from equilibrium as:

$$\ddot{x}_1 = \frac{F_x}{m_t}, \quad \ddot{y}_1 = \frac{F_y}{m_t}, \quad \ddot{z}_1 = \frac{F_z - F_{z_0}}{m_t} \quad (2.55)$$

where  $F_{z_0}$  is the constant axle load acting on the tyre rim used in the single tyre model as in previous work [8].

## 3 Tyre Parameters

The parameters used in the rigid ring tyre model have all been investigated in a previous progress report [8]. The parameters have been investigated using three different inflation pressures and two different loads. The inflation pressures are 55, 85 and 110 psi (3.8, 5.9 and 7.6 bar) and the two different loads are 13.3 and 26.7 kN. For the additional parameters in the soil calculated in this project only an inflation pressure of 110 psi was used along with loads of 26.7 kN and 40 kN. All of the parameters used can be found in Appendix D.

### 3.1 Linearisation With Respect To Vertical Load

In the start of each simulation the parameters are defined by linearising the parameters from the two loads in the previous work [8]. Each axle in the complete vehicle model has a nominal load and this is used when linearising the parameters for each tyre. The parameters that are approximated by the linearisation are:

- The stiffness and damping of the tyre and the soil (not including  $c_{tot}$  due to its likely incorrect value for 13.3 kN)
- The slip model parameters and relaxation length
- The saturation value of the slip forces

Since there are only two data points available a linearisation is the highest order approximation possible. However there is no evidence that the relation between all the parameters are linear which causes uncertainties in their true values.

### 3.2 Influence of Tyre Inflation Pressure

All the simulations in the previous work has been carried out using three different inflation pressures, 55, 85 and 110 psi. The inflation pressure is seen as constant and is defined in the start of each simulation in VTM. As only the vertical soil parameters for 110 psi is available this is the pressure that will be used when simulating driving in soil.

### 3.3 Errors and Shortcomings in the Previous Work

During the project it was discovered that the previous work contained calculation errors. This meant that all the parameters in the report for phase XII [8] needed to be looked over. The parameters that were given wrong values are the vertical residual parameters, both stiffness and damping. It was also found that the wrong belt mass and moment of inertia was used. The wrong belt mass affected the belts vertical stiffness and damping as well as lateral damping. The wrong moment of inertia lead to wrong damping in both wheel plane and out of plane rotation. This was corrected and the new values were implemented.

In addition to this the value of the total tyre damping,  $c_{tot}$ , changes dramatically between the two load levels. This is contradictory to a previous report at Volvo where the total damping stays relatively constant within the load range 13.3 - 53.3 kN. There is likely some type of error when calculating the

damping for 13.3 kN and when using the same damping as for 26.7 kN the drop test simulation gives satisfactory results.

The self aligning moment stiffness was found to be too low. In accordance to our supervisor a new self aligning moment stiffness was found using the following formula:

$$k_M = k_f \cdot a \cdot 0.37 \quad (3.1)$$

where  $k_f$  is the cornering stiffness and  $a$  is half of the contact length of the tyre.

The vertical residual damping,  $c_{vr}$ , has been seen as a tyre parameter which means that it does not change between soil and rigid ground. This however gave results that did not match the results from the FEM simulations. By increasing the parameter  $c_{vr}$  a satisfactory result was obtained which might warrant a further investigation of the parameter.

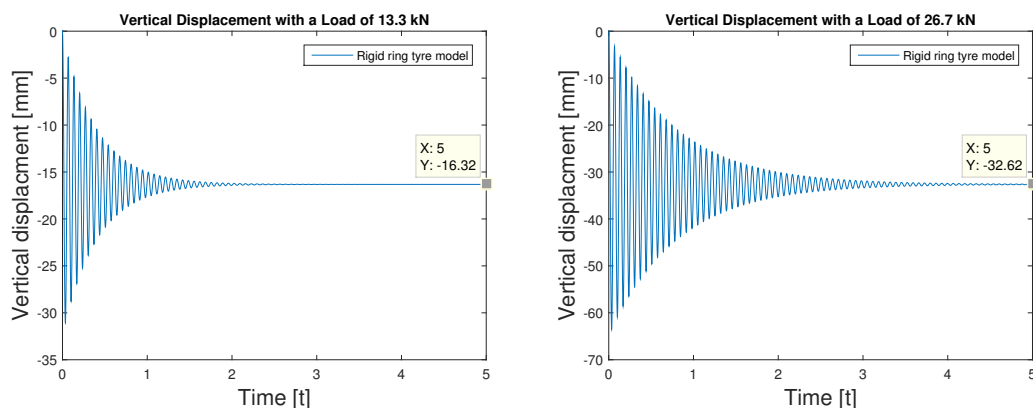
## 4 Single Tyre Verification

Since all model parameters are built upon FEA simulations the model needs to be verified against the FE-model. The results from the verification simulations described in the introduction, see Section 1.7.1, are compared with results from their FEM counterparts. Because of the non-linearity in the FEM-model exactly matching result are not likely in most cases. In the most severe cases a good fit was aimed for in the most critical regions, i.e. the most common slip values and the oscillations with large amplitudes. It was however important to reach the same steady state value in all of the simulations.

Most of these simulations were done using the 26.7 kN load since that is a more relevant load case than 13.3 kN. Some of the simulations were however made using 13.3 kN load as well to ensure correct behaviour. The difference between the parameters for the different inflation pressures are not big and a pressure of 85 psi was therefore used except for the vertical direction for soil where the only FEM-data available was for 110 psi.

### 4.1 Vertical Stiffness, Rigid Ground

The two standard forces of 13.3 kN and 26.7 kN were used and the steady state vertical displacement that is reached can be seen in Figure 4.1. If the steady state vertical displacement is plotted with the FEM results one can see that a good match is found, see Figure 4.2.



(a) Vertical displacement for a 13.3 kN vertical load

(b) Vertical displacement for a 26.7 kN vertical load

Figure 4.1: Vertical displacement of the wheel centre for two different vertical loads.

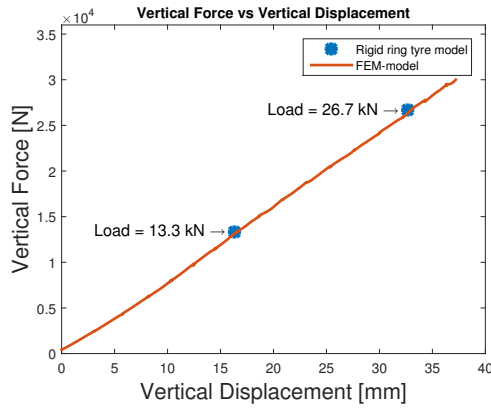


Figure 4.2: Vertical displacement data from previous work with this projects steady state values plotted on top.

## 4.2 Vertical Damping, Rigid Ground

When comparing the damping of the rigid ring tyre model with the FE-model one can see that the frequency of the rigid ring tyre model is higher in the beginning and remains constant while the FE-model's increases and becomes higher after some time, see Figure 4.3. This is due to the fact that the FE tyre stiffness is nonlinear in vertical direction as the contact area of the tyre changes while bouncing. This phenomenon is very clear for the case with a load of 13.3 kN, see Figure 4.4b. When looking at the decrement of the amplitude the match is considered good after changing the damping constant for 13.3 kN to the same as for 26.7 kN . In Figure 4.4a the simulation result using the original damping from previous work [8] is shown.

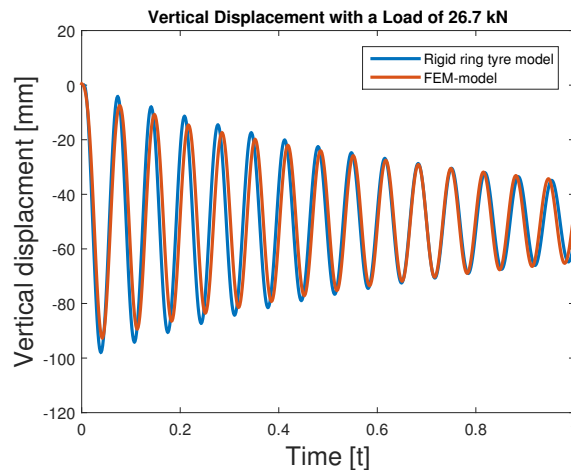
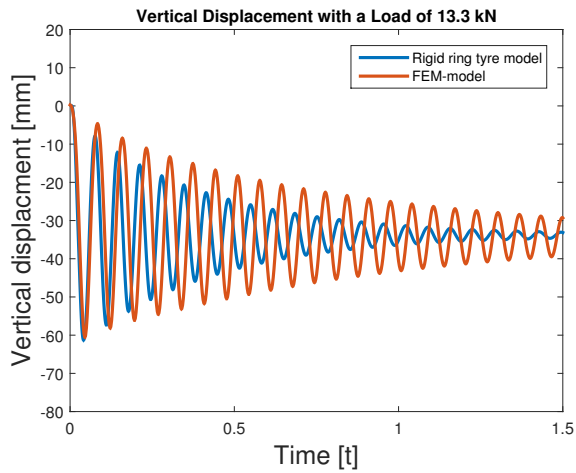
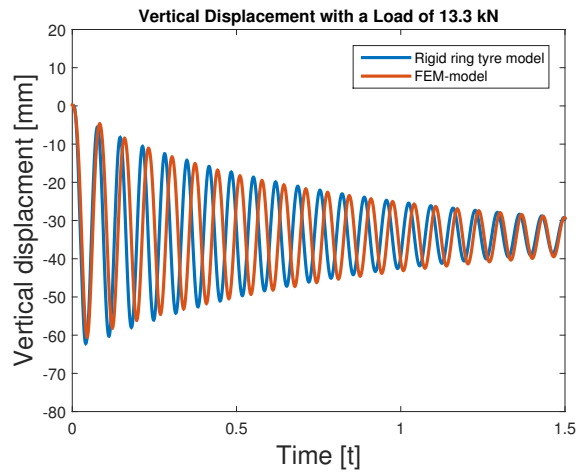


Figure 4.3: Vertical displacement of wheel centre from drop test with a 26.7 kN vertical load



(a) With original damping constant

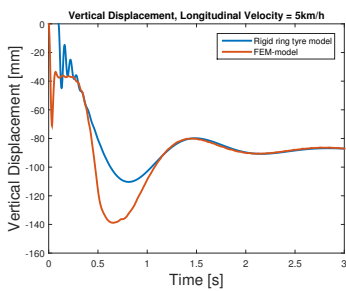


(b) With the same damping constant as for 26.7 kN

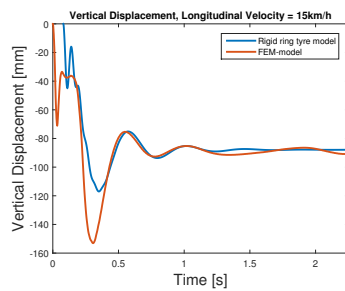
Figure 4.4: Vertical displacement of wheel centre from drop test with a 13.3 kN vertical load.

### 4.3 Soil Vertical Stiffness and Damping

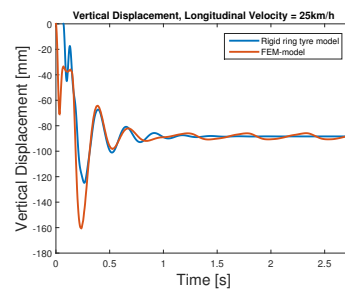
The vertical damping in the soil varies between different velocities. It is also extremely non-linear as seen below, with the big dip in the beginning. This non-linearity can not be fully captured in the soil model used in the rigid ring model. However a somewhat similar behaviour has been achieved and is considered sufficient. As the steady state vertical displacement matches the FE-model the stiffness of the model is considered sufficient as well. The reason why no stiffness simulation was done by only applying a vertical load while the tyre is standing still is because this soil model can't stand still. The fictive mass goes towards infinity when the frequency goes towards zero, see equation 2.34, which it does for low velocities.



(a) Velocity of 5 km/h



(b) Velocity of 15 km/h



(c) Velocity of 25 km/h

Figure 4.5: Wheel centre displacement when driving on soil at different velocities for a 26.7 kN vertical load.

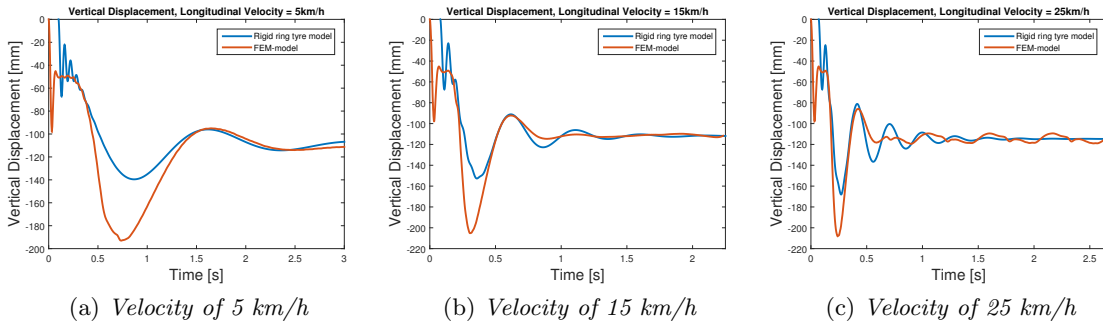


Figure 4.6: *Wheel centre displacement when driving on soil at different velocities for a 40 kN vertical load.*

#### 4.4 Wheel Plane Rotational Stiffness & Damping

It was found that the moment of inertia used when calculating the damping constant in previous work [8] was too high. By tuning this until the oscillations matched, see Figure 4.7b, appropriate constants were found that gave a correct behaviour.

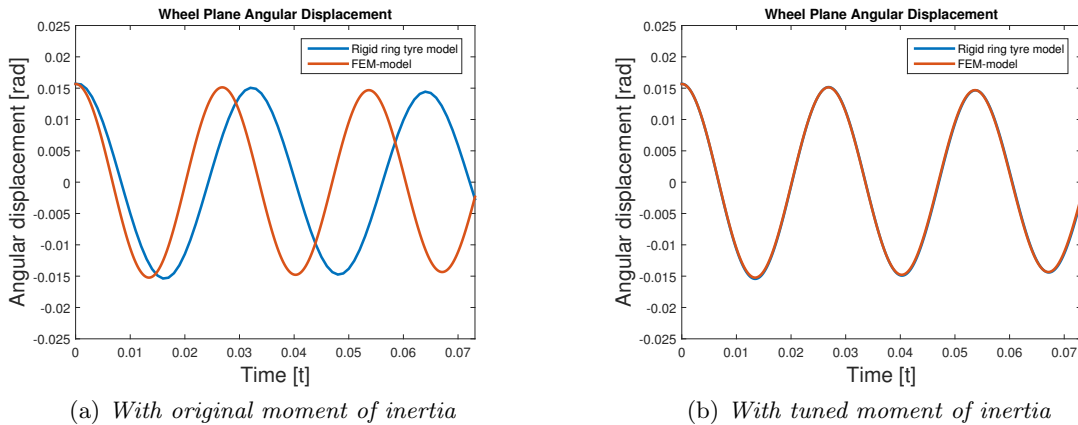
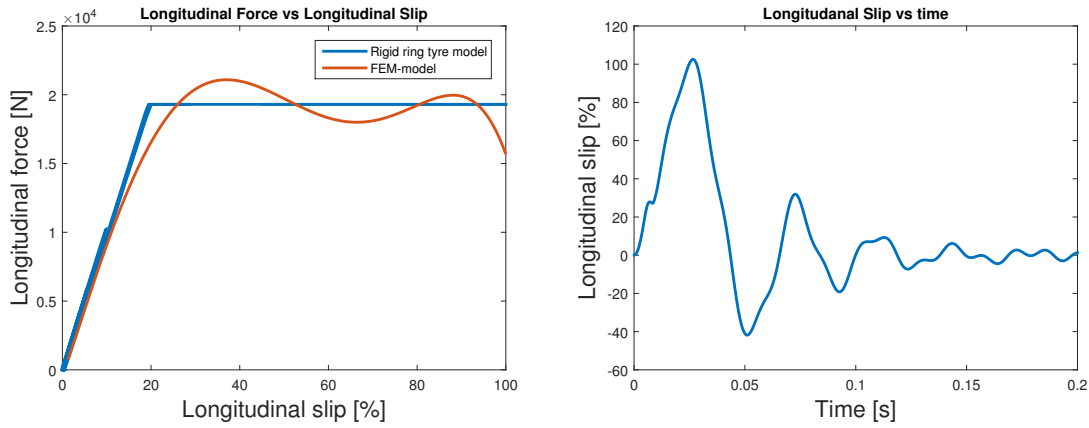


Figure 4.7: *Wheel plane angular displacement from the damping simulation.*

#### 4.5 Longitudinal Tread & Tyre Stiffness, Rigid Ground

The non linear relation between longitudinal force and slip is modelled as a bi-linear relation. Since a wheel usually operates within 0-20% slip this is the area in which the behaviour is of most importance. The dependency on the slip is cut off after reaching its saturation value, see Figure 4.8a.

The simulation for the FE-model includes a drum on which the tyre is driven. This is not possible to achieve for the single tyre model making it impossible to compare slip vs time, slip vs force can be however be compared. However, the result from the single tyre model shows a correct behaviour according to the project supervisor. In Figure 4.8b the longitudinal slip versus time can be seen from the verification simulation of the single tyre model. The FEM-model is not included in this Figure because the manoeuvres are not the same and this comparison would be misleading. The driving torque used in this simulation was 17 kN and kept for 0.02 seconds to reach 100% slip.

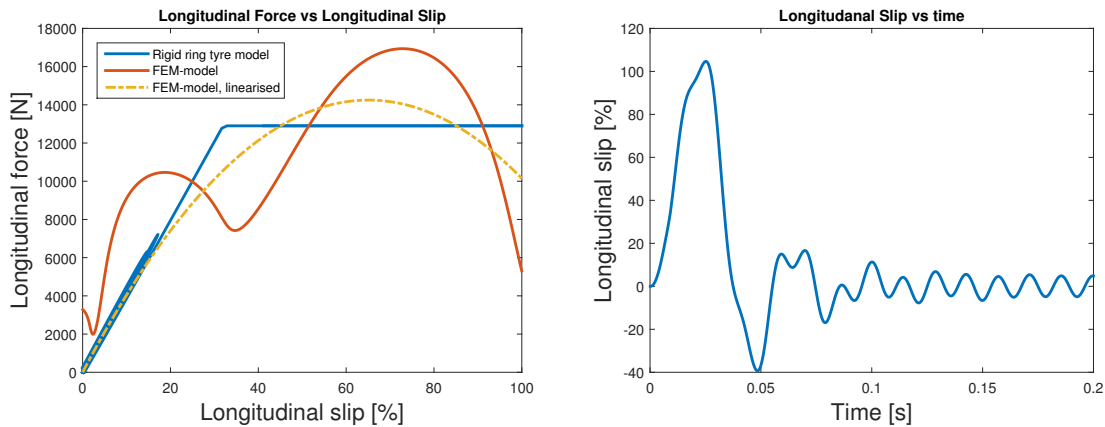


(a) The longitudinal slip/force relation which is saturated at 19.6 kN, for a 26.7 kN vertical load. (b) The longitudinal slip versus time from acceleration simulation.

Figure 4.8: Plots over the slip/force relation and the longitudinal slip.

## 4.6 Longitudinal Tread & Tyre Stiffness, Soft Soil Ground

The non-linear slip/force relation on soil is again modelled bi-linearly. The match is rather good up to 20% and beyond that the match starts to suffer. Since the wheel usually operates between 0-20% slip the fit is considered sufficient when compared to the polynomial approximation. This result is from the model without rolling resistance included. The raw results from the FEA shows some very odd behaviour which and the result considered with caution since it looks that some other kind of mechanic is influencing the results. To obtain 100% slip with this model the driving torque that need to be applied was 10 kNm.

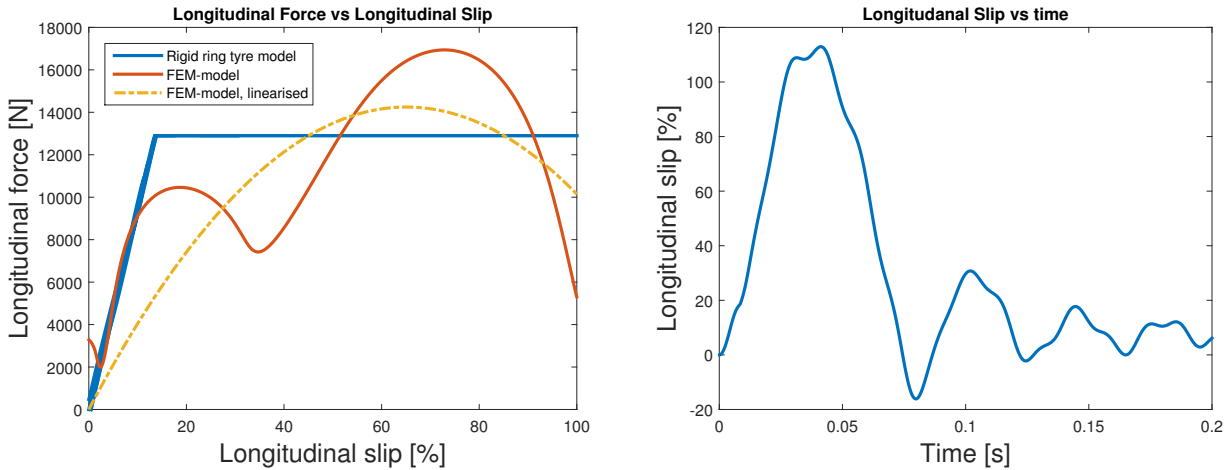


(a) The longitudinal slip/force relation which is saturated at 12.9 kN, for a 26.7 kN vertical load. (b) The longitudinal slip versus time from acceleration simulation.

Figure 4.9: Plots over the slip/force relation and the longitudinal slip for model with out rolling resistance included.

The result from using the same longitudinal tyre stiffness as for rigid ground and including the rolling resistance can be seen below. The driving torque that was applied to obtain 100% slip was 12 kNm.

The driving torque can not be completely removed after 0.02 seconds because of the rolling resistance. Some driving torque was needed to be kept to maintain constant velocity. Comparing with the actual FEA data the match can be considered good for 0-10%. It can also seen in Figure 4.10b that the slip goes towards 0% slower which seems more realistic when driving in soil.



(a) The longitudinal slip/force relation which is saturated at 12.9 kN, for a 26.7 kN vertical load.

(b) The longitudinal slip versus time from acceleration simulation.

Figure 4.10: Plots over the slip/force relation and the longitudinal slip for model with rolling resistance included.

## 4.7 Out of Plane Sidewall Translational Stiffness & Damping

When simulating the out of plane translational properties of the sidewall it was found that the mass from the previous work was too high. When this was corrected appropriate parameters were obtained and matching oscillations were found, see Figure 4.11b.

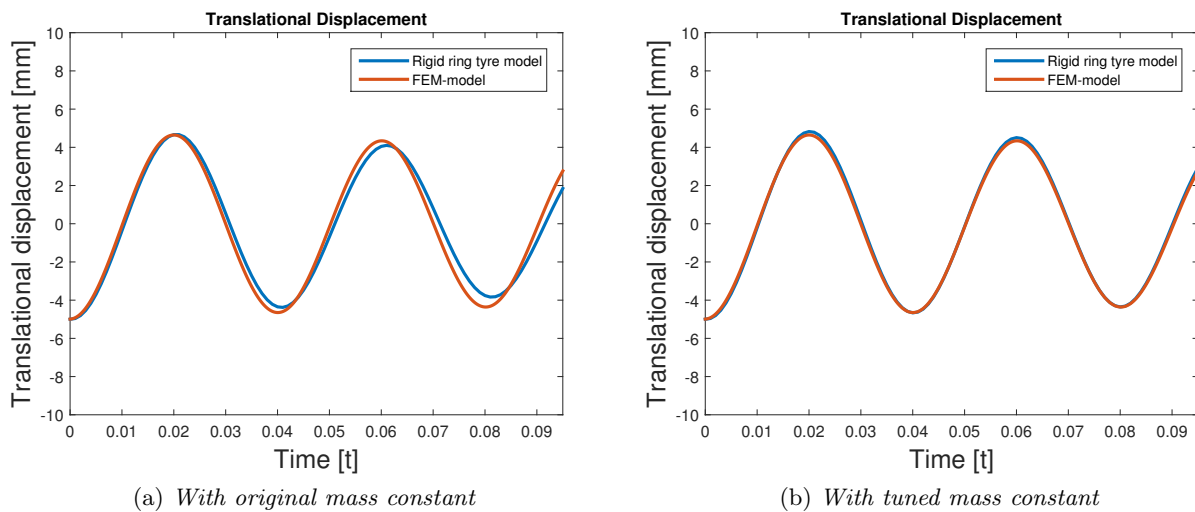


Figure 4.11: The translational displacement of the tyre tread while keeping wheel rim fixed.

## 4.8 Out of Plane Rotational Stiffness & Damping

In the previous work the moment of inertia used was found to be too high. When this was corrected matching results were found and suitable parameters obtained, see Figure 4.12b.

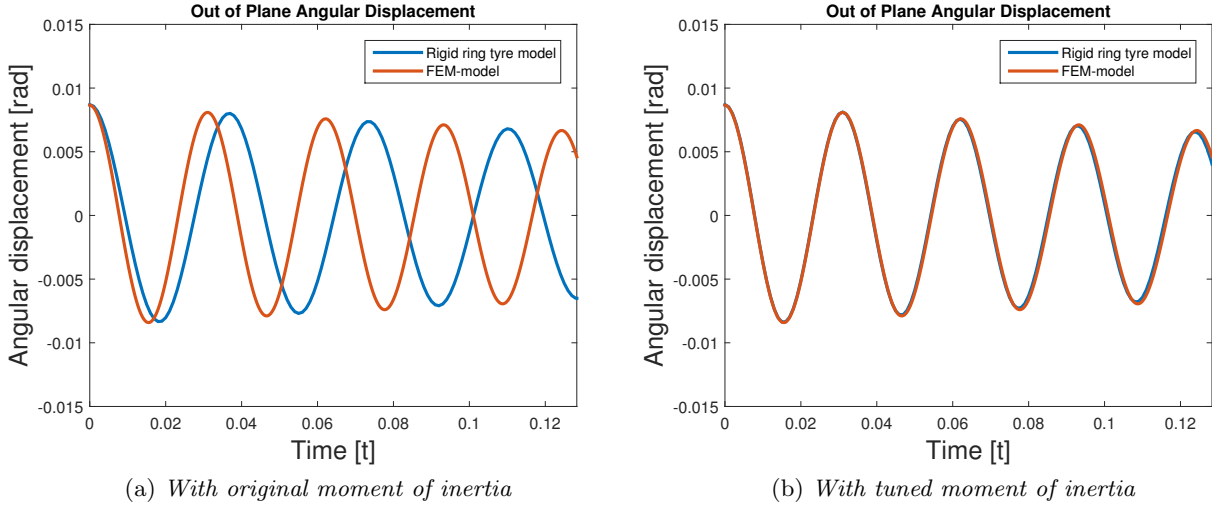
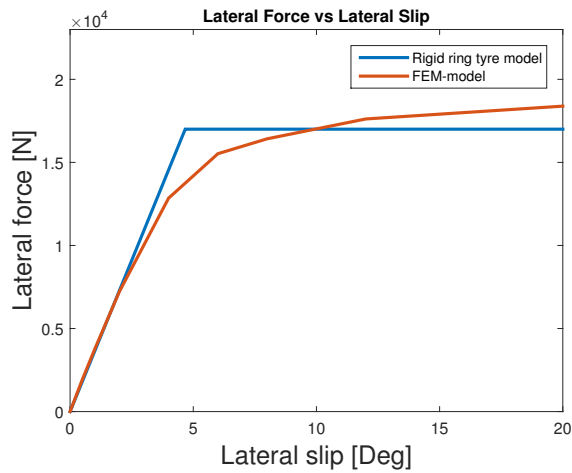


Figure 4.12: *The out of plane angular displacement of the wheel belt.*

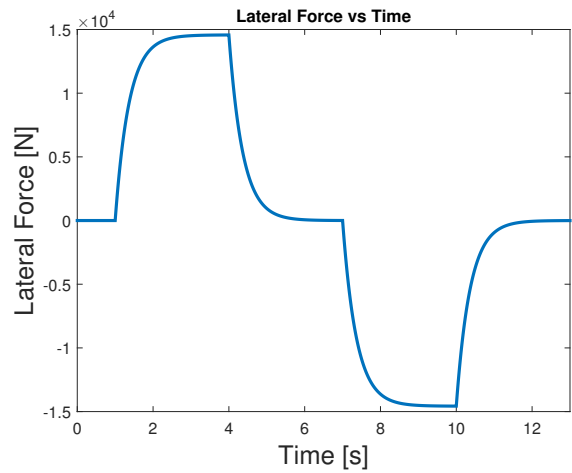
## 4.9 Cornering Stiffness, Rigid Ground

The lateral slip/force relation is also modelled bi-linearly. The first 4 degrees give a good match but above that the match starts to suffer. Since the lateral slip angle usually stays between 0-4 degrees the fit is considered sufficient.

Figure 4.13b shows the lateral force from a simulation where the tyre is driven at constant longitudinal speed. The tyre is given a instant steering angle resulting in a lateral slip angle of 4 degrees. This angle is maintained until steady state is reached. The same thing is done in the opposite direction. A correct behaviour seems to be obtained where the relaxation length causes a delay of the lateral force which can be seen in Figure 4.13b. In Figure 4.13a the result from a simulation where the lateral slip angle is increased and is plotted against the lateral force that arises.



(a) The lateral slip/force relation which is saturated at 17 kN, for a 26.7 kN vertical load.

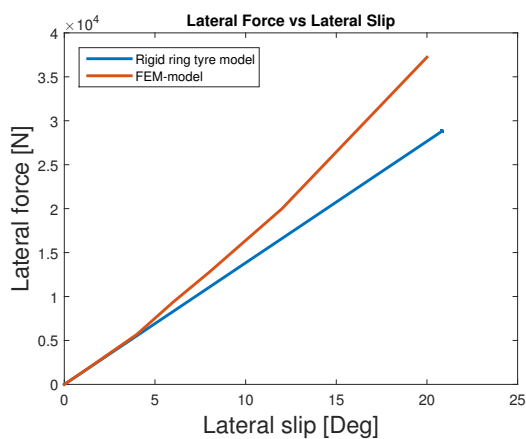


(b) The lateral slip during a simple manoeuvre.

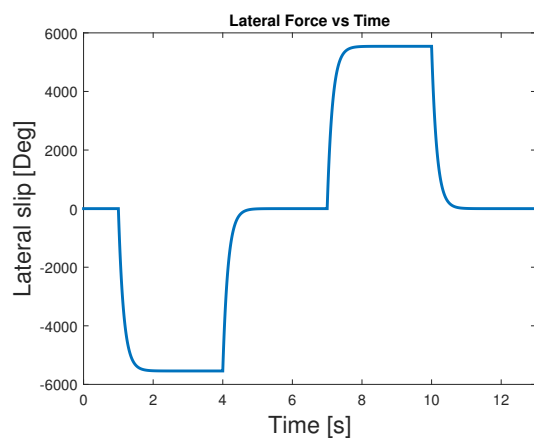
Figure 4.13: Plots over the the lateral slip/force relation and a the lateral force during two different manoeuvres.

## 4.10 Cornering Stiffness, Soft Soil Ground

The cornering stiffness for the soft soil case is verified in the same way as for the rigid ground. However, here the force is never saturated. It is unclear why the cornering stiffness does not decrease but one theory is that due to the sinkage the tyre will always push a small mound of soil in front of it, thus causing this force. As for rigid ground the match with the FE-model is good the first 4 degrees. In Figure 4.14b the result from the same manoeuvre as for rigid ground is shown and one can see that the lateral force is much lower than for rigid ground as it should be and the relaxation length is shorter as well.



(a) The lateral slip/force relation for a 26.7 kN vertical load.



(b) The lateral slip during a simple manoeuvre.

Figure 4.14: Plots over the the lateral slip/force relation and a the lateral force during two different manoeuvres.

## 5 Complete Vehicle Results

To verify the model's behaviour once implemented in the full scale VTM complete vehicle simulations were needed to be performed. A number of simulations were constructed to test all models. There are four mayor simulation types with a few variations within them:

1. Straight line acceleration test
  - (a) Instantaneous acceleration test
  - (b) Delayed acceleration test
  - (c) Delayed acceleration test with resistance compensation
2. Step-steer test
  - (a) Instantaneous steer test
  - (b) Delayed step-steer test
  - (c) Delayed step-steer test with resistance compensation
3. Zigzag test
  - (a) Instantaneous zigzag test
  - (b) Delayed zigzag test
  - (c) Delayed zigzag test with resistance compensation
4. Figure-8 test

The acceleration test was designed to test the longitudinal properties of the models. The step-steer test was designed to test the cornering properties of the models. The zigzag test was designed to further test the cornering properties as well as the overall dynamics of the models. Lastly the figure-8 test was designed to test the a combination of all of the above.

The sub-tests were designed to further investigate each category. The instantaneous tests were used so no prior results were affecting the results. The models are behaving differently during the start-up due to different initial conditions and model differences. Therefore the delayed tests were introduced where the models are kept with a constant speed until 10 s, after which the test is started. To keep the soil models speed constant a driving torque was applied to overcome the resistance forces. During the last test this torque was not removed causing the soil model to manoeuvre more like the other models. The figure-8 test will not be ran with the different sub-test since the resistance compensation will be needed to complete the simulation

The models are started with an initial speed of 15 km/h since the model should operate between 5-25 km/h. All results come from the front left tyre of the vehicle and are represented in its local coordinate system. All the following simulations have used the ode3 solver in Simulink together with a time step of 1/1000 of a second.

There is noticeable difference in the steady state vertical force in the delayed tests. One theory of why this might occur is illustrated in Figure 5.1. Because the torque is applied on the rear wheels, which experience more sinkage, a moment on the vehicle is generated. Thus causing the front wheels to experience a lower vertical reaction force.



Figure 5.1: *Illustration of one theory of why the vertical force is different for the soil model for the delayed tests.*

Also worth noting is that the steady state wheel speed for the rigid ring model differs from the PAC2002 model. This is because they use tyres with different diameters.

Simulations using the delayed test with resistance compensation for 5 and 25 km/h can be found in Appendix A - C

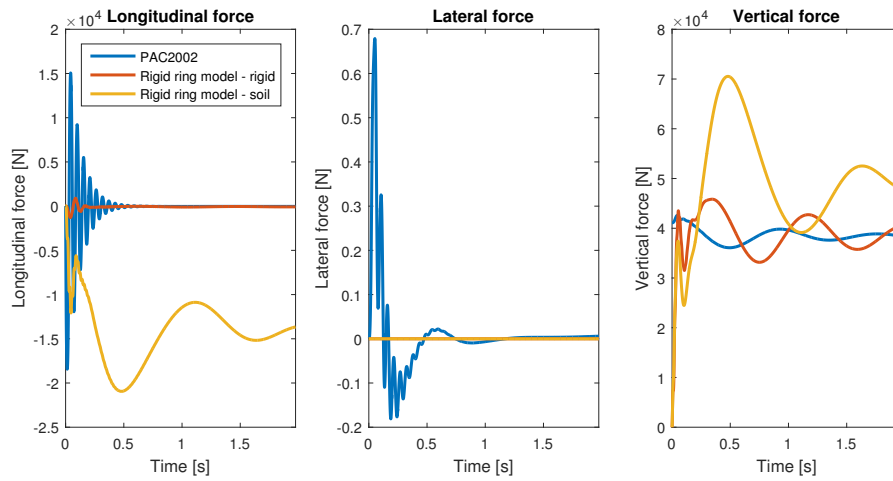
## 5.1 Straight Line Acceleration Tests

The models are started with a constant driving torque of 3000 Nm on each wheel on the two rear axles. The results are from the left front wheel and both rigid models show zero longitudinal force since no torque is applied on this tyre. The longitudinal force in the soil model does however show a negative value due to the resistance forces.

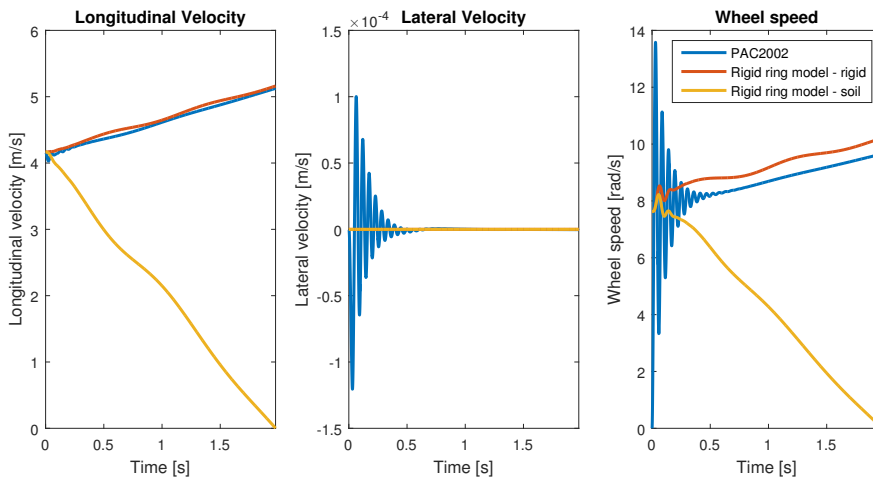
In the vertical direction the force is higher for the soil model since the other models are accelerating and thus rearing. One can also see that the amplitude and period is higher for the soil model. The peak force is higher due to the strong deceleration of the truck making it tilt forward and the period is longer since the total vertical stiffness is lower with the soil inclusion.

Both of the rigid ground models are without resistance forces and are accelerating in a similar manner, the soil model does however decelerate because the applied driving torque is not enough to keep the speed constant.

Keep in mind that the last results, just before the crash when the model for soil reaches zero longitudinal velocity, might not be accurate for the model for soil.



(a) Forces, 15 km/h



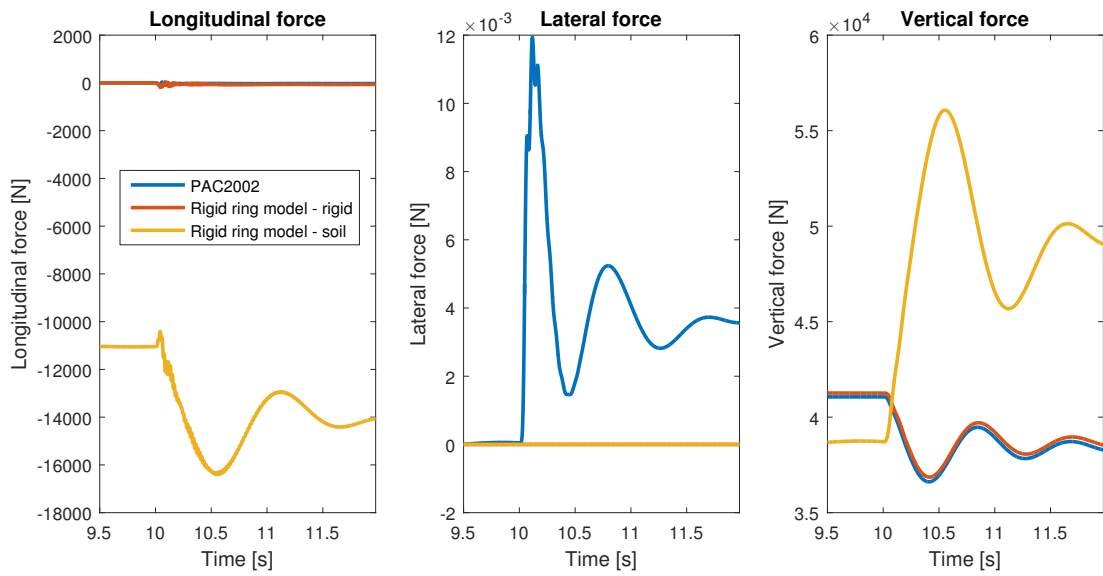
(b) Velocities, 15 km/h

Figure 5.2: The forces and velocities during an acceleration test starting at 15 km/h.

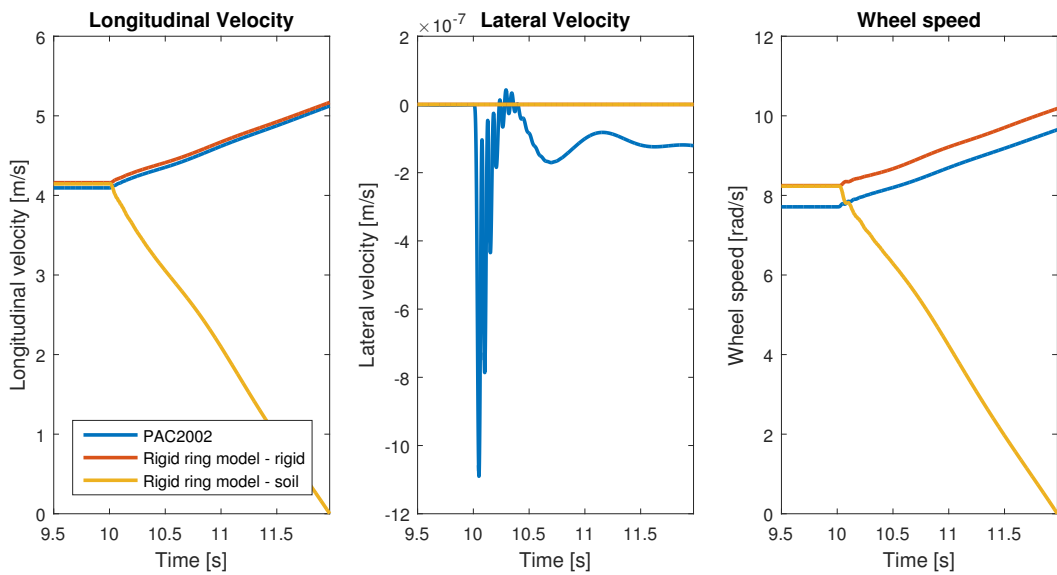
A second test was constructed to negate the effects of the initial start-up of the model. Here a torque was applied on the soil model from the start in order to keep a constant velocity. After 10 s a torque of 3000 Nm is applied on each wheel on the two rear axles causing the rigid models to accelerate and the soil model to decelerate, since the compensating torque was removed from the soil model. One can see that the vertical force between the rigid ground models behave extremely similar. The soil model has again a higher vertical force due to the deceleration.

One can see that the rigid ground models have different steady state values for the vertical force. This is very odd since both should arrive at the same steady state value and no explanation for this has been found. Only the upward pointing reaction force is modelled within the tyre model and the downward facing gravity force is modelled outside the tyre model. Since both models have reached equilibrium this indicates that this counter force has been affected and is not giving a correct value. The difference of around 0.6% is however very small and will likely not affect the overall result, but the error is still there and no cause has been found. A follow up simulation was conducted where no driving torque was applied and it was found that the PAC2002-model reaches the expected value,  $(m \cdot g)$ , while the new model gets a slightly higher value. This confirms that it is the rigid ring model that is behaving incorrectly. Additionally, the soil models vertical steady state force value differs even more from the rigid model. The difference might come from the fact that the model is being kept at a constant speed by applying a torque. Since it is impossible for the soil model to stand still no further test were done for this model.

Keep in mind that the last results, just before the crash, might not be accurate for the model for soil.



(a) Forces, 15 km/h

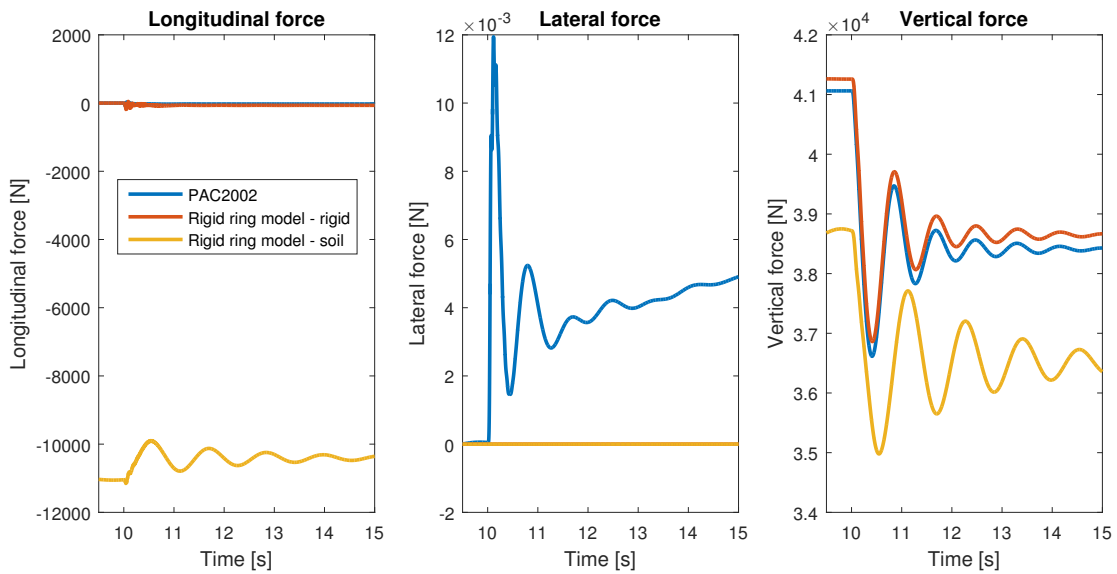


(b) Velocities, 15 km/h

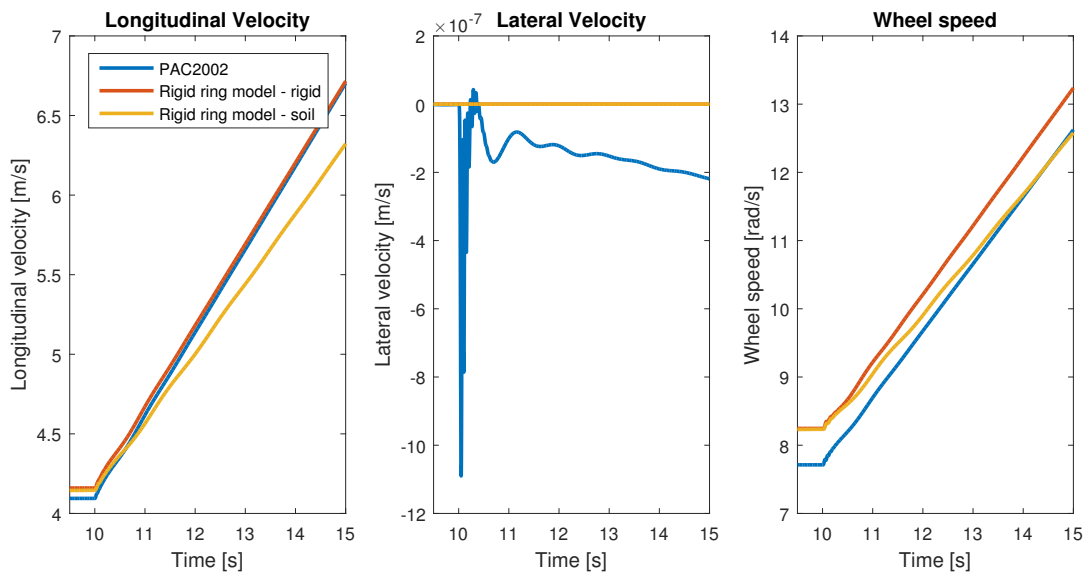
Figure 5.3: The forces and velocities during a delayed acceleration test starting at 15 km/h.

A third test was constructed where all models are allowed to accelerate. This was constructed by starting the soil model with an applied driving torque to keep the speed constant. Then an additional torque, 3000 Nm on each wheel of the two rear axles, was applied on all three models causing them to accelerate.

One can see that the soil model does not accelerate as much as the other models. This is because the soil model reaches its saturation value for the slip force and cannot match the other models. The torque used to keep the soil model driving at a constant speed gives a slip of around 18 % which is already close to the saturation limit. Once the additional torque is applied the slip goes beyond the saturation value and can accommodate for all the extra torque from the rolling resistance force.



(a) Forces, 15 km/h



(b) Velocities, 15 km/h

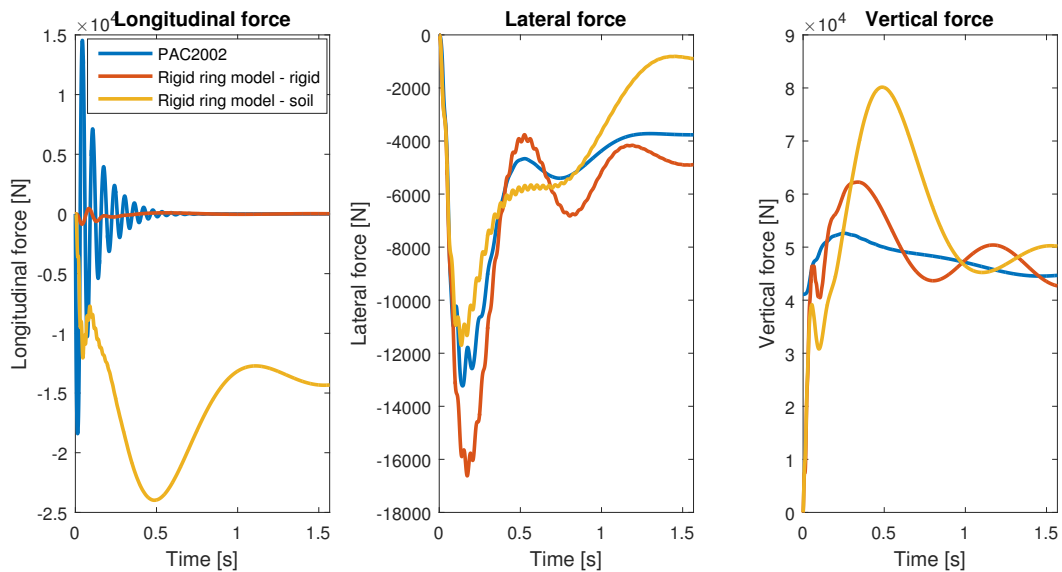
Figure 5.4: The forces and velocities during a delayed acceleration test with counter torque on soil model starting at 15 km/h.

## 5.2 Step Steer Test

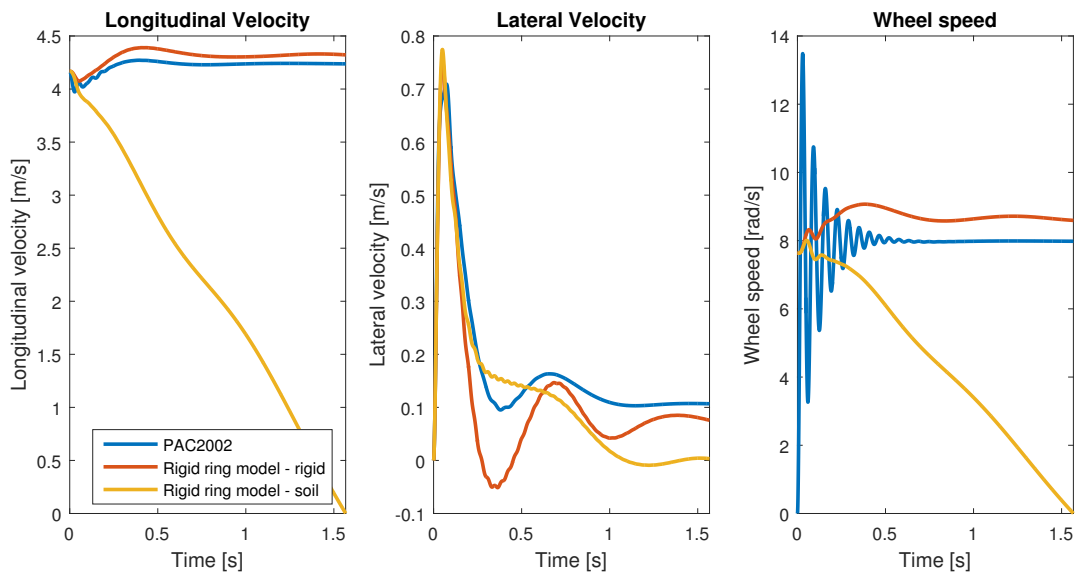
In the same manner as in the acceleration test three tests are set up for the step steer test. In the first test the models are started with constant steering angle of  $12^\circ$  to the right. The models are ran until the soil model crashes due to too low longitudinal velocity.

The lateral force shows a similar behaviour between the models, with the PAC2002 model showing a more damped behaviour than the rigid ring model. The soil model has the overall lowest lateral force which makes sense due to its lower cornering stiffness and relatively low lateral velocity. The vertical force shows a much larger amplitude than the other models.

Keep in mind that the last results, just before the crash, might not be accurate for the model for soil.



(a) Forces, 15 km/h



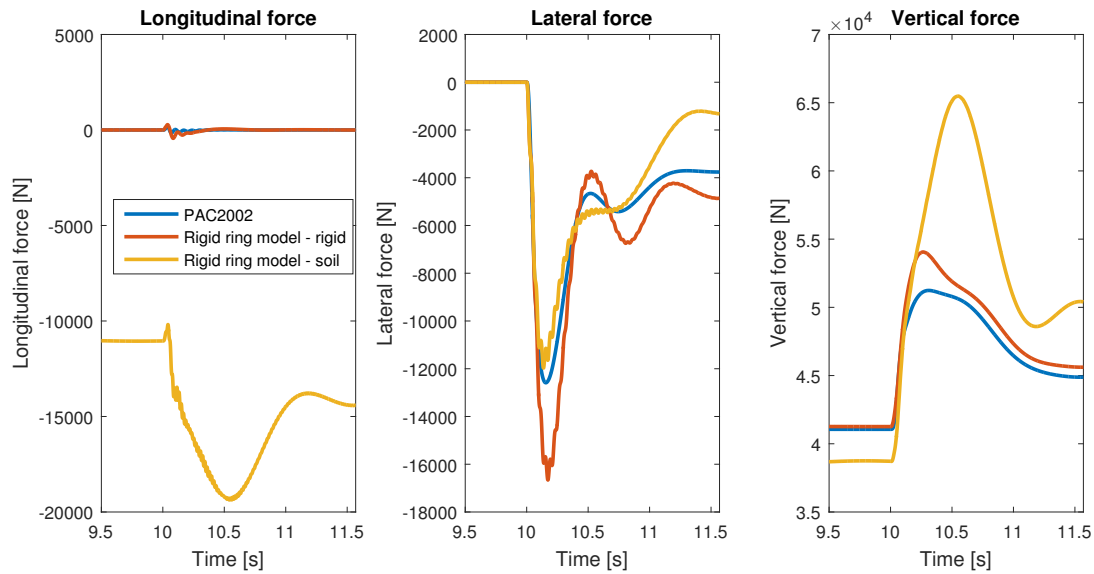
(b) Velocities, 15 km/h

Figure 5.5: The forces and velocities during a step steer test starting at 15 km/h.

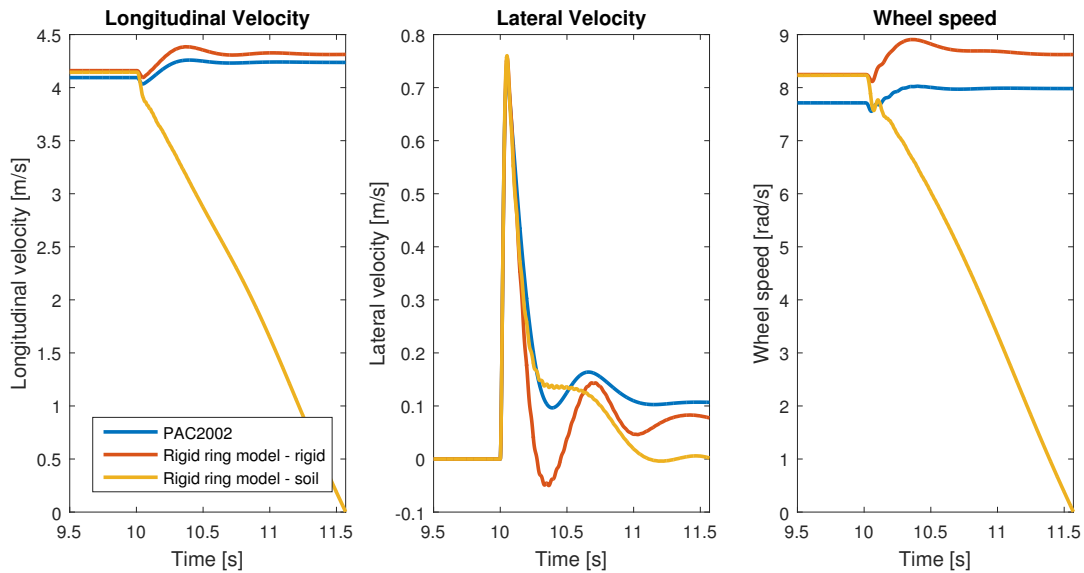
In the second test the models are kept at a constant speed to negate the difference in initial conditions between the models. The applied torque on the soil model, countering the resistance force, is then removed as the steering angle is applied.

The results from this simulation is very similar to the previous one. The only real difference seems to be that the initial effects on the longitudinal force and wheel speed are negated.

Keep in mind that the last results, just before the crash, might not be accurate for the model for soil.



(a) Forces, 15 km/h

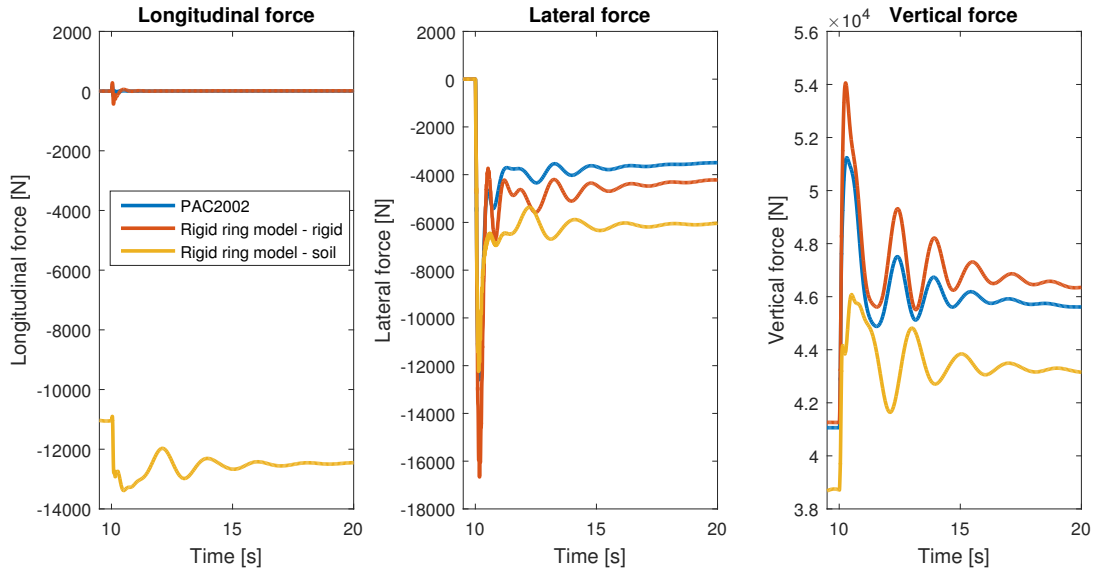


(b) Velocities, 15 km/h

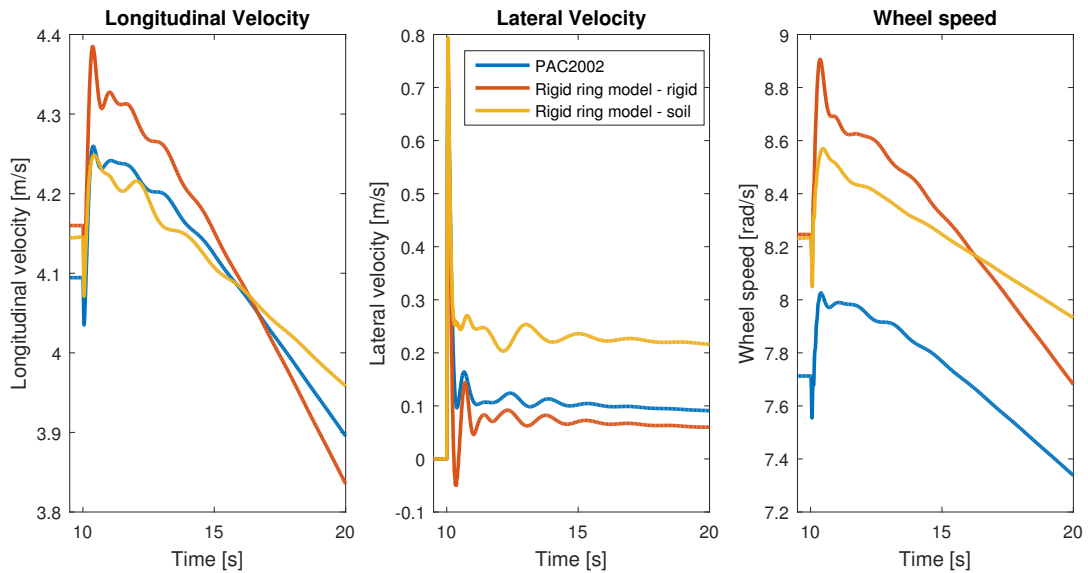
Figure 5.6: The forces and velocities during a delayed step steer test starting at 15 km/h.

A third test was performed where the torque that counters the resistance was continued throughout the entire simulation.

During this simulation the soil model gets the highest lateral reaction force. This is because the compensating torque causes this model to do a slightly different manoeuvre. One can also see that the soil model is the least decelerating model which also causes a lower vertical force on the front of the vehicle. The overall results show the same characteristics for all three models during this simulation.



(a) Forces, 15 km/h



(b) Velocities, 15 km/h

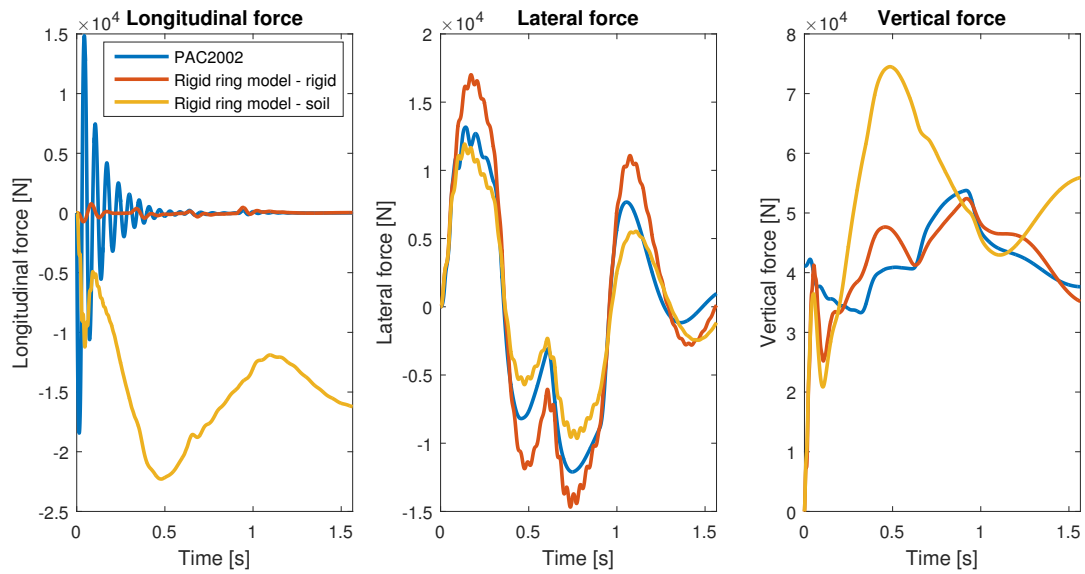
Figure 5.7: The forces and velocities during a delayed step steer test with counter torque starting at 15 km/h.

### 5.3 Zigzag Steer Test

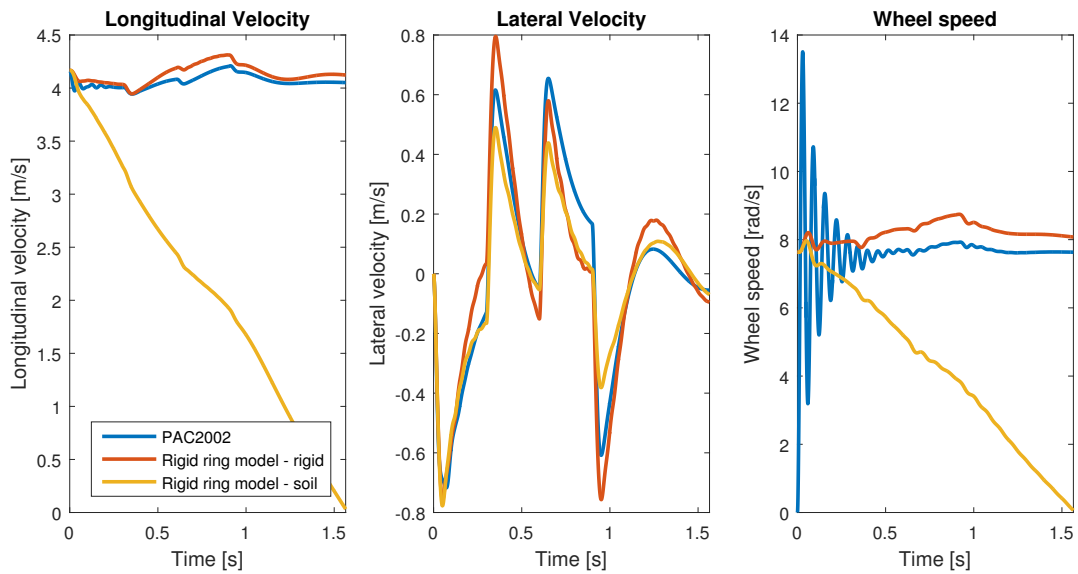
This test is similar to the step steer test but a bit more complex. As before both models are given an initial speed and once steady state is reached a steer input of  $12^\circ$  is applied for 0.3 seconds. After this the vehicle drives straight ahead for another 0.3 seconds until a steer input of  $12^\circ$  is applied in the other direction for 0.3 seconds. After that the vehicle is driven straight ahead.

The lateral response, both force and velocity, all show very similar behaviour for all models. For these quick manoeuvres the lateral force is, however, lower for soil ground than rigid.

Keep in mind that the last results, just before the crash, might not be accurate for the model for soil.



(a) Forces, 15 km/h



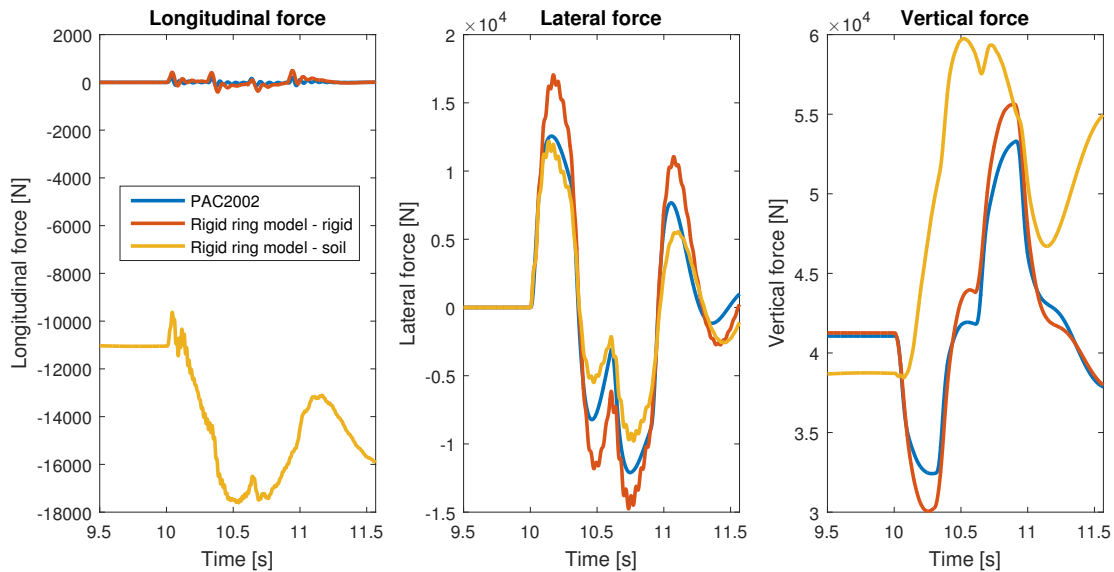
(b) Velocities, 15 km/h

Figure 5.8: The forces and velocities during a zigzag steer test starting at 15 km/h.

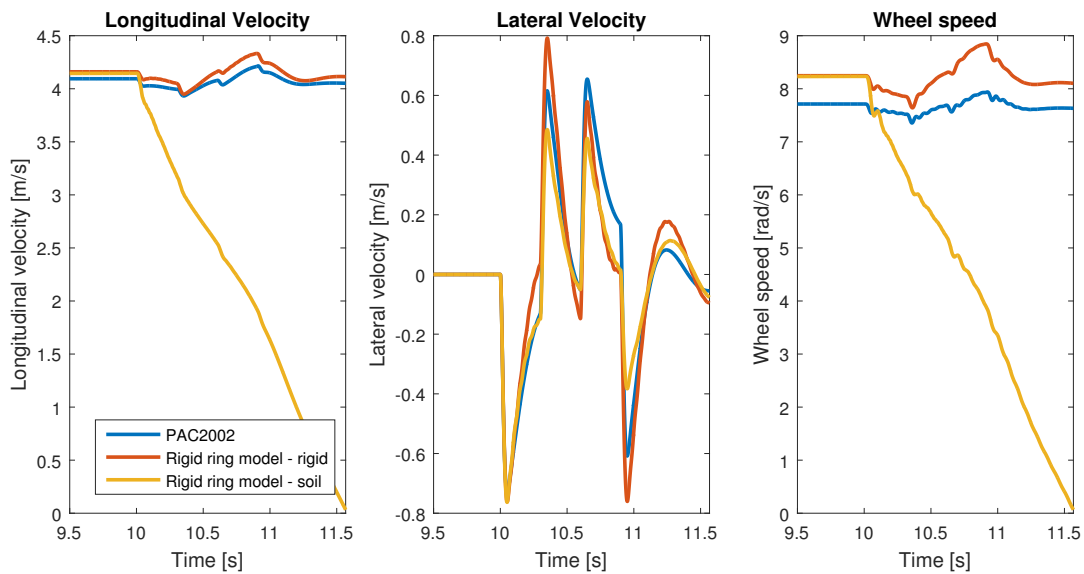
During this simulation a torque countering the resistance force is applied on the soil model giving all three models a constant speed. After 10 s the torque is removed and the manoeuvre began. This was done to negate effects from the simulation start up.

Again in this test it is the vertical force that stands out. It does however follow the other models results closer than the previous simulation. All other properties follow the behaviour from the previous simulation.

Keep in mind that the last results, just before the crash, might not be accurate for the model for soil.



(a) Forces, 15 km/h

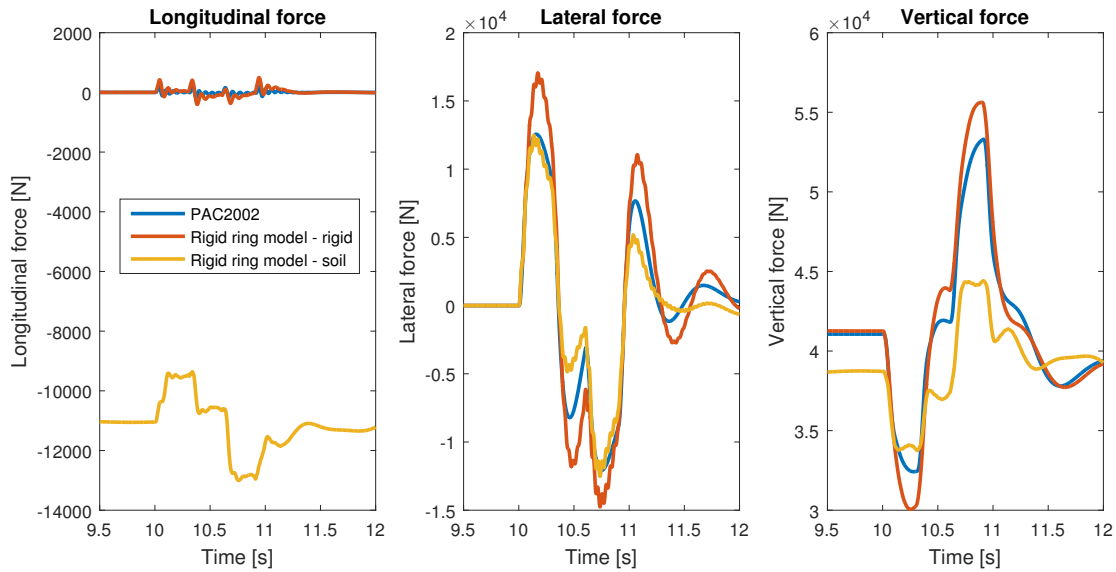


(b) Velocities, 15 km/h

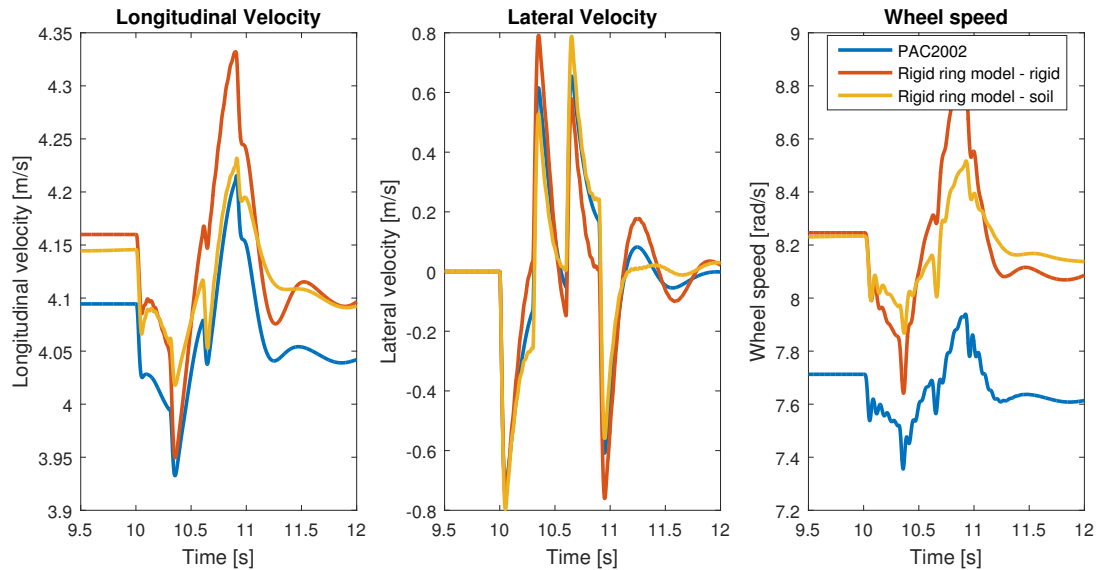
Figure 5.9: The forces and velocities during a zigzag steer test starting at 15 km/h.

This simulation is identical to the previous one with the difference that the counter torque on the soil model is not removed.

The longitudinal properties in the soil behaves as expected with the counter torque applied, they also behave very similar to the other models. In the previous simulations the soil models vertical force has deviated greatly from the other models. During this simulation it does however behave as the other models. One theory in the previous results was that it was the vertical properties of the soil causing this behaviour. This result does however indicate that it might rather be the longitudinal resistance forces from the soil that caused the previous behaviour.



(a) Forces, 15 km/h



(b) Velocities, 15 km/h

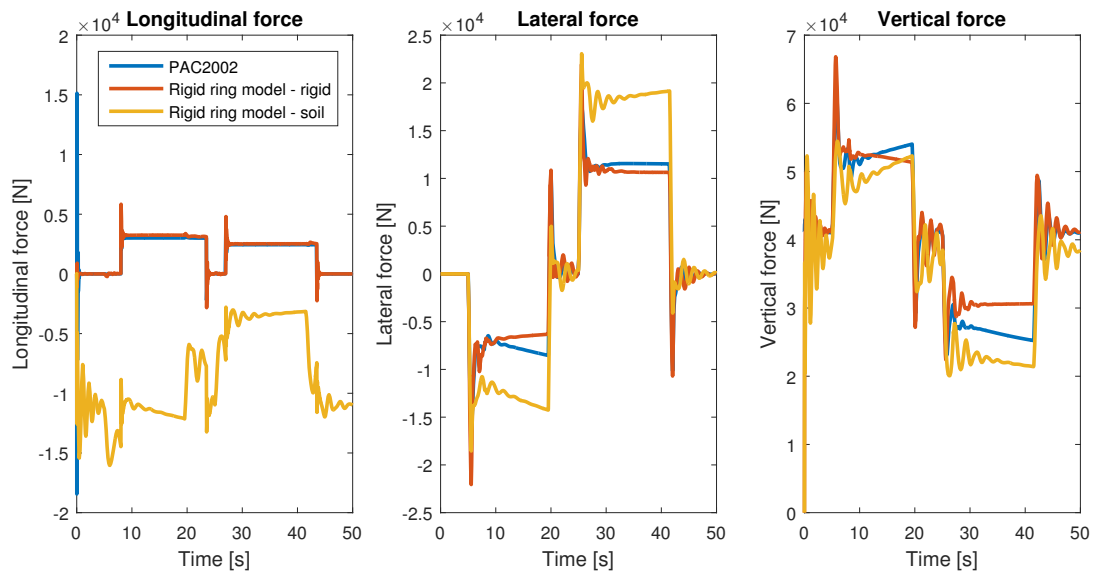
Figure 5.10: The forces and velocities during a delayed zigzag steer test with counter torque starting at 15 km/h.

## 5.4 Figure-8 test

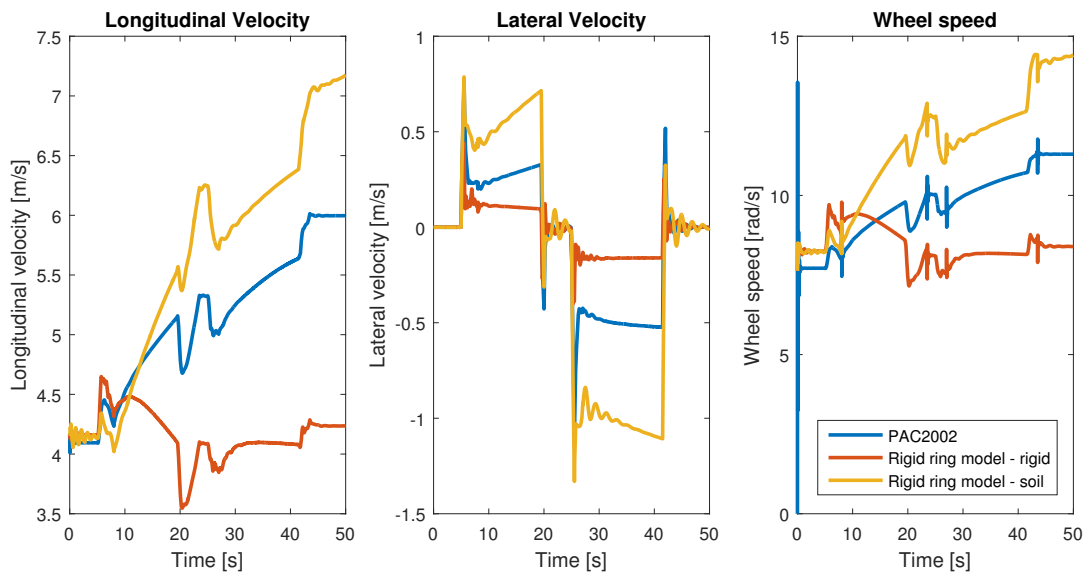
During this test the initial speed is tried to be maintained, during a steering manoeuvre, by applying a driving torque. The steering manoeuvre consists of driving in a figure-8 with wheel angles of 25 degrees ramped up over half a second. The applied driving moment is tuned so that the rigid ring model is driving at a somewhat constant speed. To be able to include the soil model in the simulation the constant counter torque used in the previous simulations is used here as well.

As seen below the overall behaviour shows some resemblance. It is however clear that the models are reacting differently to the applied torque. The rigid ground, for which the inputs are designed, shows the least amount of acceleration. The PAC2002 model does show a significant amount of acceleration. Since the acceleration test show a great resemblance between these two models it is likely the higher lateral forces causing the slow down. Since the vehicle is turning some part of the local lateral forces will be pointing in the reverse longitudinal direction on a global scale.

The soil model has an additional torque that is kept constant during the entire manoeuvre. This torque is designed to keep the soil model at a constant speed while driving straight ahead. It is this additional moment that causes this model to accelerate further.



(a) Forces, 15 km/h



(b) Velocities, 15 km/h

Figure 5.11: The forces and velocities during a figure-8 test starting at 15 km/h.

## 6 Future Work

Due to the time frame of this project there was not enough time to further investigate certain behaviours and models. In order to not lose this information some of the more interesting further suggestions are presented here for future reference.

### 6.1 More Detailed Rolling Resistance Modelling

The resistance forces are for now approximated from one simple test in previous work [7]. The resistance forces could be modelled more thoroughly using theory derived by Bekker.

One effect that should be taken into consideration is the rolling resistance force arising from deformation of the soil underneath the tyre, the rut formation. There are several ways to describe this force; the empirical WES-model developed by a US army research group and the semi-empirical model based on Bekker's work are the ones most suitable for implementation in VTM. In the previous progress reports the constants in Bekker's equation have been determined and therefore his model is the most suitable to implement [5]. The rut rolling resistance force,  $F_R$ , can be calculated as in equation 6.1 as described by Bekker and compiled by Macmillan [13].

$$F_R = \frac{\left(\frac{3W}{(3-n)\sqrt{D}}\right)^{\frac{2n+2}{2n+1}}}{(n+1)(k_c + bk_\Phi)^{\frac{1}{2n+1}}} \quad (6.1)$$

Here  $b$  is the width of the contact area,  $D$  is the diameter of the tyre,  $k_c$ ,  $k_\Phi$  and  $n$  are soil parameters from the Bekker equation and  $W$  is the vertical force on the tyre.

The bulldozing resistance is another force acting in the direction opposing the motion of the vehicle. It represents the force needed to push a small mound of soil in front of the tyre, see Figure 6.1.

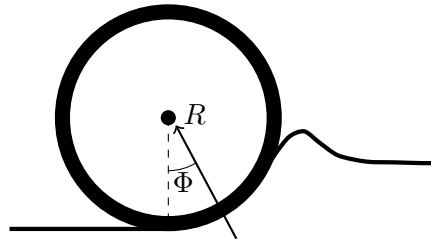


Figure 6.1: *Illustration of a soil mound causing the bulldozing effect.*

The bulldozing resistance force can be calculated as seen in equation 6.2 developed by Bekker.

$$F_B = \left[ \frac{b \sin(\alpha + \Phi)}{2 \sin(\alpha) \cos(\Phi)} (2z_3 c K_c + \rho g z_3^2 K_\gamma) + \frac{\pi t^2 \rho g (90^\circ - \Phi)}{540} + \frac{\pi c t^2}{180} + c t^2 \tan\left(45^\circ + \frac{\Phi}{2}\right) \right] \quad (6.2)$$

where  $K_c$  and  $K_\gamma$  are constants which can be found in "Introduction to the Mechanics of Space Robots" [14].

$c$  is the cohesive bearing strength and  $\Phi$  represents the angle of the reaction force.  $\alpha$  and  $t$  are

calculated as:

$$\alpha = \arccos\left(1 - \frac{z_3}{R_0}\right), \quad t = z_3 \tan^2\left(45^\circ - \frac{\Phi}{2}\right)$$

The total longitudinal force acting on the outer ring can then be found as:

$$F_x = F_{sx} - F_{wx} - F_R - F_B \quad (6.3)$$

## 6.2 Different Vertical Soil Models

The non-linear soil model adopted in the latter parts of this project needs further investigation. This is one of the next steps at the University of Ontario Institute of Technology. With further studies in this model a more refined approximation of the soil can be found. This requires more tests to be able to find more precise values than the ones approximated in this project.

In this project the soil model have not been used in its entirety, since it could not be made to behave correctly. The stiffness is considered constant which means that the equivalent stiffness,  $k'_{\text{soil}}$ , has been removed from the model. This, supposedly low, stiffness gave values higher than the static stiffness even at low frequencies and was therefore removed. The equivalent damping,  $c'_{\text{soil}}$ , however gave a good fit due to its frequency dependency.

More advanced ways of modelling the soil can be achieved by including other types of building blocks in addition to spring, damper and mass components. The friction damper could give the model another energy dissipation method which could more accurately depict soil behaviour.

Only one soil has been implemented and studied in this project, Clayey soil (Thailand), and it is unclear how accurate the model will be for soils with lower cohesion, e.g. dry sand, which has proven problematic in the previous work.

### 6.2.1 Local slope

The local slope behaviour implemented in this project has not been investigated enough. While an effect like this is needed for the investigated soil model it might not be needed for more refined models.

## 6.3 Further Studying of Parameters

Besides the flaws mentioned in previous sections, 6.1 and 6.2, the model seems to be working as it should. However, some thoughts have been put into the need of further investigating the accuracy of the parameters in the model.

### 6.3.1 Fictive Mass, Soil Damping and Removing Masses

Since the fictive mass and the soil damping had not been considered before this project, further studying is needed. By designing soil tests, with a rigid wheel, the soil damping can be found without interference from frequencies in the tyre. In addition the fictive soil mass, giving the soil its inertial properties, needs to be further investigated to find appropriate values and how it depends on other physical quantities.

One could also try removing some masses like the tyre belt mass,  $m_2$ . The low level dynamics occurring at that point might not be relevant for the complete vehicle dynamics.

### 6.3.2 Vertical Residual Damping

The vertical residual damping,  $c_{vr}$ , needs further investigation when coupled with soil. In order to get a behaviour corresponding to the FEA results this parameter needed to be increased significantly, by a factor of 10. The parameter has been treated as a tyre parameter in the previous work and was therefore not investigated for soil. However, since this parameter acts in the contact between the soil and the tyre it is possible that the soil will have an effect.

### 6.3.3 Longitudinal Tyre Stiffness for Soil

In the current soil tyre model the longitudinal tyre stiffness that is used is the one calculated for rigid ground. This is because there were suspicions about the calculations being wrong as the rolling resistance were included when calculating the longitudinal tyre stiffness.

## 6.4 Friction limit

Now the longitudinal and lateral slip forces are saturated independently. This does not follow the theory of the friction circle which states that it is the combined slip forces that should be saturated. This is only a problem when operating on the extreme friction limit which means that it should not have affected the results.

## 6.5 Optimising the S-function

Not much time has been put into optimising the S-function. The main focus has been on making the model work properly leaving no time to optimise it. Some thought about possible optimisation has however been had. First is to change the states to the difference between the states that are defined now. For example the states,  $x_1$  and  $x_2$  can be changed to one state that is the difference between them. This can be done in most cases as the springs and dampers depends on the difference between two positions and velocities.

Another area which has not been investigated thoroughly is the influence of solver and the time step. During this project the fixed step solver ode3 has been used together with a time step of 1/1000 of a second. With a variable step solver or a longer time step faster simulations could be achieved as well.

## 6.6 Real World Test Data

The results for the soft soil do not have any data to be verified against. To further improve and verify the soft soil model, real world tests would need to be conducted. By comparing real world manoeuvres one could investigate how well the model behaves overall as well as pinpointing where problems occur in the model. It would be difficult to design such a test since giving and keeping the soil at certain conditions could be very hard.

## 7 Conclusion

This project treats a tyre model called the "Rigid ring model" and an accompanying soil model. The tyre model has been tested using a single tyre, disconnected from the complete vehicle. The tyre model has also been tested in a complete vehicle by simulating a set of manoeuvres.

For the single tyre model, good results were found for rigid ground. Most of the simulations showed really good results with some errors due to the non-linearity of the FE-model. The slip/force relation has shows relatively good results for the most crucial slip values. However, the result for higher slip values of the bi-linear model is not satisfactory and relatively high errors are present. The behaviour is still considered acceptable because a vehicle usually does not experience those levels of slip.

With the rigid ring model implemented in the complete vehicle model good results has been found for both implemented with rigid and soft soil ground. When comparing outputs for the rigid ring model and PAC2002 for the same manoeuvre, on rigid ground, the outputs behave very similarly. The behaviour is not an exact match but that is not expected since these are two different models, one physical and one semi-empirical, with a large difference in the number of degrees of freedom. The steady state value of the vertical force,  $F_z$ , differs between the two models which is very strange but no reason for this has been found.

Since the only existing results for soft soil ground are the verification tests for single tyre the overall dynamic behaviour for the complete vehicle model is uncertain. The behaviour does, however, feel intuitively correct on an overall level and the single tyre verification gave satisfactory results.

The soil modelling has proved to be problematic in the vertical direction and a completely physical working model has not been found. The non-linear soft soil model introduced by Wong [10] has given successful results with some modification, the equivalent stiffness,  $k'_{soil}$ , that arises from the spring in series with the damper was neglected since it gave a very high stiffness contribution, even at low frequencies. The modified model, however, captures the soil behaviour accurately with the shortcoming that it can not capture the extreme non-linearity in the FE-model.

There were also uncertainties in the longitudinal tyre stiffness due to questionable results and methods in progress report phase XII [8]. The rolling resistance force was included by lowering the tyre stiffness which was not an satisfactory way of modelling. By further research and FE-simulations a better longitudinal soil model could be found which could easily be verified in the single tyre model since the underlying dynamics are implemented.

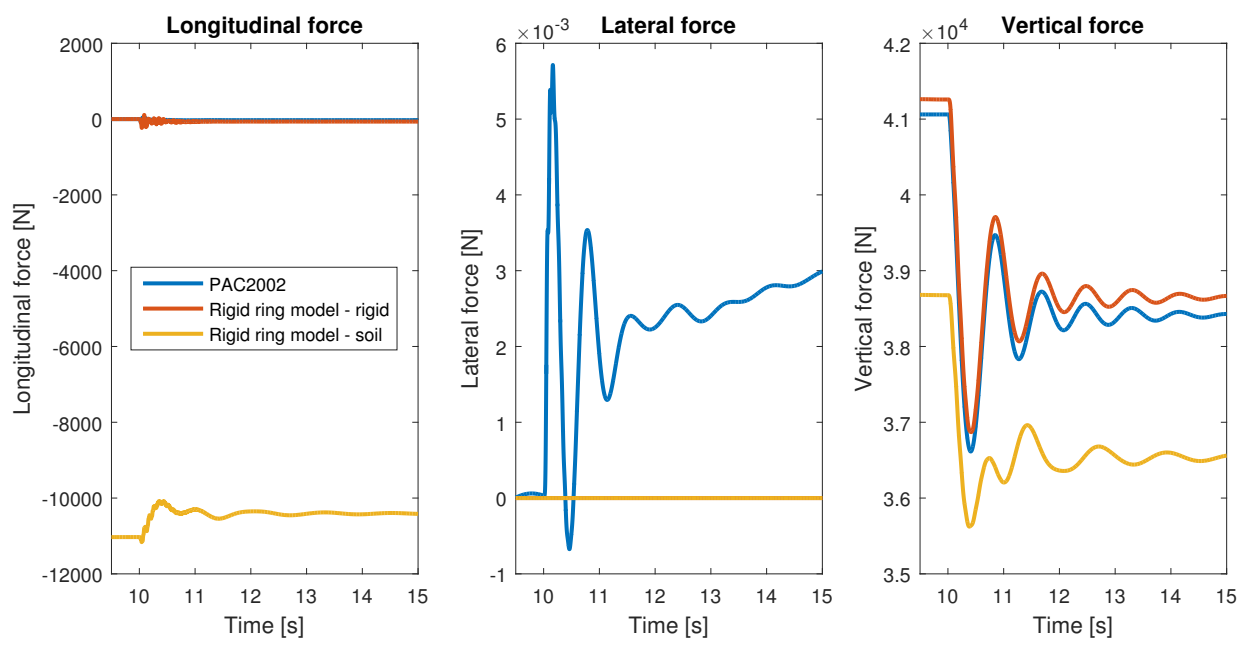
For both the rigid and soft soil ground problems occur when the longitudinal velocity is close to zero. This is due to the definition of longitudinal slip that includes division with the longitudinal velocity. This ends up causing a singularity of the longitudinal slip for low velocities. The slip force has, however, been modeled to be independent of the actual slip but as the actual slip is an output this is still a problem. As the range of the velocity was set to 5-25 km/h this problem was not prioritised. In PAC2002 it is mentioned that this model also had problems at low speeds but by implementing a modified definition of the slip the problem was mitigated. This solution has not been investigated and therefore not been implemented in the rigid ring model. A similar solution might be able to implement if velocities close to zero are wanted to be investigated.

For soft soil ground, the same problem occurs when calculating the fictive mass. As the frequency goes towards zero with the velocity and the calculation of the fictive mass includes division with the frequency the same problem occurs as for the longitudinal slip.

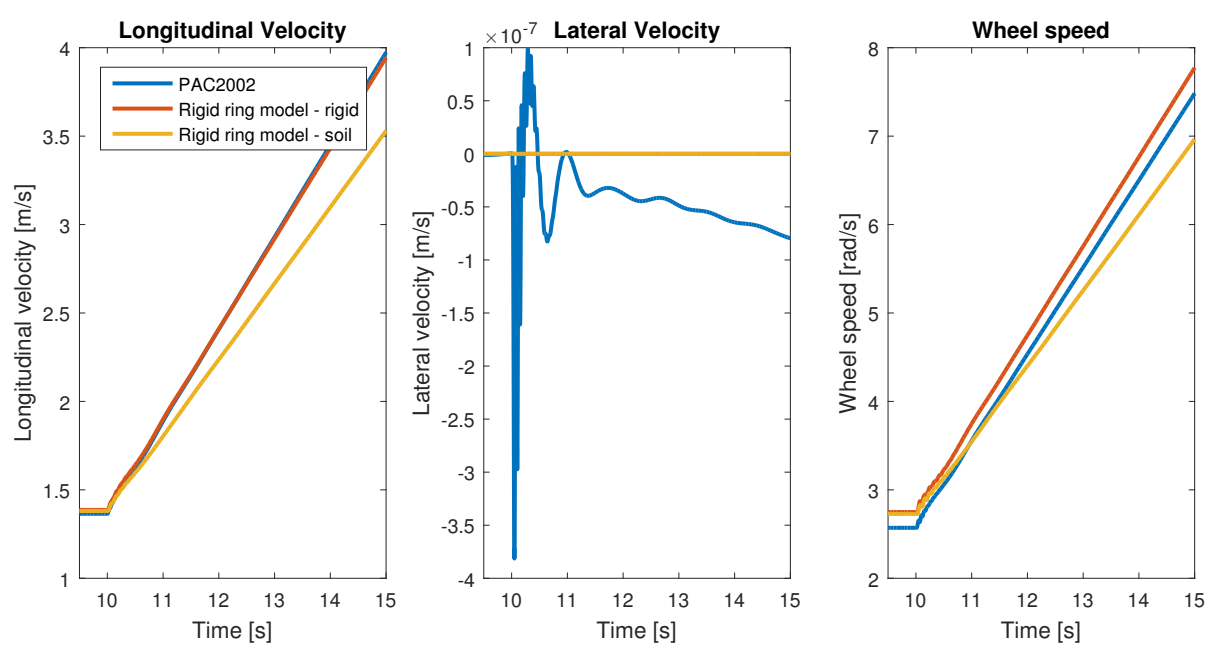
## References

- [1] J. Allen-II and M. El-Gindy. “Phase V: Tire-Soft Terrain Modeling and Interaction Simulation”. Volvo project in collaboration The Pennsylvania State University. May 2007.
- [2] J. Slade, R. Lescoe, and M. El-Gindy. “Part 1: Determination of the In-Plane Rigid Ring Parameters for the Off-Road Tire RHD 315/80R22.5 on Rigid and Soft Soil”. Volvo project in collaboration The Pennsylvania State University. Nov. 2008.
- [3] J. Slade, R. Lescoe, and M. El-Gindy. “Part 2: Determination of the Out-Of-Plane Rigid Ring Parameters for the Off-Road Tire RHD 315/80R22.5 on Hard and Soft Soil”. Volvo project in collaboration The Pennsylvania State University. Nov. 2008.
- [4] D. Maciejewski, R. Lescoe, and M. El-Gindy. “Part 2: Determination of the Out-Of-Plane Rigid Ring Parameters for the 3-Groove Tire on Rigid and Soft Soil”. Volvo project in collaboration The Pennsylvania State University. Aug. 2009.
- [5] J. Slade, R. Lescoe, and M. El-Gindy. “Phase VIII: Advanced Soil-Modeling”. Volvo project in collaboration University of Ontario Institute of Technology. Mar. 2012.
- [6] M. El-Gindy, R. Ali, and R. Dhillon. “Phase VIII: Advanced Soil-Modeling”. Volvo project in collaboration with University of Ontario Institute of Technology. Apr. 2012.
- [7] M. El-Gindy, R. Ali, and R. Dhillon. “Phase VIII: Advanced Soil-Modeling Soiltype: clayey soil (Thailand)”. Volvo project in collaboration with University of Ontario Institute of Technology. June 2012.
- [8] A. Reid, D. M. El-Gindy, and R. Dhillon. “Development of an off-road rigid ring tire model for RHD truck tires in soft soil”. Volvo project in collaboration with University of Ontario Institute of Technology. Aug. 2013.
- [9] A. Reid and D. M. El-Gindy. “Rolling resistance results of august 2014 Volvo test track experiment”. Volvo project in collaboration with University of Ontario Institute of Technology. Jan. 2015.
- [10] J. Y. Wong. *Theory of Ground Vehicles*. 4th. John Wiley and sons, 2008.
- [11] MSC-Software. *Adams/Tire Using the PAC2002 Tire Model*.
- [12] M. Emam et al. A tyre-terrain interaction model for off-road vehicles. **3(7)** (July 2011).
- [13] R. Macmillan. *The Mechanics of Tractor - Implement Performance: Theory and Worked Examples*. University of Melbourne. 2002.
- [14] G. Genta. *Introduction to the Mechanics of Space Robots*. Springer Verlag, 2012.
- [15] A. Schmeitz. “A Semi-Empirical Three-dimensional Model of the Pneumatic Tyre Rolling over Arbitrarily Uneven Road Surfaces”. PhD thesis. De Technische Universiteit Delft, 2004. ISBN: 90-9018380-9.
- [16] P. Tomaraee et al. Relationships among the contact patch length and width, the tire deflection and the rolling resistance of a free-running wheel in a soil bin facility. **13.2** (June 2015). Spanish Journal of Agricultural Research.

# A Straight Line Acceleration Test

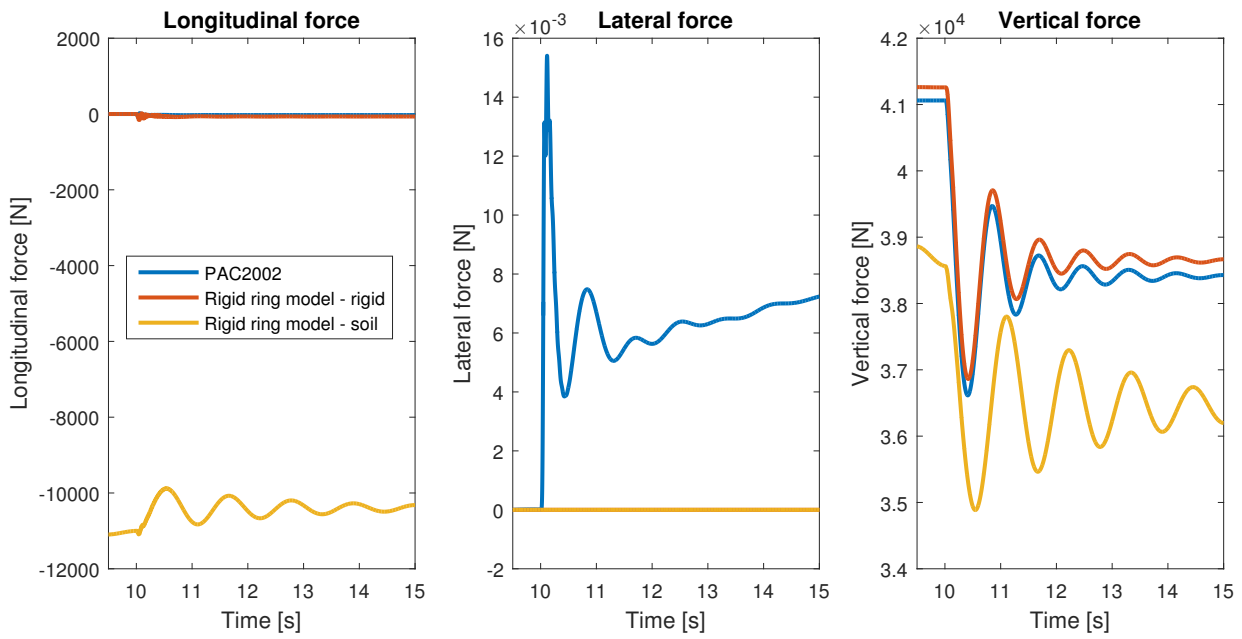


(a) Forces, 5 km/h

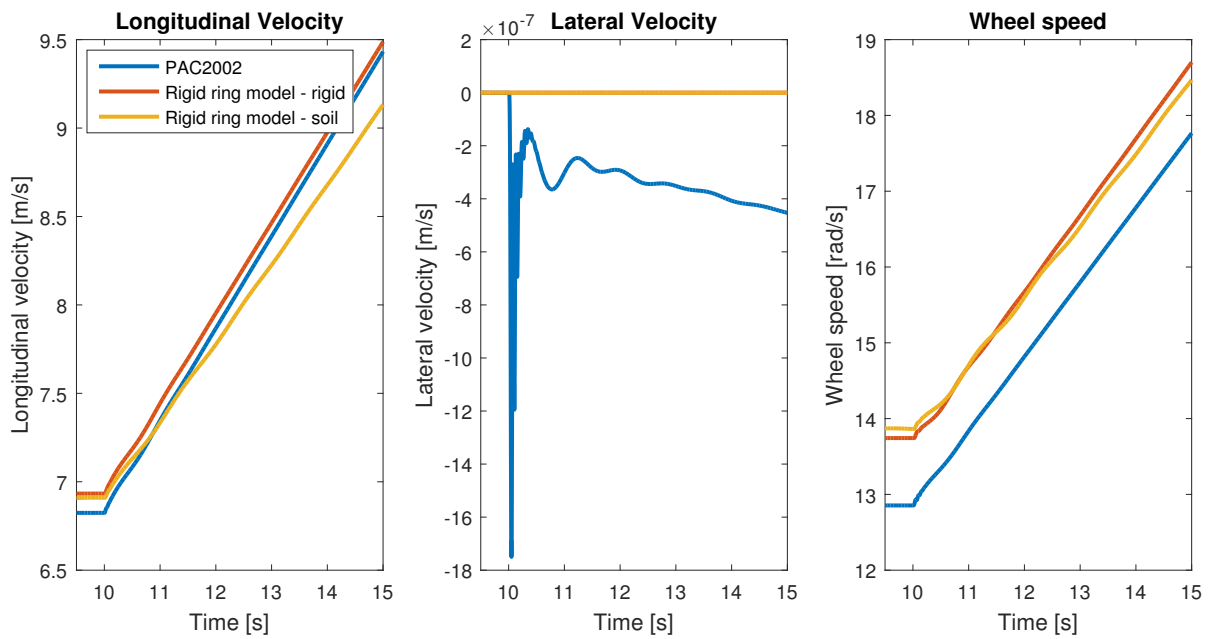


(b) Velocities, 5 km/h

Figure A.1: The forces and velocities during a straight line acceleration test starting at 5 km/h.



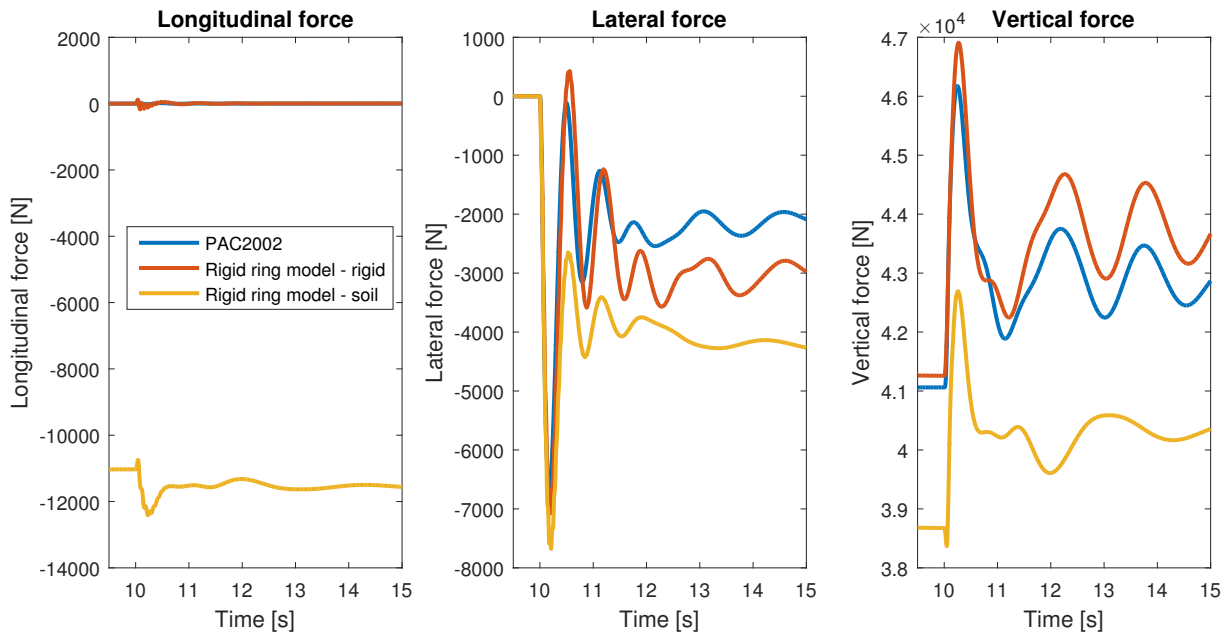
(a) Forces, 25 km/h



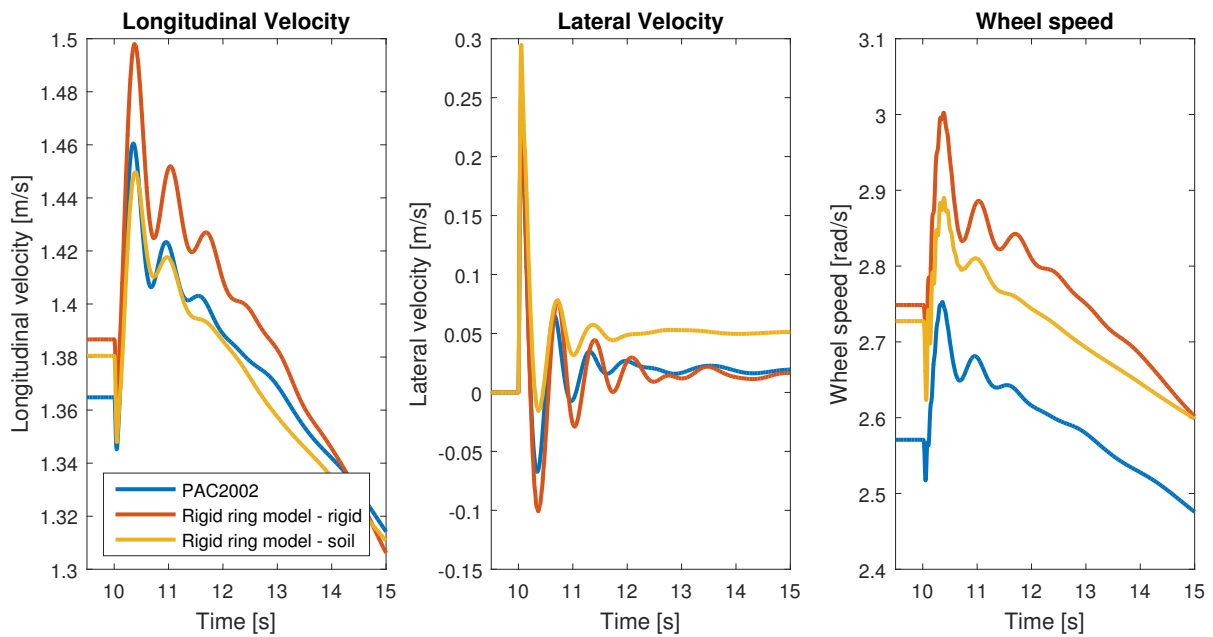
(b) Velocities, 25 km/h

Figure A.2: The forces and velocities during a straight line acceleration test starting at 25 km/h.

## B Step-Steer Test

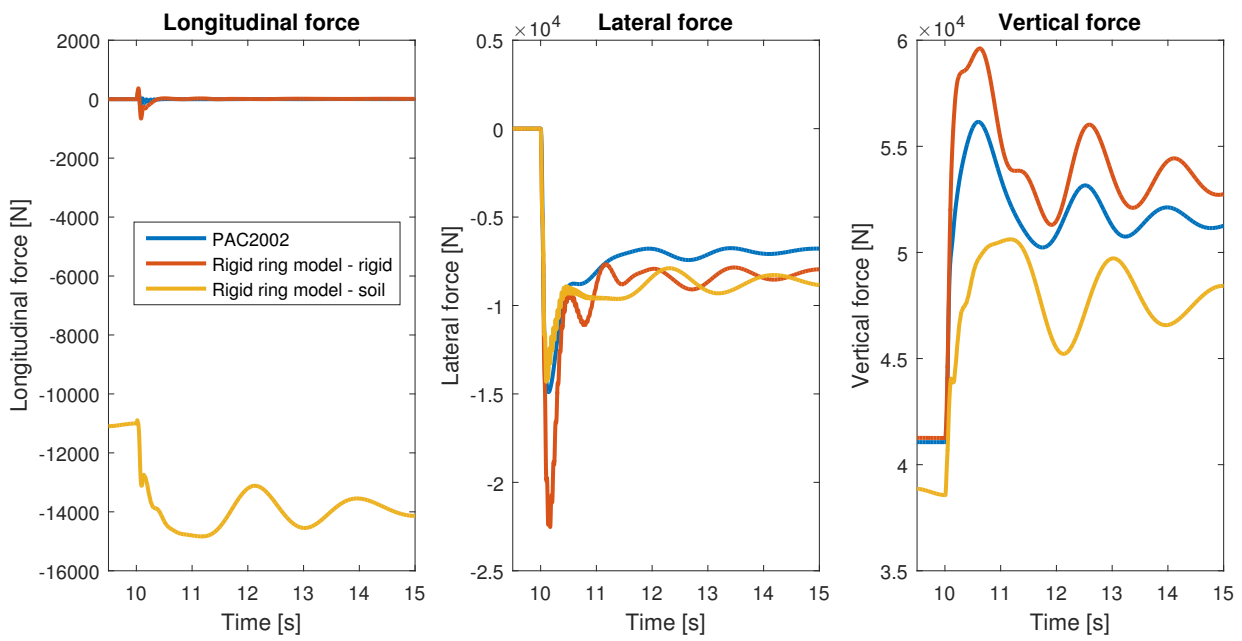


(a) Forces, 5 km/h

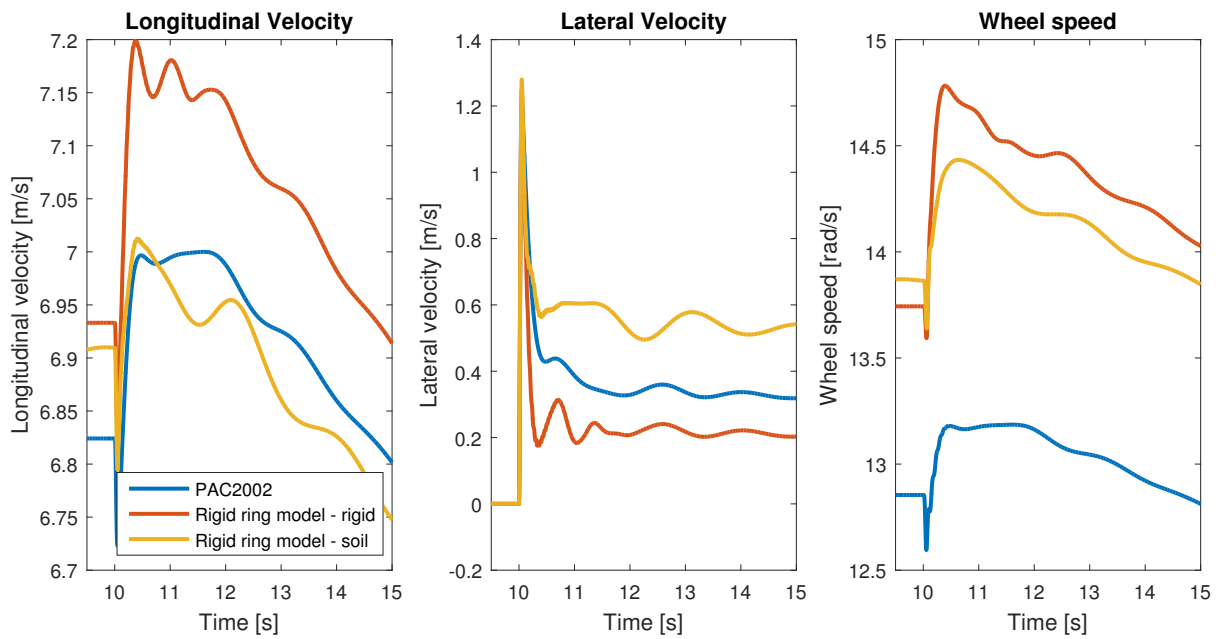


(b) Velocities, 5 km/h

Figure B.1: The forces and velocities during a step-steer test starting at 5 km/h.



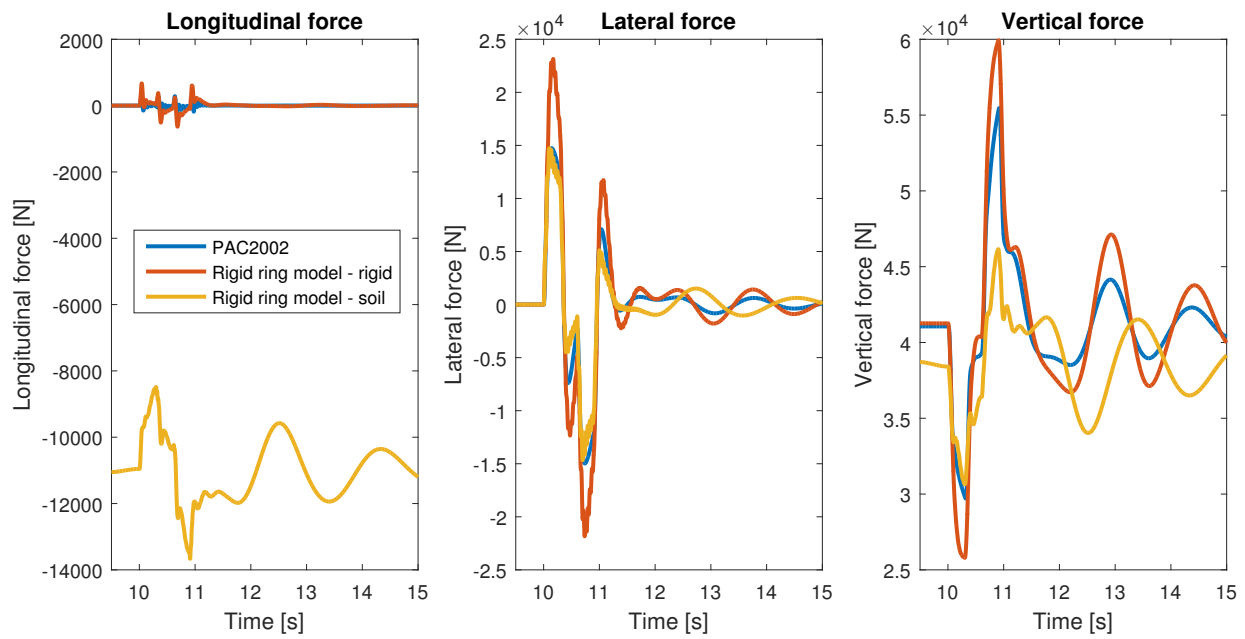
(a) Forces, 25 km/h



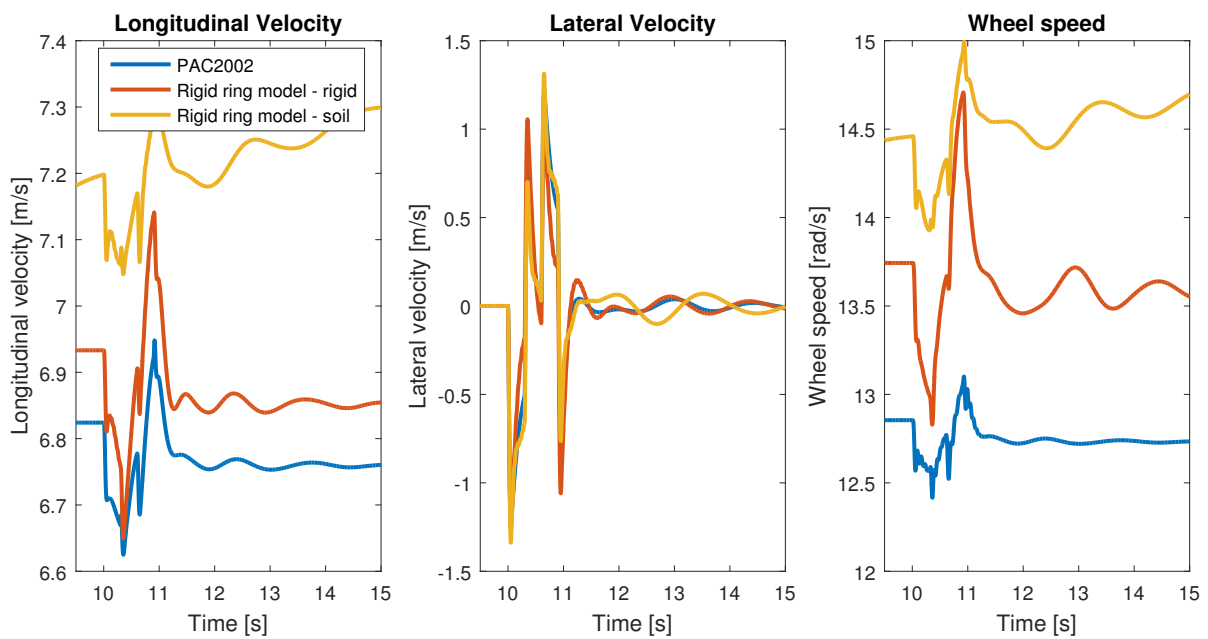
(b) Velocities, 25 km/h

Figure B.2: The forces and velocities during a step-steer test starting at 25 km/h.

# C Zigzag Test

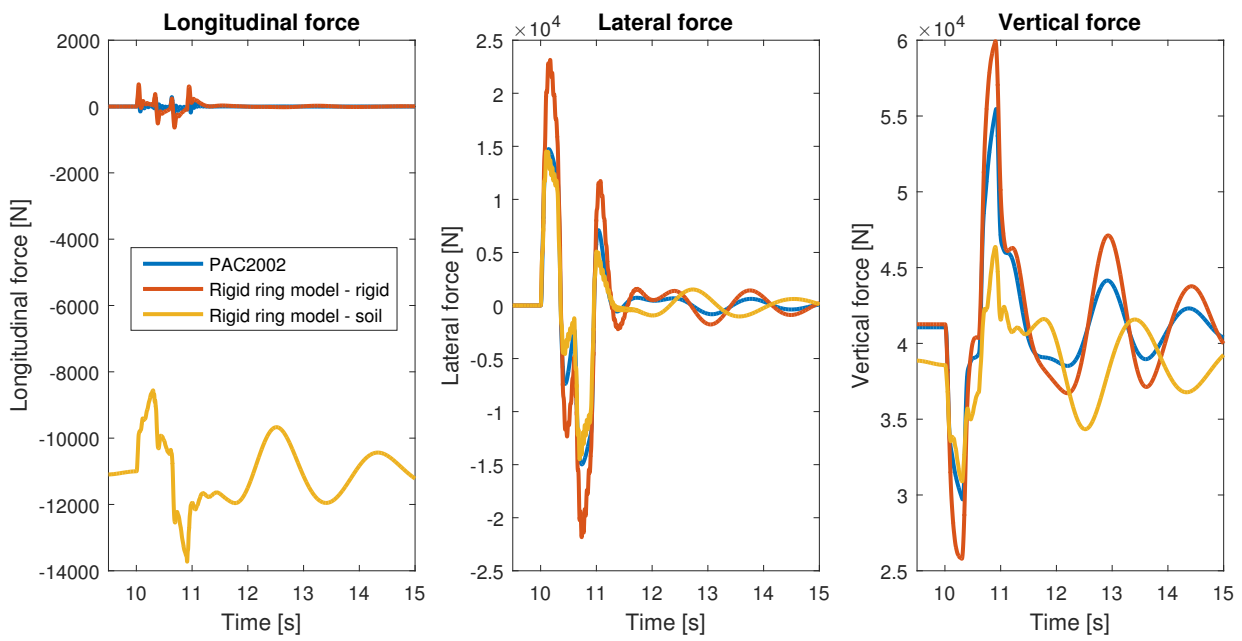


(a) Forces, 5 km/h

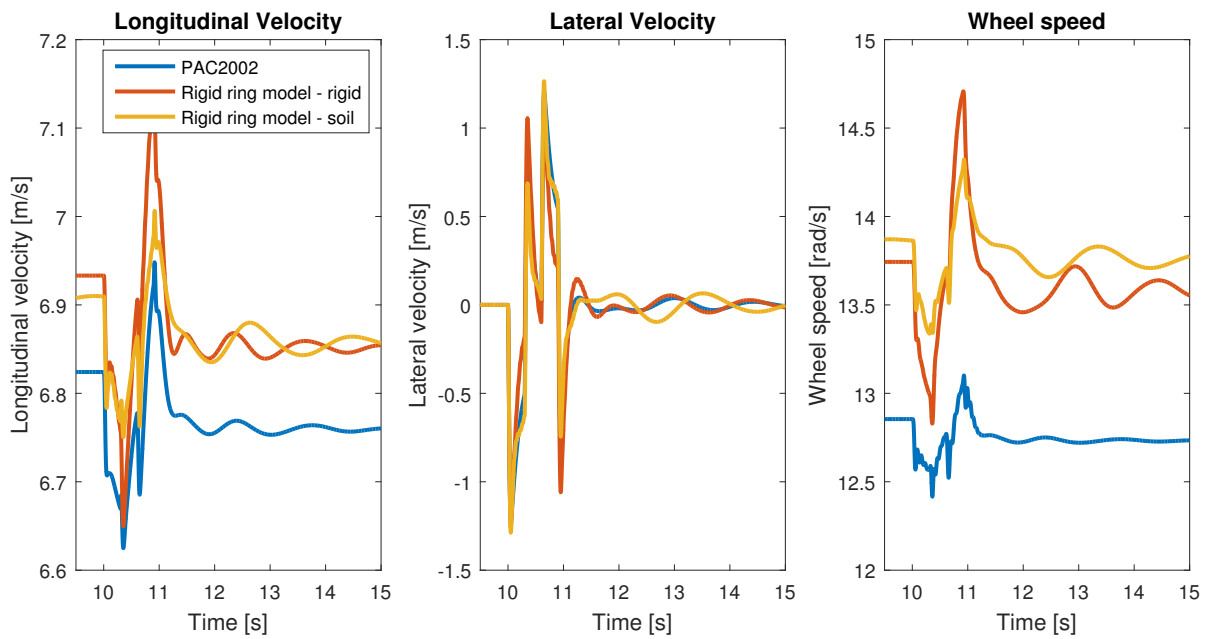


(b) Velocities, 5 km/h

Figure C.1: The forces and velocities during a zigzag test starting at 5 km/h.



(a) Forces, 25 km/h



(b) Velocities, 25 km/h

Figure C.2: The forces and velocities during a zigzag test starting at 25 km/h.

## D Rigid Ring Tyre Model Parameter Values Used in This Project

Table D.1: Mass and moment of inertia of tyre

Parameter	Symbol	Value	Unit
Total tyre mass	$m_{tot}$	108.6	kg
Mass of tyre belt	$m_b$	36.8066	kg
Mass of tyre rim	$m_r$	69.9933	kg
Wheel plane moment of inertia of belt	$I_{by}$	8.5718	$\frac{kg}{m}$
Out of plane moment of inertia of belt	$I_{bx}$	4.8564	$\frac{kg}{m}$
Wheel plane moment of inertia of rim	$I_{ry}$	3.5012	$\frac{kg}{m}$
Out of plane moment of inertia of rim	$I_{rx}$	1.9836	$\frac{kg}{m}$

Table D.2: Wheel plane parameters for rigid ring tyre model for rigid and Clayey soil (Thailand) ground, 13.3 kN

Parameter	Symbol	55 PSI	85 PSI	110 PSI	Unit
Vertical stiffness of tyre belt	$k_{bz}$	3168.3	3954.8	4779.7	$\frac{kN}{m}$
Vertical damping of tyre belt	$c_{bz}$	1.0961	1.2247	1.3463	$\frac{kN}{m/s}$
Vertical residual stiffness	$k_{vr}$	703.17	1031.2	1254.4	$\frac{kN}{m}$
Vertical residual damping	$c_{vr}$	0.2757	0.2963	0.3266	$\frac{kN}{m/s}$
Wheel plane rotational stiffness of tyre belt	$k_{b\theta}$	405.34	467.51	516.72	$\frac{kN}{rad}$
Wheel plane rotational damping of tyre belt	$c_{b\theta}$	0.0212	0.0219	0.0223	$\frac{kN}{rad/s}$
Longitudinal tread stiffness	$k_{cx}$	1392.6	1588.9	1809.7	$\frac{kN}{m}$
Longitudinal tyre stiffness	$k_k$	96.088	99.309	104.06	$\frac{kN}{slip}$
Longitudinal tyre stiffness, soft soil	$k_{k,soil}$	19.231	18.182	17.857	$\frac{kN}{slip}$
Vertical stiffness of soil	$k_{soil}$	337.49	360.14	370.25	$\frac{kN}{m}$
Longitudinal slip force saturation	$F_{x,max}$	9.5	9.5	9.5	$kN$
Longitudinal slip force saturation, soil	$F_{x,max,soil}$	7.0	6.7	6.4	$kN$
Damping constant in equivalent damping of soil	$c_{soil}$	-	-	-	$\frac{kN}{m/s}$
Stiffness constant in equivalent damping of soil	$k_{soil,2}$	-	-	-	$\frac{kN}{m}$
Frequency derivative	$\frac{d\omega}{dv_x}$	-	-	-	$\frac{rad/s}{m/s}$
Nominal frequency	$\omega_0$	-	-	-	$\frac{rad}{s}$
First slope compensation constant	$c_a$	-	-	-	$\sim$
Second slope compensation constant	$c_b$	-	-	-	$\sim$
Third slope compensation constant	$c_c$	-	-	-	$\sim$

Table D.3: Out of plane parameters for rigid ring tyre model for rigid and Clayey soil (Thailand) ground, 13.3 kN

Parameter	Symbol	55 PSI	85 PSI	110 PSI	Unit
Translational stiffness of tyre belt	$k_{by}$	742.93	911.21	1017.6	$\frac{kN}{m}$
Translational Damping of Tyre belt	$c_{by}$	0.1224	0.1248	0.1269	$\frac{kN}{m/s}$
Out of plane Rotational Stiffness of tyre belt	$k_{b\gamma}$	163.71	200.09	227.92	$\frac{kN}{slip}$
Out of plane rotational damping of tyre belt	$c_{b\gamma}$	0.0209	0.0213	0.0206	$\frac{kN}{rad/s}$
Cornering stiffness	$k_f$	150.75	150.75	150.75	$\frac{kN}{rad}$
Cornering stiffness, soil	$k_{f,soil}$	50.247	50.247	50.247	$\frac{kN}{rad}$
Self-aligning torque stiffness	$k_M$	5.1	5.1	5.1	$\frac{kN}{slip}$
Self-aligning torque stiffness, soil	$k_{M,soil}$	10.708	10.708	10.708	$\frac{kN}{slip}$
Relaxation length	$\sigma$	0.6874	0.5633	0.4881	$m$
Relaxation length, soil	$\sigma_{soil}$	0.2878	0.2357	0.1990	$m$
Lateral slip force saturation	$F_{y,max}$	8.5	8.5	8.5	$kN$

Table D.4: Wheel plane parameters for rigid ring tyre model for rigid and Clayey soil (Thailand) ground, 26.7 kN

Parameter	Symbol	55 PSI	85 PSI	110 PSI	Unit
Vertical stiffness of tyre belt	$k_{bz}$	3237.5	4205.9	4779.7	$\frac{kN}{m}$
Vertical damping of tyre belt	$c_{bz}$	1.1081	1.2629	1.3463	$\frac{kN}{m/s}$
Residual stiffness	$k_{vr}$	699.84	1015.4	1254.4	$\frac{kN}{m}$
Residual Damping	$c_{vr}$	0.2749	0.2942	0.3266	$\frac{kN}{m/s}$
Wheel plane rotational stiffness of tyre belt	$k_{b\theta}$	410.08	468.44	518.88	$\frac{kN}{rad}$
Wheel plane rotational damping of tyre belt	$c_{b\theta}$	0.0215	0.0219	0.0219	$\frac{kN}{rad/s}$
Longitudinal tread stiffness	$k_{cx}$	648.42	1076.8	1338.7	$\frac{kN}{m}$
Longitudinal tyre stiffness	$k_k$	84.393	93.566	96.211	$\frac{kN}{slip}$
Longitudinal tyre stiffness, soft soil	$k_{k,soil}$	40.718	40.742	36.931	$\frac{kN}{slip}$
Vertical stiffness of soil	$k_{soil}$	337.49	360.14	370.25	$\frac{kN}{m}$
Longitudinal slip force saturation	$F_{x,max}$	19.3	19.3	19.3	$kN$
Longitudinal slip force saturation, soil	$F_{x,max,soil}$	13.3	12.9	12.2	$kN$
Damping constant in equivalent damping of soil	$c_{soil}$	-	-	113.01	$\frac{kN}{m/s}$
Stiffness constant in equivalent damping of soil	$k_{soil,2}$	-	-	537.64	$\frac{kN}{m}$
Frequency derivative	$\frac{d\omega}{dv_x}$	-	-	0.4977	$\frac{rad/s}{m/s}$
Nominal frequency	$\omega_0$	-	-	0.0683	$\frac{rad}{s}$
First slope compensation constant	$c_a$	-	-	0.00183	$\sim$
Second slope compensation constant	$c_b$	-	-	2.9	$\sim$
Third slope compensation constant	$c_c$	-	-	0.2753	$\sim$

Table D.5: Out of plane parameters for rigid ring tyre model for rigid and Clayey soil (Thailand) ground, 26.7 kN

Parameter	Symbol	55 PSI	85 PSI	110 PSI	Unit
Translational stiffness of tyre belt	$k_{by}$	742.93	911.21	1017.6	$\frac{kN}{m}$
Translational damping of tyre belt	$c_{by}$	0.1224	0.1248	0.1269	$\frac{kN}{m/s}$
Out of plane rotational stiffness of tyre belt	$k_{b\gamma}$	163.71	200.09	227.92	$\frac{kN}{slip}$
Out of plane rotational damping of tyre belt	$c_{b\gamma}$	0.0209	0.0213	0.0206	$\frac{kN}{rad/s}$
Cornering stiffness	$k_f$	208.42	208.42	208.42	$\frac{kN}{rad}$
Cornering stiffness, soil	$k_{f,soil}$	79.248	79.248	79.248	$\frac{kN}{rad}$
Self-aligning torque stiffness	$k_M$	6.9	6.9	6.9	$\frac{kN}{slip}$
Self-aligning torque stiffness, soil	$k_{M,soil}$	8.3709	8.3709	8.3709	$\frac{kN}{slip}$
Relaxation length	$\sigma$	0.9096	0.8108	0.7177	$m$
Relaxation length, soil	$\sigma_{soil}$	0.4060	0.3327	0.2860	$m$
Lateral slip force saturation	$F_{y,max}$	17	17	17	$kN$

Table D.6: Wheel plane parameters for rigid ring tyre model for rigid and Clayey soil (Thailand) ground, 40 kN

Parameter	Symbol	55 PSI	85 PSI	110 PSI	Unit
Vertical stiffness of tyre belt	$k_{bz}$	-	-	-	$\frac{kN}{m}$
Vertical damping of tyre belt	$c_{bz}$	-	-	-	$\frac{kN}{m/s}$
Residual stiffness	$k_{vr}$	-	-	-	$\frac{kN}{m}$
Residual damping	$c_{vr}$	-	-	-	$\frac{kN}{m/s}$
Wheel plane rotational stiffness of tyre belt	$k_{b\theta}$	-	-	-	$\frac{kN}{rad}$
Wheel plane rotational damping of tyre belt	$c_{b\theta}$	-	-	-	$\frac{kN}{rad/s}$
Longitudinal tread stiffness	$k_{cx}$	-	-	-	$\frac{kN}{m}$
Longitudinal tyre stiffness	$k_k$	-	-	-	$\frac{kN}{slip}$
Longitudinal tyre stiffness, soft soil	$k_{k,soil}$	-	-	-	$\frac{kN}{slip}$
Vertical stiffness of soil	$k_{soil}$	-	-	-	$\frac{kN}{m}$
Longitudinal slip force saturation	$F_{x,max}$	-	-	-	$kN$
Longitudinal slip force saturation, soil	$F_{x,max,soil}$	-	-	-	$kN$
Damping constant in equivalent damping of soil	$c_{soil}$	-	-	100.72	$\frac{kN}{m/s}$
Stiffness constant in equivalent damping of soil	$k_{soil,2}$	-	-	486.09	$\frac{kN}{m}$
Frequency derivative	$\frac{d\omega}{dv_x}$	-	-	0.4111	$\frac{rad/s}{m/s}$
Nominal frequency	$\omega_0$	-	-	0.0000	$\frac{rad}{s}$
First slope compensation constant	$c_a$	-	-	0.0061	$\sim$
Second slope compensation constant	$c_b$	-	-	2.492	$\sim$
Third slope compensation constant	$c_c$	-	-	0.7862	$\sim$